NASA CR → /56762

Semi-Annual Status Report

RESEARCH IN MILLIMETER WAVE TECHNIQUES

NASA Grant No. NSG-5012
GT/EES Project No. A-1642

Report Period
15 December 1976 - 15 June 1977

Project Director/Principal Investigator
R. W. McMillan

Project Monitor for NASA/GSFC
J. L. King

15 July 1977

Electromagnetics Laboratory

ENGINEERING EXPERIMENT STATION

Georgia Institute of Technology

Atlanta, Georgia 30332

Semi-Annual Status Report

RESEARCH IN MILLIMETER WAVE TECHNIQUES

NASA Grant No. NSG-5012
GT/EES Project No. A-1642

Report Period
15 December 1976 - 15 June 1977

Project Director/Principal Investigator
R. W. McMillan

Project Monitor for NASA/GSFC
J. L. King

15 July 1977

Electromagnetics Laboratory

TABLE OF CONTENTS

LIST OF ILLUSTRATIONS

FOREWORD

This is the sixth semi-annual status report on NASA Grant NSG-5012.
The Grant period is from June 15, 1974 to January 31, 1978 and includes
five extensions and increases to the scope and funding of the programs.
The total funding to date is $423,933 of NASA funds and $22,681 in Georgia
Tech cost-sharing funds, for a total from both sources of $446,614.
Current grant funding is at a level of $150,000 with Georgia Tech pro-
viding $7,500, and the current grant period extends through January 31,
1978.

As indicated in previous reports, and although not required by the
Grant, informal monthly letter-type reports have been written and fur-
nished to the NASA/GSFC technical monitor, J. Larry King, in order to
keep him abreast of project activities on a current basis. We believe
this provides a better opportunity for NASA to direct the technical efforts
on the program for the maximum benefit of the government. Copies of each
of these monthly reports for the current period (thirty-two through
thirty-six) are attached as an Appendix. This sixth semi-annual report
will replace the thirty-seventh monthly letter (since this semi-annual
report is being furnished during the time the thirty-seventh monthly report
would normally be written).

Responsibility for technical effort on this grant lies in the Electro-
magnetics Laboratory, under the general supervision of J. W. Dees, Director.
R. W. McMillan has been appointed Project Director of this program, which
has the internal project number A-1642. The program technical effort is
divided between the Radiation Systems Division, responsible for source and
mixer development, and the Electro-Optics Division, responsible for radio-
metric measurements, quasi-optical techniques, and analysis. During the
past 1 1/2 years, Professor G. T. Wrixon of University College, Cork,
Ireland has served as a consultant to this program in the area of mm-wave
mixer design. Contributors to the technical effort and/or this report
during the six six-month periods include: V. T. Brady, J. W. Dees, J. J.
Gallagher, D. O. Gallentine, J. B. Langley, R. W. McMillan, H. Muzika,
J. H. Rainwater, J. M. Schuchardt, R. G. Shackelford, G. T. Wrixon (con-
sultant), and Student Assistants H. C. Branch, A. M. Cook, R. E. Forsythe,

H. Homayun, N. K. O'Rourke, W. M. Penn, and D. H. Smith.

A paper entitled "Calculations of Antenna Temperature, Horizontal Path Attenuation, and Zenith Attenuation Due to Water Vapor in the Frequency Band 150 - 700 GHz", by R. W. McMillan, J. J. Gallagher, and A. M. Cook, supported by funds from this grant, was published in the June 1977 issue of IEEE Transactions on Microwave Theory and Techniques (Vol. MTT-25, No. 6, pp. 484-488). A second paper entitled "Quasi-Optical Techniques for Millimeter Wave Radar Applications", by R. W. McMillan and J. J. Gallagher has been submitted to the Symposium/Workshop on Effective Utilization of Optics in Radar Systems to be held in Huntsville, Alabama on September 27-29, 1977. In addition, work has begun on a third paper whose subject will be the quasi-optical grid interferometers analyzed and tested during this program. These devices are also treated in some detail in this report.

During the period covered by this semi-annual report, the following trips related to this grant, but not necessarily charged to this grant, were made:

1. Airborne Instruments Laboratory, Long Island, New York and NASA Goddard Institute, New York, New York by V. T. Brady, J. W. Dees, and J. M. Schuchardt on 20 and 21 April, 1977 to discuss millimeter wave mixer techniques.

2. TRG and Microwave Associates in the Boston area by J. W. Dees and J. M. Schuchardt on 22 April, 1977, also for discussion of millimeter wave mixer techniques.

1.0 INTRODUCTION

During the past six months, efforts on this project have been devoted to: (1) design of fundamental mixers at 183 GHz, (2) construction and testing of a 6 GHz subharmonic mixer model, (3) beginning construction of a 183 GHz subharmonic mixer based on the results of tests on the 6 GHz model, (4) ground-based radiometric measurements at 183 GHz, (5) fabrication and testing of wire grid interferometers, and (6) preliminary calculations of antenna temperatures expected to result from reduction of data obtained during the NASA Convair 990 flights during March and April, 1977. Significant events during the past six months include: (1) design of a 183 GHz single-ended fundamental mixer by G. T. Wrixon to serve as a back-up mixer to the subharmonic mixer for airborne applications, (2) attainment of 6 dB single sideband conversion loss with the 6 GHz subharmonic mixer model, together with initial tests to determine the feasibility of pumping this mixer at $\omega_s/4$, (3) additional ground-based radiometric measurements, and (4) derivation of equations for power transmission of wire grid interferometers, and initial tests to verify these equations. Each of these areas of effort and achievement are treated in this report.

2.0 MIXER DEVELOPMENT

2.1 Fundamental Mixers

G. T. Wrixon of University College, Cork, Ireland, who has been serving as a consultant to this program, has designed a 183 GHz fundamental mixer to serve as a back-up device to the subharmonic mixer for airborne applications. Figure 1 shows how this mixer will be constructed.

This device is an improved version of the Sharpless type single diode mixer used in the Convair 990. It incorporates a 17 Ω impedance low-pass IF filter with a cut-off at 14.2 GHz. Leakage down this filter at the signal frequency is prevented by making the first two sections $\frac{3\lambda_s}{4}$ long. In this way it is hoped that the mixer can work at inter-
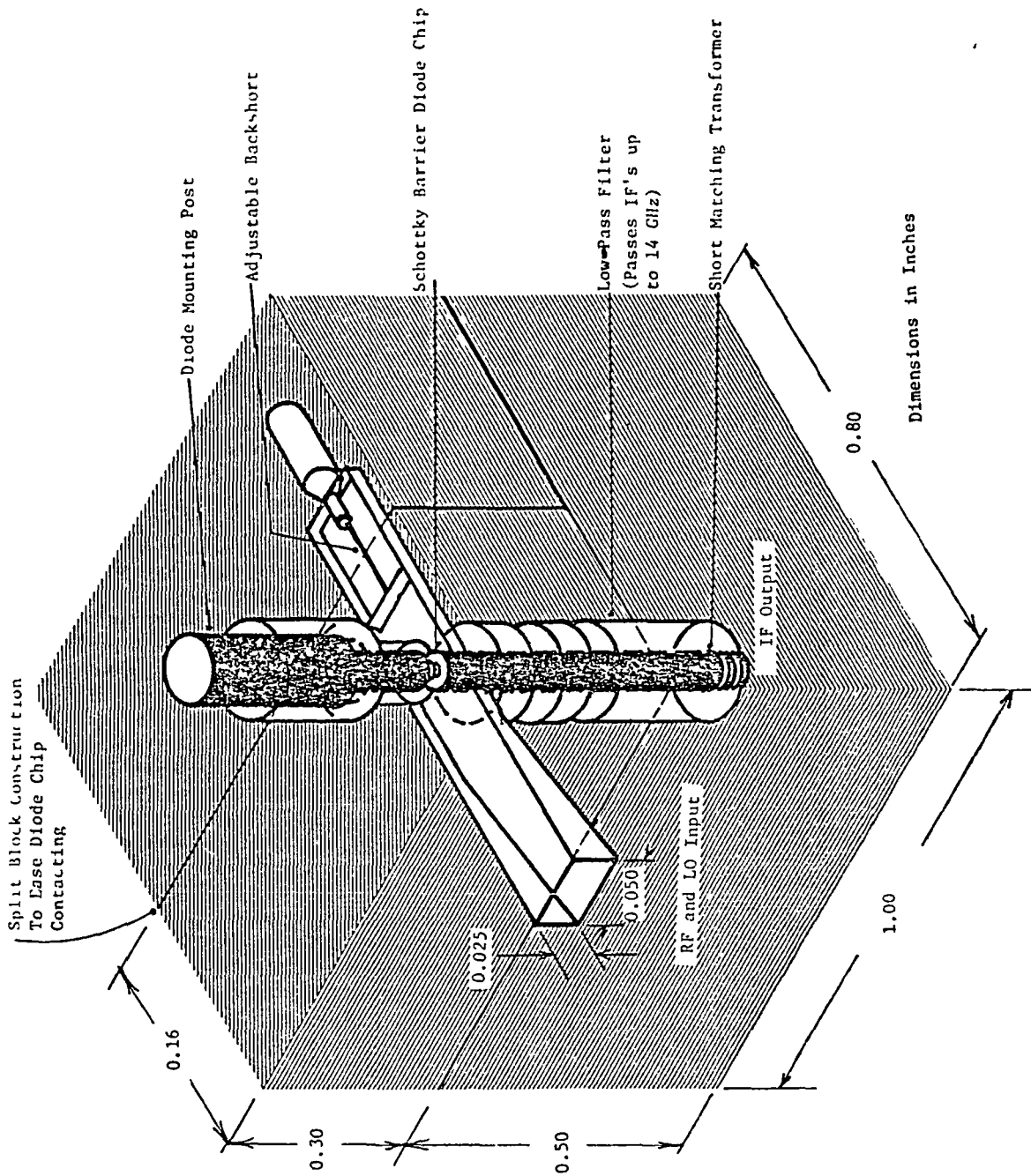
Split Block Construction
To Ease Diode Chip
Contacting

Diode Mounting Post

Adjustable Backshort

Schottky Barrier Diode Chip

Low-Pass Filter
(Passes IF's up
to 14 GHz)

Short Matching Transformer

Dimensions in Inches

0.80

IF Output

0.050

0.025

RF and LO Input

0.16

0.30

0.50

1.00

Figure 1. Schematic of 183 GHz Fundamental Mixer.

2

mediate frequencies of from 1 up to 10 GHz while still presenting an impedance which is very nearly real. This should greatly facilitate matching to the IF amplifiers.

The mixer body itself is split along the H-plane and one of the front sections forming part of the waveguide transformer is removable to enable visual contacting of the diode to be carried out. This mixer is specifically designed to provide for the use of multiple broadband IF's so that multichannel radiometry at 183 GHz will be possible.

2.2 Subharmonic Mixers

It will be recalled that the approach used to build and test a subharmonic mixer at 183 GHz is to first construct a model at some convenient frequency at which the microwave components are large, optimize the model, and then scale the model to the proper size corresponding to 183 GHz. For this work, a modeling frequency of 6 GHz was chosen and a model subharmonic mixer was constructed to operate at this frequency.

The results of tests on this model have been good. At the 6 GHz modeling frequency, it has been possible to achieve a single sideband mixer conversion loss of 6 to 8 dB, for a range of signal input power varying from 0 dBm to -70 dBm and for intermediate frequencies over the range 30 - 300 MHz. These IF's scale to 1-10 GHz in the final version. A detailed discussion of the results of this modeling is given in Appendix A-2. These results were considered good enough to begin construction of the final version of the mixer, which is scaled to a frequency of 183 GHz. The mixer body is being machined and the stripline filters are in the process of being made by Jerry Lamb at NASA/GSFC.

In addition to pumping a subharmonic mixer with a local oscillator frequency equal roughly to one-half the signal frequency, it is also possible to use any even submultiple of the signal frequency. The mixer model discussed above is being pumped in this way to compare results to the $\omega_s/2$ case. Preliminary single sideband conversion loss measurements

3

give about 9 dB for the case of pumping at $\omega_s/4$. Such a mixer would be very useful in spaceborne applications because it would extend the range of solid state local oscillator pumped mixers to almost 400 GHz. Appendix A-2 also contains a discussion of this type of subharmonic pumping.

3.0 RADIOMETRIC AND PROPAGATION CALCULATIONS

During the recently completed NASA Convair 990 flights, which covered a variety of terrain from Southern California to Greenland, it was noted in Arctic regions that the antenna temperature measured by the Georgia Tech 183 GHz radiometer varied depending upon whether the radiometer antenna was pointed at open water or ice. This variation indicates that the radiometer can "see" the ground in the Arctic regions, which is contrary to earlier opinions on this subject. In order to see if this result agrees with theory, the atmospheric modeling computer programs developed at Georgia Tech under this grant were used to calculate expected downlooking antenna temperature for both water and ice backgrounds under Arctic conditions. Calculations of horizontal path attenuation under these conditions were also made. These results show that it is possible for the radiometer to "see" the ground in the Arctic. These calculations are discussed in the thirty-sixth monthly progress report (MPR) in Appendix A-1.

From high altitudes, it is possible to calibrate a radiometer operating a few GHz away from the center frequency of an absorption line by using it to look upward at the cold sky. In this case the radiometer should measure the cosmic background of about 3°K. The Georgia Tech 183 GHz radiometer was used in this manner during the Convair 990 flights to observe the sky from an altitude of 11.9 km (39,000 ft.). Calculations were made of the expected result of this measurement using a computer program similar to those mentioned above. The results of these calculations are also given in the thirty-sixth MPR. Comparison of theory and experiment in this case must await reduction of the Convair 990 radiometer data, but the calculations show that the 5 GHz radiometer channel should indeed measure the 3°K

4

cosmic background.

4.0 RADIOMETRIC MEASUREMENTS

As part of the radiometric and propagation measurements program at Georgia Tech, a fully instrumented propagation range has just been completed. This range extends from the roof of the Baker Building to any one of several sites on or near the campus. Instruments associated with this range are capable of measuring temperature, relative humidity, wind speed and direction, rainfall level and rate, and aerosol droplet size. The terminus of this range situated on the roof of the Baker Building is an air conditioned laboratory mounted on a concrete slab. The 183 GHz radiometer has been moved from its former location on the roof of the Electronics Research Building to this new laboratory.

In moving the radiometer to its new location, some problems were encountered with performance of this instrument. Erratic behavior of the radiometer output, caused by persons moving around the laboratory, was ascribed to the proximity of the transmitting antenna of Channel 17 television. Although the earlier lab location was also near this antenna, the earlier location was better shielded. This problem was solved by shielding the windows of the new lab, rebuilding all IF cables from semi-rigid coax, shortening the remaining cables, and improving the shielding of the mixer bias box. These steps are described in the thirty-sixth MPR.

Another problem arose with the cross-guide harmonic mixer used in this radiometer. The diode chip had been contacted so many times that it was almost impossible to contact a diode with useable noise performance. Fortunately, G. T. Wrixon arrived from Ireland with some new chips, one of which was used in the mixer to achieve a total system double sideband noise figure of about 15 - 17 dB, including 5 dB of loss in the Fabry-Perot filter placed in front of the radiometer horn.

The Fabry-Perot pre-filter is being used to eliminate antenna temperature contribution from the third harmonic of the 90 GHz local oscillator, which has the effect of lowering the temperature at 180 GHz, because the sky temperature is low at 270 GHz. Results obtained so far

with this filter in the frequency range 160 - 170 GHz indicate that the filter is working as desired because these temperatures are in the range 250 - 290°K, which is higher than expected for these frequencies.

Preliminary results show the erratic temperature-versus-frequency behavior that has characterized earlier 183 GHz radiometric measurements. After carefully rebuilding and refining measurement techniques with this instrument for almost a year, it is becoming increasingly evident that all of the anomalous results obtained to date are not being given by the radiometer. There is strong precedent for anomalous atmospheric absorption in the short millimeter wavelength region [1]. Furthermore, this absorption fluctuates greatly with atmospheric conditions, being an especially strong function of the absolute humidity. It was speculated earlier that this absorption was due to the water dimer $(H_2O)_2$, but Gebbie [2] has shown conclusively that all of the absorption cannot be accounted for by this explanation, thus he has called this phenomenon "anomalous absorption". Measurements in the frequency range near 183 GHz are continuing in an effort to be sure that this absorption is indeed causing the erratic results. Of particular interest are the results of measuring the sky temperature directly on the 183 GHz water line peak, which should be slightly below ambient temperature regardless of whether or not anomalies are present, and will therefore provide some assurance that the radiometer is working properly.

Figure 2 shows the results of measuring antenna temperature over the frequency range of 160 - 200 GHz. A klystron is not available to cover a narrow region near the line peak. The circles and triangles are measured points and the solid curve is calculated using the measured temperature and water vapor density. Note that the measured radiometric temperature does reach ambient, showing that the Fabry-Perot filter is effectively eliminating the contribution from the third harmonic of the local oscillator at 270 GHz. The temperature is higher than expected over a broad range, however, and additional measurements must be made to verify this behavior. Since these measurements have not been repeated, they should be regarded as preliminary.
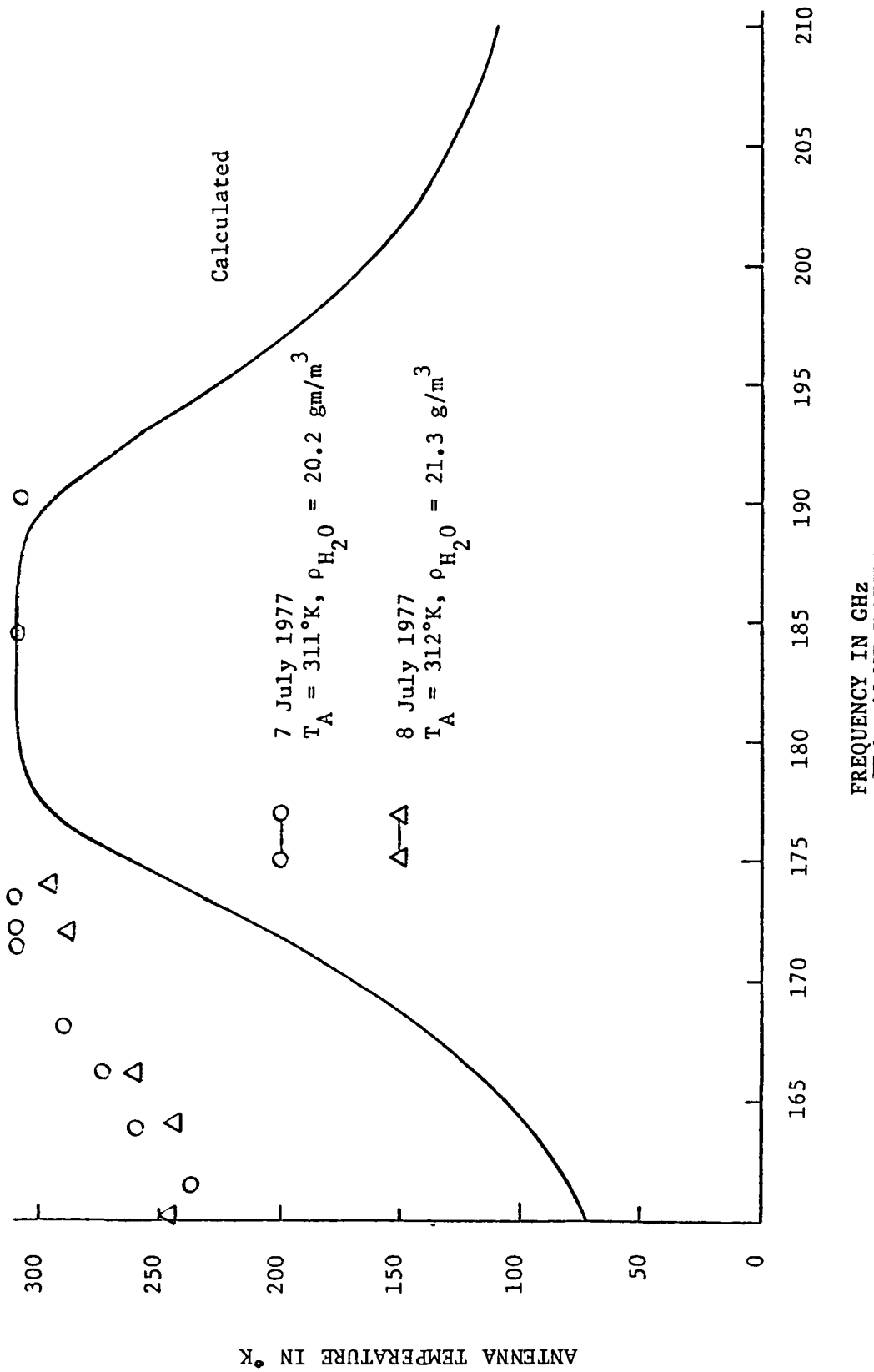
Figure 2. Measured and Calculated Radiometric Data.

It would also be of interest to measure the antenna temperature in the range 240 - 270 GHz by using the third harmonic of the local oscillator klystron together with a high-pass waveguide filter. Such filters are available at Georgia Tech with cut-off frequencies in the range 190 - 600 GHz.

5.0 WIRE GRID INTERFEROMETERS

Significant progress has been made in the analytical characterization of four-grid Fabry-Perot interferometers for use as microwave quasi-optical devices. An expression for lossless transmission has been derived, which shows that these interferometers are bandpass tunable by two different methods: (1) varying the angle between elements of a grid pair, and (2) varying the spacing between these elements. Further analysis resulted in an expression for transmission with losses considered, showing that narrow bandpass interferometers are more susceptible to losses than wideband devices, in agreement with basic Fabry-Perot theory. These results are discussed in some detail in the thirty-second monthly progress report (MPR), which is included as part of the appendix to this report. Additional results, including some preliminary measurements, are given in the thirty-third through thirty-fifth MPR's, which are also included in the appendix.

In addition to being bandpass tunable, a very general expression for grid interferometer transmission shows that it should be possible to build a polarization-twisting device which works in the forward direction. The matrix

$$\begin{pmatrix} \cos\theta_1 \cos\theta_2 & \sin\theta_1 \cos\theta_2 \\ \cos\theta_1 \sin\theta_2 & \sin\theta_1 \sin\theta_2 \end{pmatrix} ,$$

where θ_1 and θ_2 are the angles with the horizontal made by the normals to the grid wires of the input and output grids of the interferometer, is the general transmission matrix appearing in the grid transmission

8

equation. For a graphical definition of the angles θ_1 and θ_2, see Section VI of the Semi-Annual Status Report dated 22 July 1976. Note that choosing $\theta_1 = \pi/2$ and $\theta_2 = 0$ gives for this matrix

$$\begin{pmatrix} 0 & 1 \\ 0 & 0 \end{pmatrix} .$$

Operation on a column vector $\begin{pmatrix} 0 \\ e_y \end{pmatrix}$ representing a vertically polarized input gives $\begin{pmatrix} e_y \\ 0 \end{pmatrix}$ which shows that the output polarization is horizontal and that the plane of polarization has thus been rotated through 90°. Unfortunately, it has not yet been possible to solve this general transmission equation in closed form, so that the above result cannot be stated with certainty. Further analysis also needs to be done on the grid reflection equations, because a power reflection equation has not yet been derived. These problems will receive attention when time permits.

Additional measurements on grid transmission as a function of angle have been made. The results of the individual grid transmission measurements given in the thirty-third MPR were used in the interferometer transmission equations to compare measured and calculated results. Reflectivity losses were treated by comparing peak transmission to the calculated value and determining the best fit to the data. This approach was taken because of the difficulty in making reflectivity measurements due to grid edge effects. The results of these measurements are shown plotted in Figures 3 - 6 for grid angles of 60°, 80°, 85°, and 89°. Theoretical curves are shown as solid lines and measured curves are dashed. Figures 7 - 10 are essentially the same curves replotted as a function of frequency to show the bandpass characteristics of these filters. The agreement between these curves is fair in some cases and poor in others. The essential features of bandpass tunability are shown however, together with the expected poorer transmission as the bandpass becomes narrower.
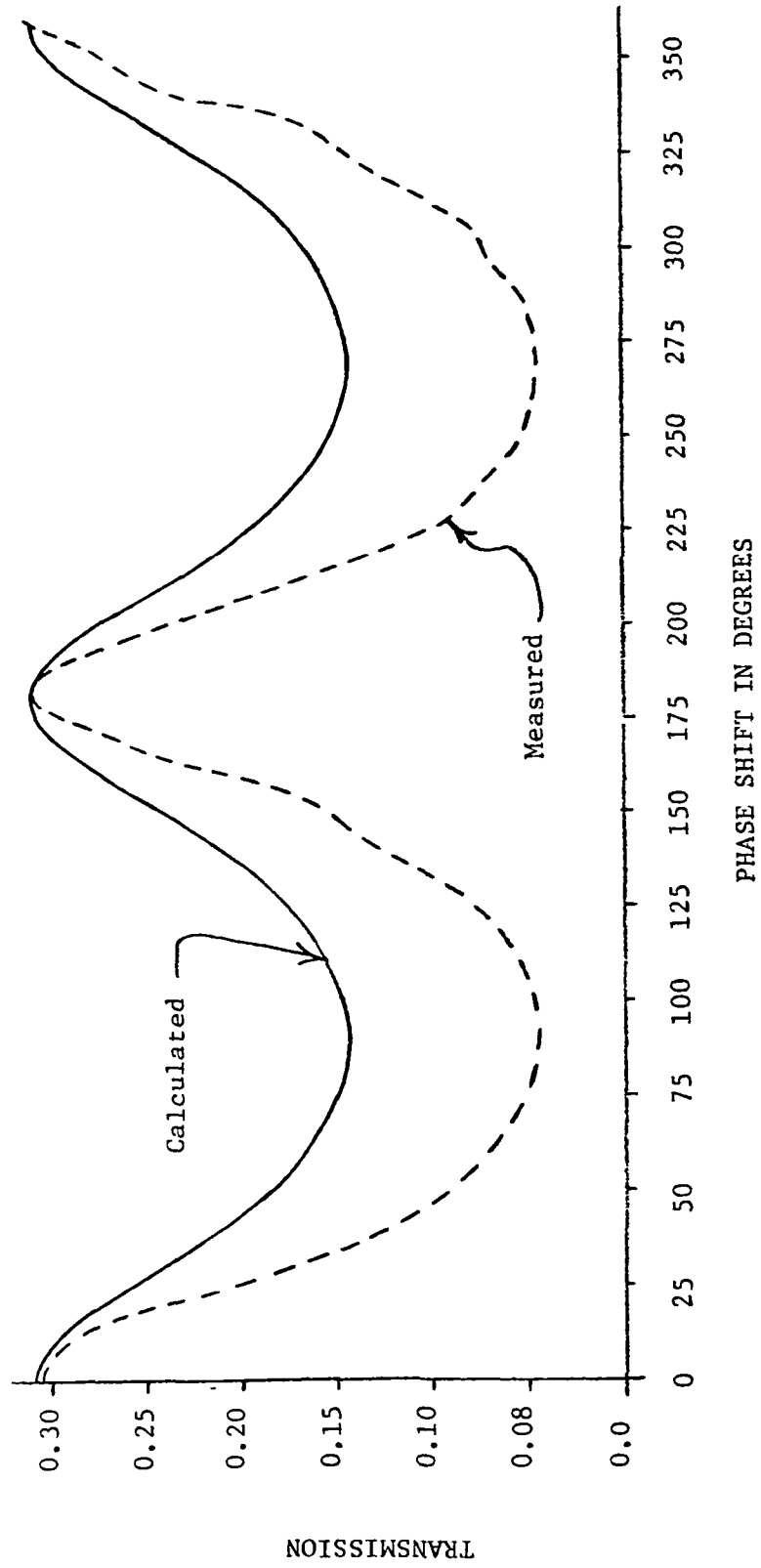
9

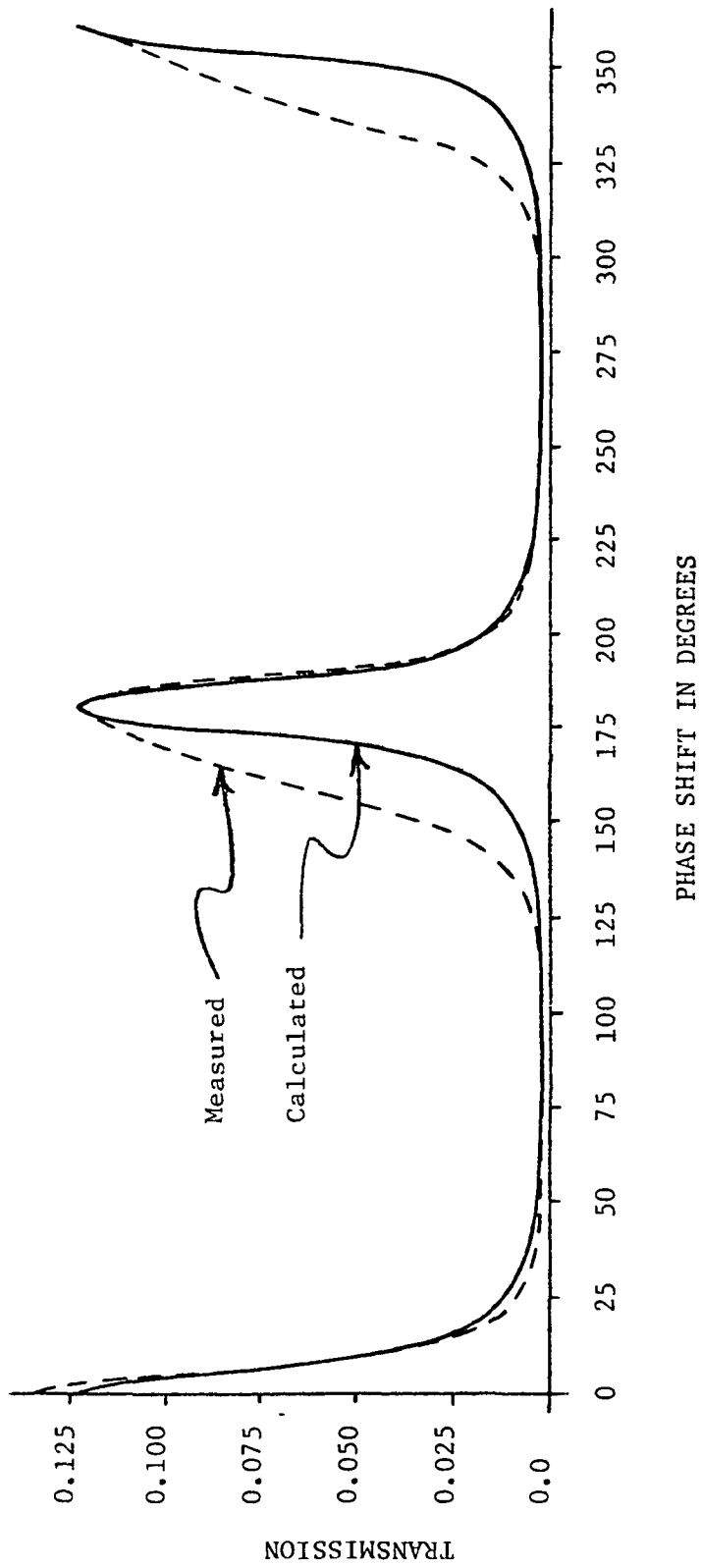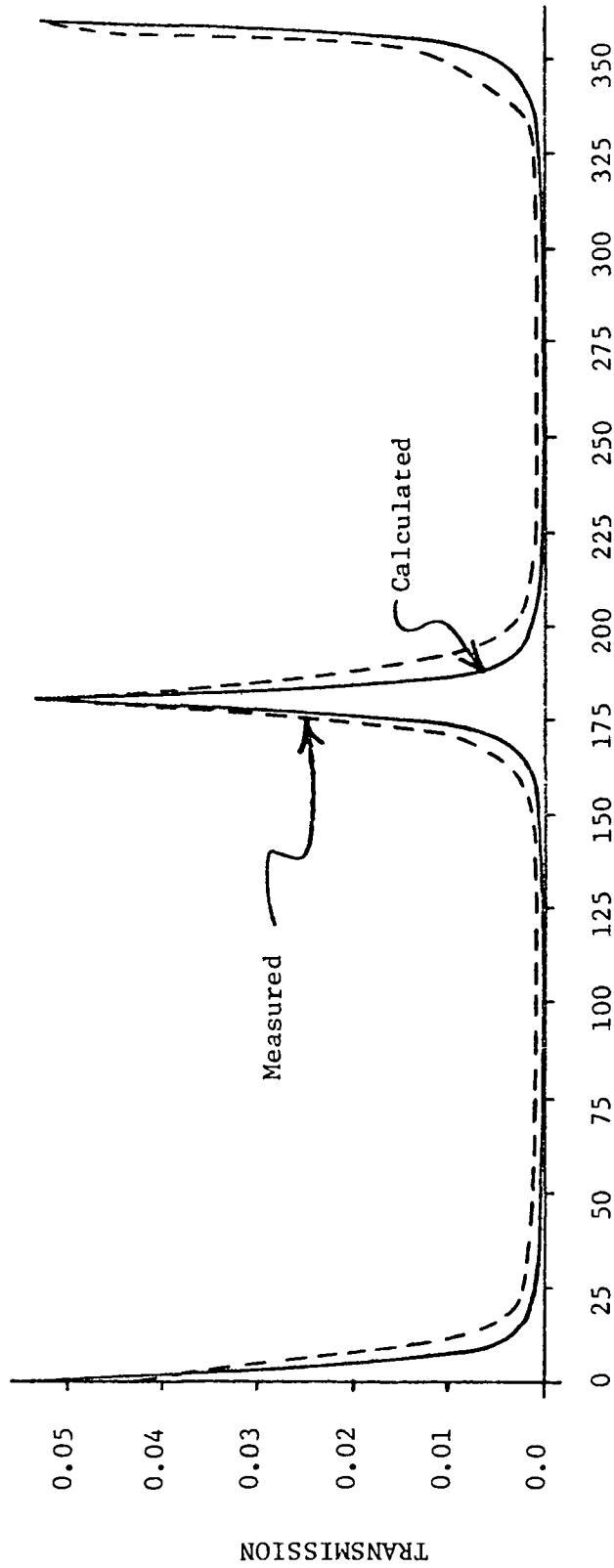Figure 3. Grid Interferometer Transmission vs. Phase for Grid Angle $\gamma = 60°$.

Figure 4. Grid Interferometer Transmission vs. Phase for Grid Angle γ = 80°.

11

Figure 5. Grid Interferometer Transmission vs. Phase
for Grid Angle $\gamma = 85°$.

12
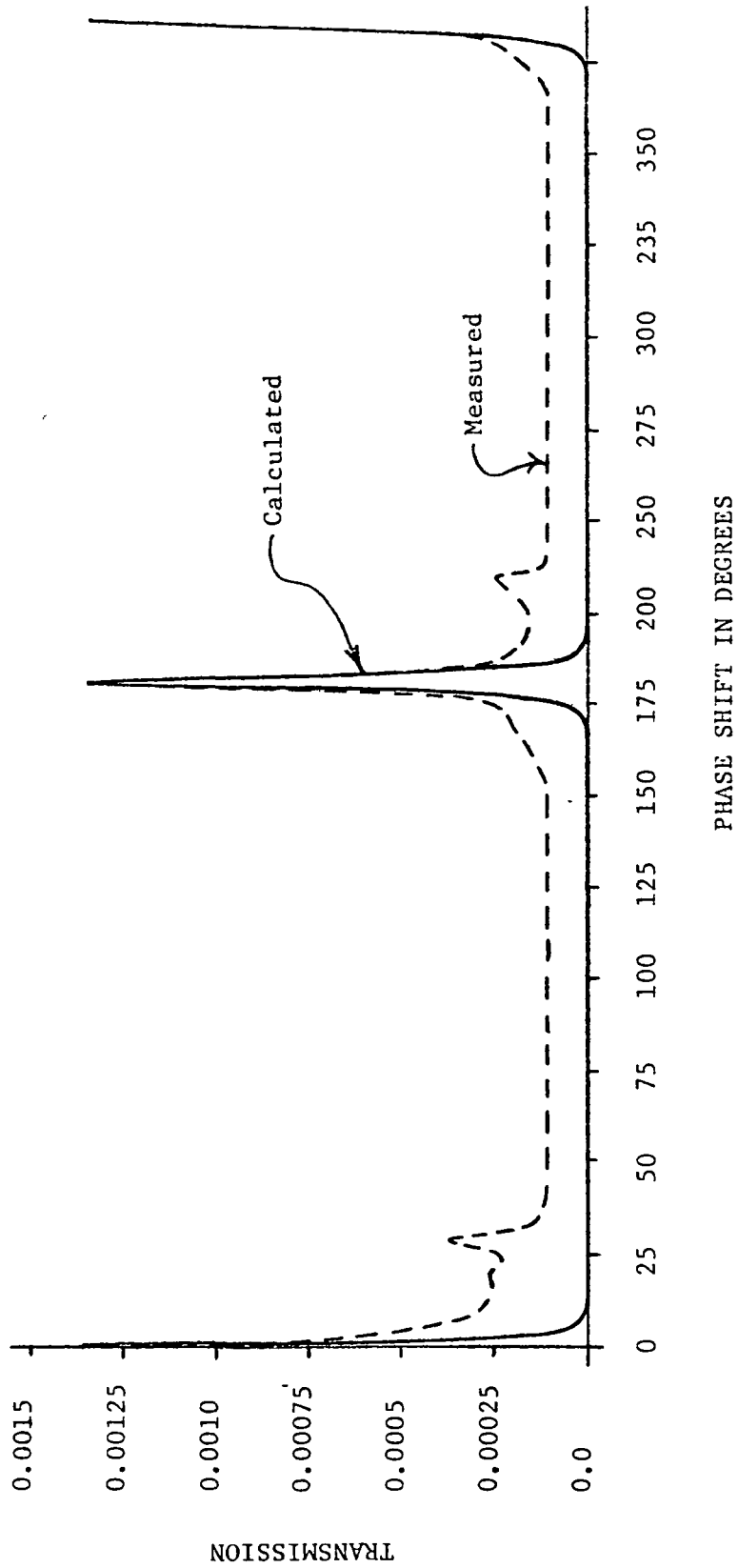
Figure 6. Grid Interferometer Transmission vs. Phase for Grid Angle $\gamma = 89°$.
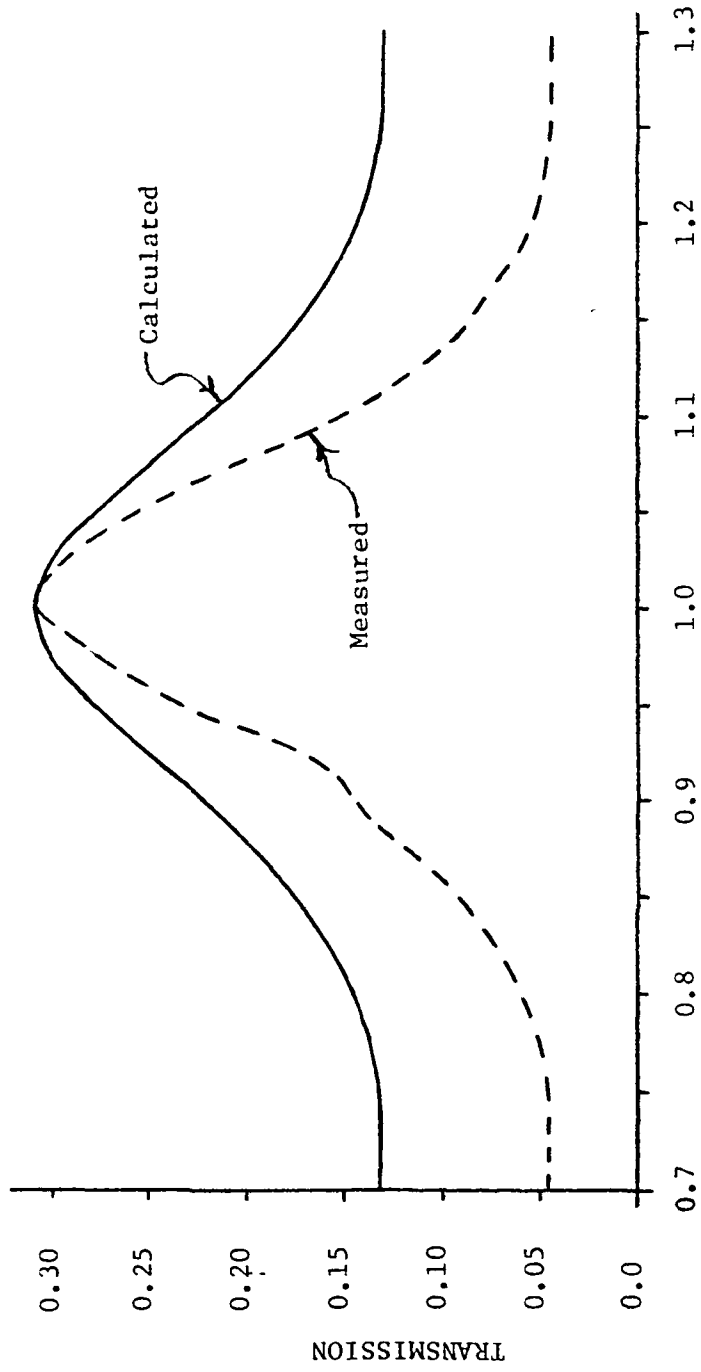
Figure 7. Grid Interferometer Transmission vs. Frequency for Grid Angle $\gamma = 60°$.
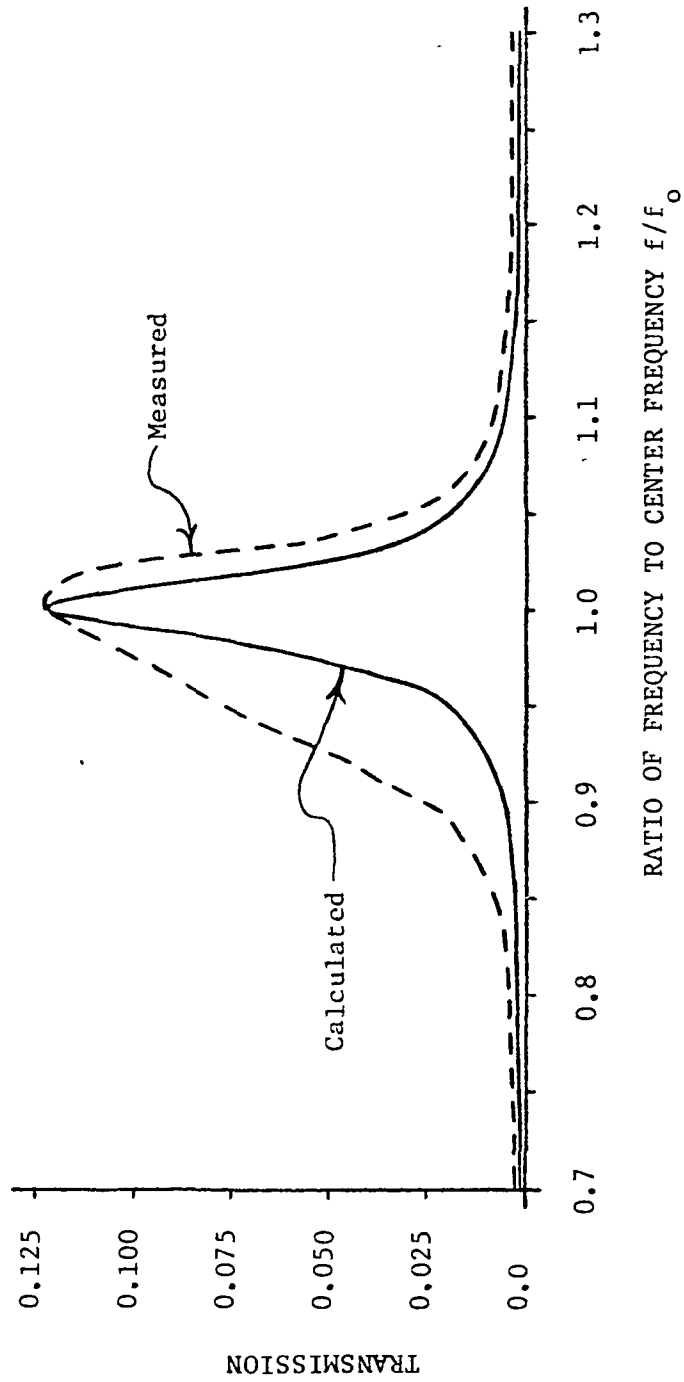
Figure 8. Grid Interferometer Transmission vs. Frequency for Grid Angle γ = 80°.
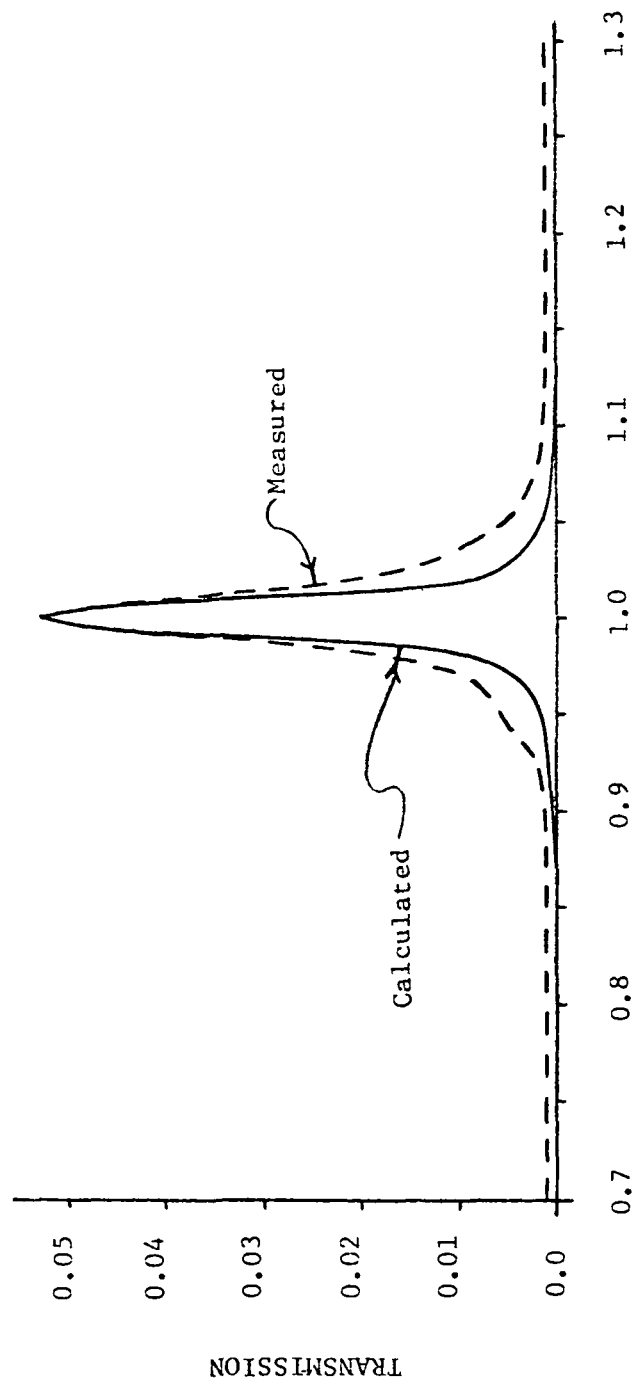
Figure 9. Grid Interferometer Transmission vs.
Frequency for Grid Angle γ = 85°.

16

Figure 10. Grid Interferometer Transmission vs. Frequency for Grid Angle $\gamma = 89°$.

17

The reason for the poor agreement of the above results with theory is probably caused by the fact that the grid conductor thickness is only 800 angstroms, which is about one-fifth of a skin depth for aluminum at 50 GHz. This thickness is such that part of the radiation incident on the grid, polarized parallel to the grid wires, will be transmitted. A basic assumption on which the derivation of the grid interferometer equations is based is that the conductors are many skin depths thick so that incident radiation, polarized parallel to the grid wires, is totally reflected. Jerry Lamb of NASA/GSFC has agreed to try to furnish some grids with thicker conductors so that more meaningful measurements can be made.

6.0 EFFORTS PLANNED FOR THE LAST HALF OF 1977

6.1 Calculations

Radiometric and propagation calculations have reached the point where they will only be performed for the purpose of comparing theory to experiment or to look at some particular special cases of interest, such as those of Section 3.0. Computer programs have been developed during this effort which will treat a wide variety of atmospheric effects with little or no modification.

Some additional calculations need to be made on the wire grid interferometers. The results obtained thus far need to be expanded to include an expression for reflected power. Also, the general case, with all grid angles and phases arbitrary, needs to be treated to determine conditions on which polarization twisting on transmission depends. The technical paper describing this work, begun during the last six-month reporting period, should be completed during the next period.

6.2 Measurements

All of the components for the noise figure test facility have been received and will be assembled into the test facility when time permits. This set-up will provide a means for evaluating mixer performance at assembly, and will be a valuable addition to the mixer lab. It is anticipated that this facility will be operational during the next six-month period.

Measurements of grid interferometer performance will be continued, and methods of constructing useful components from these grids will be studied. This effort will support the grid calculation work mentioned above.

Radiometric measurements will be continued unless it becomes obvious that anomalous absorption effects make them meaningless. An attempt will be made to measure antenna temperature in the range 240 - 270 GHz using filters available at Georgia Tech.

Performance measurements will be continued on the subharmonic mixer model using $\omega_s/4$ pumping. The actual 183 GHz subharmonic mixer should be available early in the reporting period, and its performance will also be evaluated.

6.3 Component Development

Work will continue on the development of the subharmonic mixer and it is anticipated that this work will result in a useful mixer during the next six-month period, barring unforeseen difficulties.

In addition to the grid interferometers already tested, methods of building quasi-optical millimeter wave components from wire grids such as isolators, diplexers, duplexers, and circulators will be studied. Also, interferometer grids with improved characteristics will be constructed.

REFERENCES

1. H. A. Gebbie, "New Molecular Absorbers in the Earth's Atmosphere and Their Submillimeter Spectra", Second International Conference on Submillimeter Waves and Their Applications, San Juan, Puerto Rico, December 1976.

2. H. A. Gebbie, private communication, May, 1977.

APPENDIX A-1

Monthly Letters 32 - 36

Period Covered

15 January 1977 - 15 June 1977

RESEARCH IN MILLIMETER WAVE TECHNIQUES

Thirty-Second Monthly Progress Report

Report Period

15 January to 15 February 1977

NASA Grant No. NSG-5012

GT/EES Project No. A-1642

Project Director: R. W. McMillan

Project Monitor: J. L. King

Engineering Experiment Station
Electromagnetics Laboratory
Georgia Institute of Technology
Atlanta, Georgia 30332

SUMMARY OF WORK

1.0 MIXERS

Two additional 183 GHz mixer wafers are being assembled to be used as spares for the Convair 990 radiometer. Measurements of the η-factor on these diodes consistently gave results greater than the η = 1.2 limit. Since the same technique has been used throughout the course of this program for contacting the mixer diodes, it was decided to try to use the scanning electron microscope (SEM) to examine these devices to see if the source of the problem could be determined. There was some reservation about taking this approach, because of the possibility of damage to the diodes by the electron bombardment. For this reason, a poor diode was chosen to be examined first. This diode was characterized so that changes due to the SEM examination, if present, could be easily determined. Testing of this device after being irradiated in the SEM showed no measurable change in characteristics, and it was decided to proceed with examination of the other diodes.

Figure 1 is an SEM photograph of the first, poor diode that was studied. The photograph shows clearly that the bent whisker is the cause of its poor performance. The η of this diode was measured to be 1.14, its series resistance was 4.4 Ω and its rectified current was 0.32 mA; measured with the klystron, doubler and coupling cavity. Figure 2 is a photograph of a normal diode, which has η = 1.13, R_s = 7.5, and I_r = 0.60 mA. Note the significance of the rectified current, which indicates that the bent whisker has a large effect on this performance parameter.

Examination of these mixers by the SEM has provided insight into the problems associated with contacting the diodes. In the future, all mixer diodes will be checked by this method, and some thought is being given to devising a method of contacting the diodes while viewing the process with the SEM.
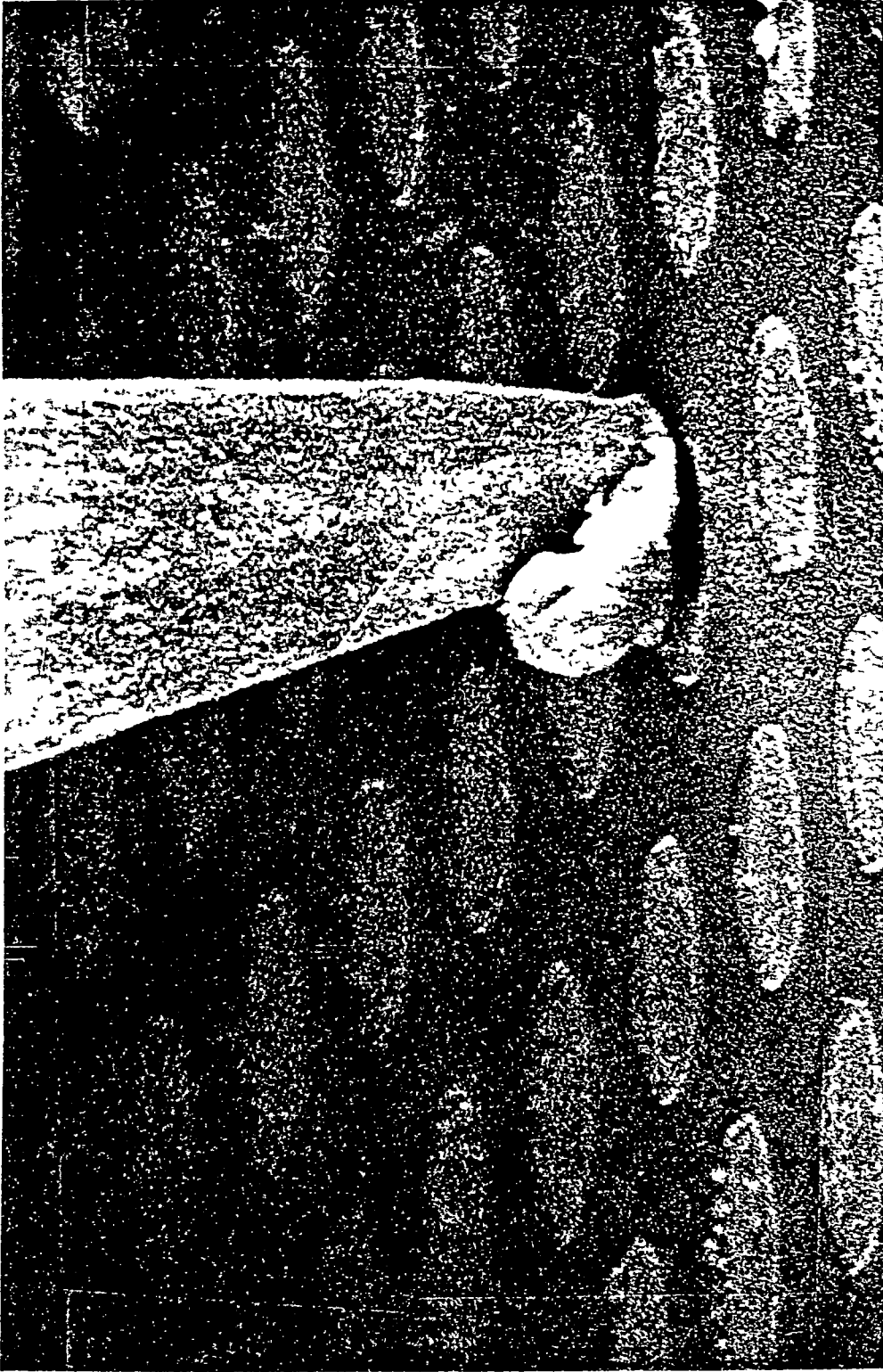
Figure 1. SEM photograph of poor diode showing bent whisker, magnification ~ 11,000X.

Figure 2. SEM photograph of normal diode, magnification ~ 11,000X.

A mixer test facility including a 1-2 GHz local oscillator and a 1-18 GHz mixer, to be used with the AIL receiver furnished by NASA/GSFC, is on order and delivery is expected in late March. This facility will provide a means for determining mixer conversion losses to an accuracy of less than 0.1 dB.

Both the local oscillator input stripline filter and the IF output stripline filter for the Model A subharmonic mixer are complete. Both of these filters show less than 0.2 dB insertion loss at the desired frequencies and greater than 40 dB attenuation an octave higher. More complete details of this performance are given in the B-57 program progress reports.

The Model A mixer body is currently being modified in the machine shop to place the signal input waveguide port perpendicular to the plane of the stripline. This change is expected to require two weeks, during which time the completion of the Model B mixer body is being delayed because of shop priorities.

2.0 RADIOMETRIC MEASUREMENTS

The radiometer is currently being modified to place a Fabry-Perot bandpass filter in front of the horn, to eliminate received power corresponding to the third harmonic of the 90 GHz LO which gives an error in antenna temperature measurements. This change requires the addition of a lens and modifications to the chopper to provide for a larger aperture. An existing adjustable mount will be used to hold the interferometer plates. These modifications are expected to be complete during the next monthly reporting period.

The bandpass filter to be used in the radiometer employs the square mesh reflectors described in the Twenty-Sixth Monthly Progress Report. These reflectors have very little loss at 200 GHz so that one would expect the contrast to be low, in accordance with the Fabry-Perot equations. Essentially all losses measured in the interferometer have been attributed to the associated lenses and horns. A test fixture, consisting of a 50 GHz klystron, run-in multiplier, and detector was set up to measure the performance of the filter in the laboratory. The output of the multiplier was WR-5 waveguide so that the third and higher harmonics of the klystron were present in the resonator signal. Evidently, however, very little of

26

the third harmonic was present, because the response of the filter, given in Figure 3, shows regularly spaced resonances corresponding to 200 GHz. Note that the contrast ratio is only 3 dB, which is consistent with the low filter loss. Part of the poor contrast is probably due to 150 GHz resonances, which are much weaker, superimposed on the 200 GHz peaks. This filter will be tried initially on the radiometer, but other inteferometer plates can be easily substituted if the contrast is not good enough. In particular, the quasi-optical filters discussed in the next section should be useful in this application.

3.0 QUASI-OPTICAL CALCULATIONS

Significant progress has been made in the analysis of the four-grid array Fabry-Perot interferometer filter. The algebraic difficulties encountered earlier have been overcome and an expression for power transmission has been derived. This expression shows the characteristic Fabry-Perot resonant peaks, and shows also that these filters have bandpass characteristics tunable by two different methods in addition to the polarization shifting properties discussed in earlier reports. The expression for lossless transmission has been determined to be

$$T = \frac{\cos^2(\theta-\beta)}{1 + \tan^4(\alpha-\theta)\left[\dfrac{\sin \delta + \cos^2(\alpha-\theta) \sin (2\phi_1-\delta)}{1-\cos 2\phi_1}\right]^2} , \qquad (1)$$

where α and θ are the grid angles, β is the input polarization, ϕ_1 is the phase shift between elements of a grid pair, and δ is the total phase shift through the interferometer. Figure 4 is a family of curves showing transmission normalized to $\cos^2(\theta-\beta)$ as a function of phase shift δ, with ϕ_1 held constant. The angle between grids $\gamma = \alpha-\theta$ is a parameter. Figure 5 is a similar family in which γ is held constant and ϕ_1 is varied as a parameter. Note that the bandpass may be tuned by varying either of these parameters.

In designing any filter, it is necessary to know the transmission losses before a reasonable design can be realized. Losses were treated in this analysis by modifying the transmission and reflection matrices derived earlier by multiplying them by a parameter which accounts for
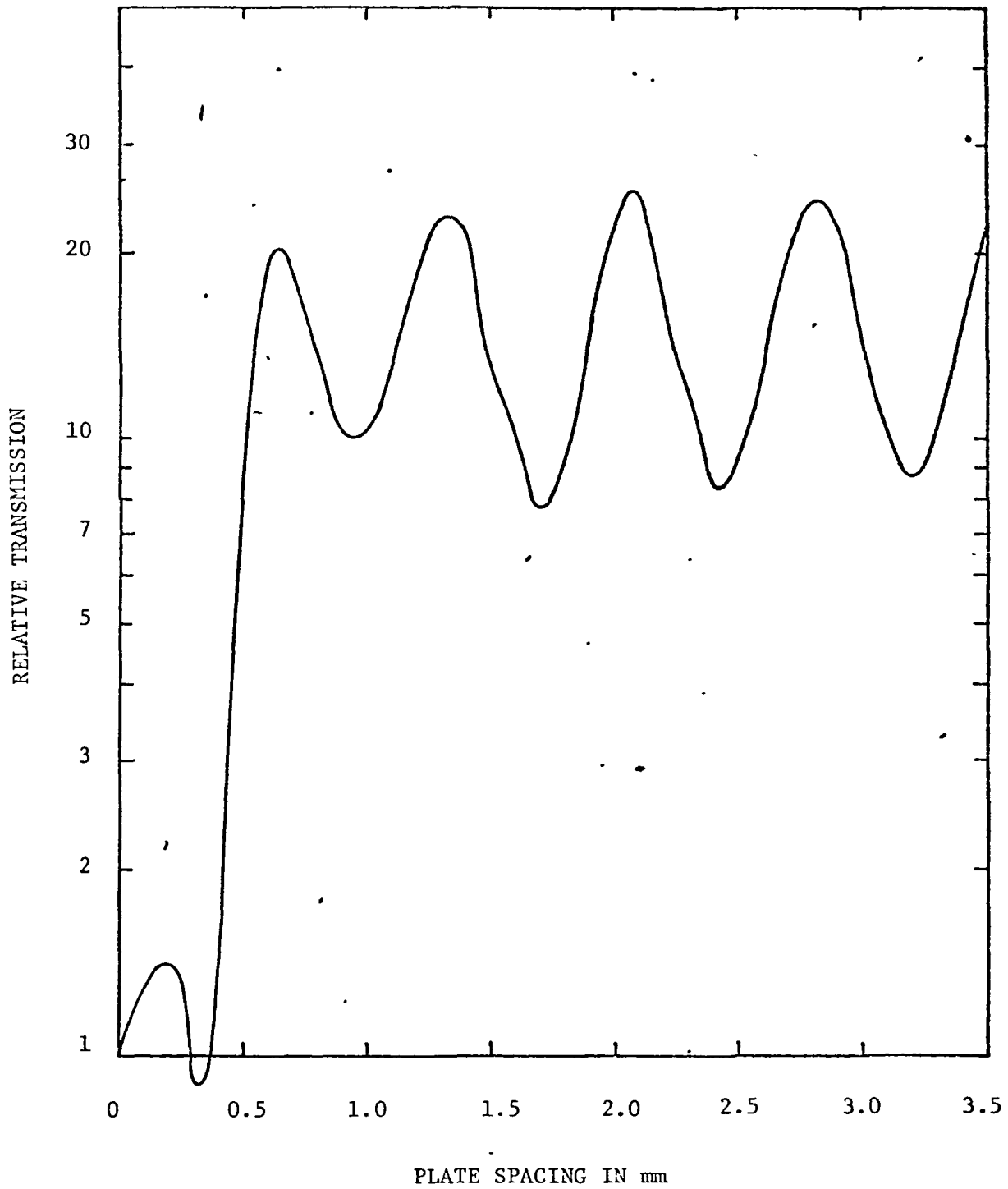
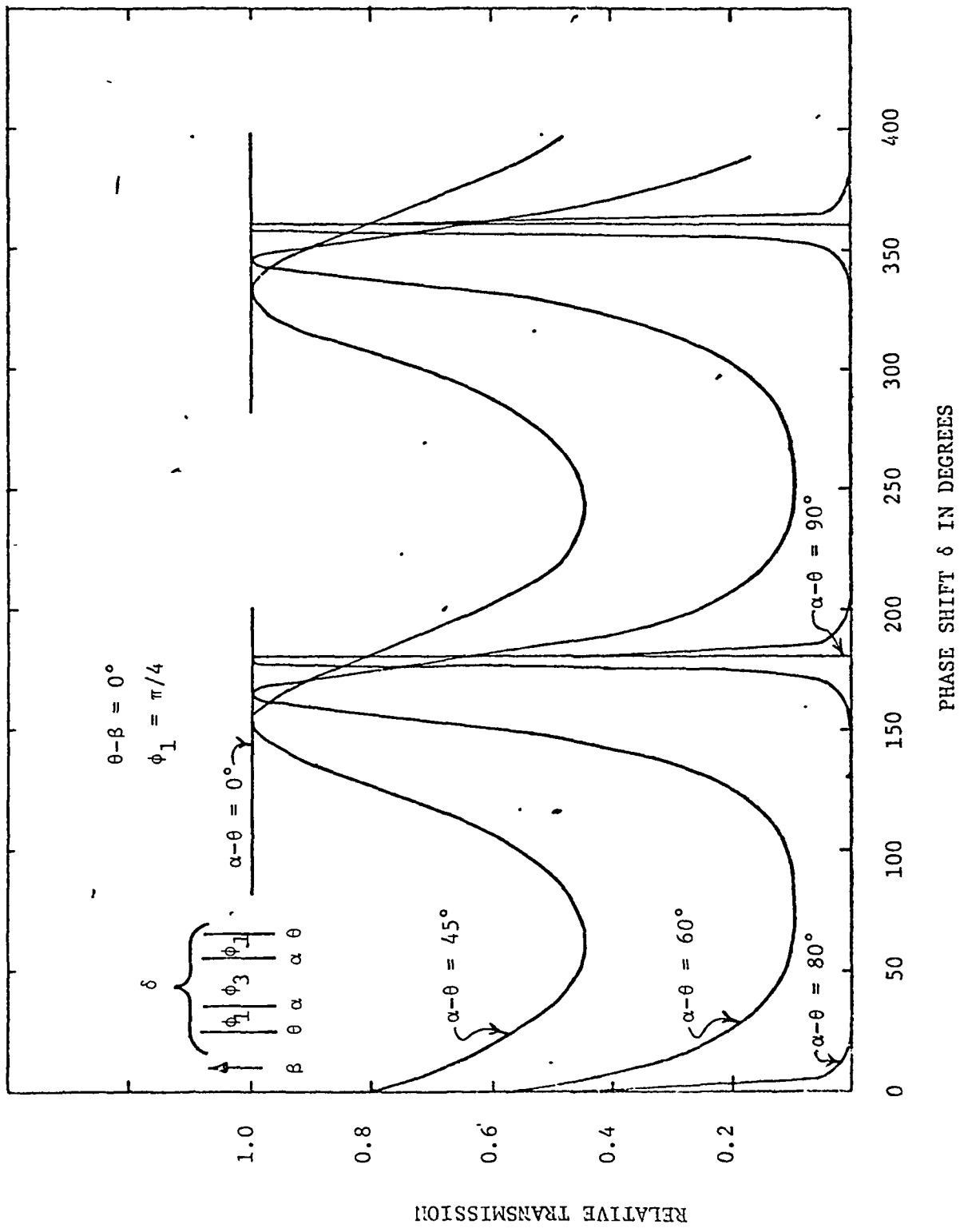Figure 3. Transmission of Fabry-Perot interferometer using mesh reflectors.

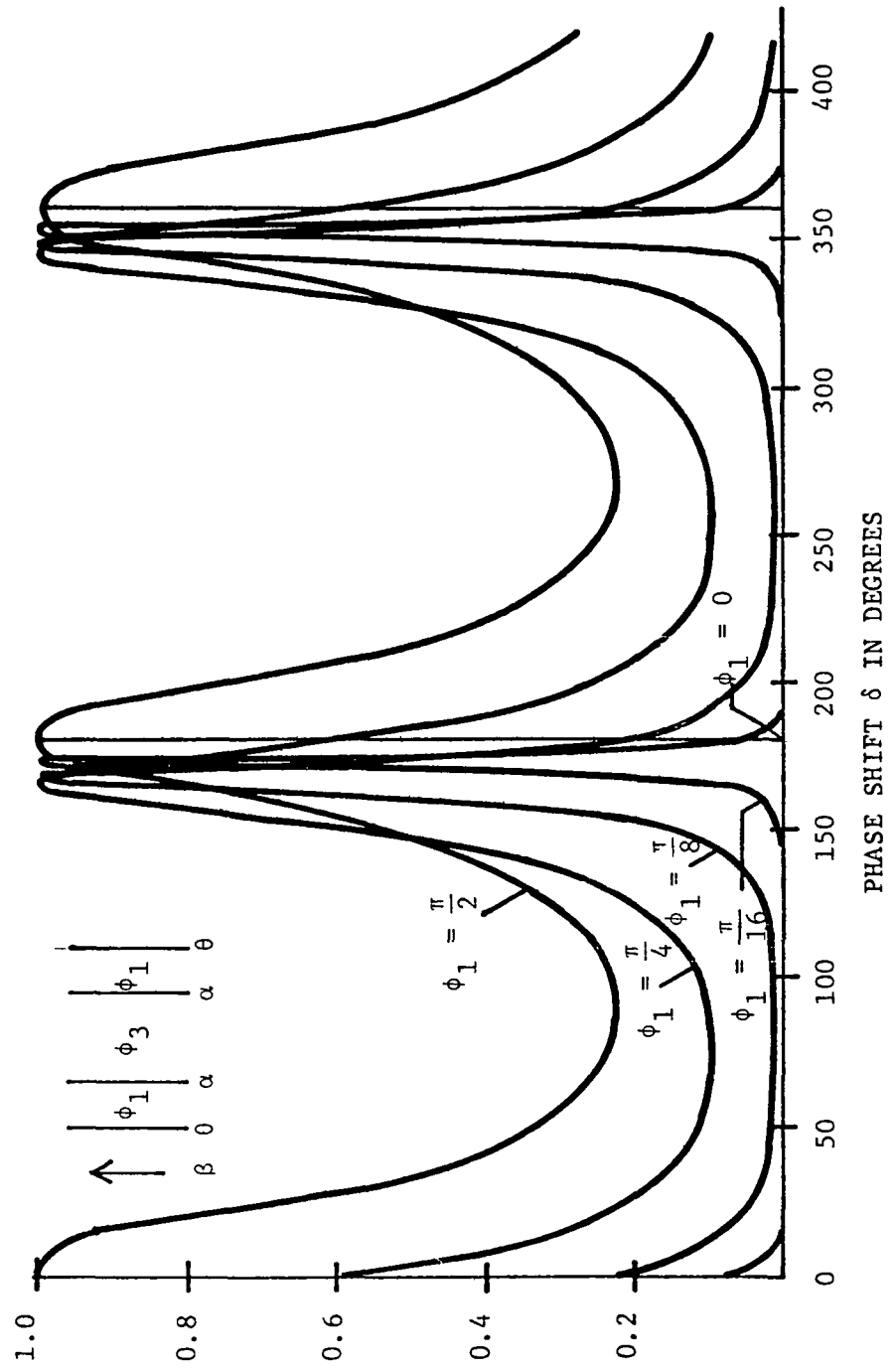Figure 4. Calculated transmission of grid-reflector interferometer with grid angle as a parameter.

Figure 5. Calculated transmission of grid-reflector interferometer with phase shift as a parameter.

imperfect transmission and reflection as follows:

$$t_\theta = T_\theta \begin{pmatrix} \cos^2\theta & \cos\theta\,\sin\theta \\ \sin\theta\,\cos\theta & \sin^2\theta \end{pmatrix}, \qquad t_\alpha = T_\alpha \begin{pmatrix} \cos^2\alpha & \cos\alpha\,\sin\alpha \\ \sin\alpha\,\cos\alpha & \sin^2\alpha \end{pmatrix},$$

$$r_\theta = R_\theta \begin{pmatrix} -\sin^2\theta & \sin\theta\,\cos\theta \\ \cos\theta\,\sin\theta & -\cos^2\theta \end{pmatrix}, \qquad r_\alpha = R_\alpha \begin{pmatrix} -\sin^2\alpha & \sin\alpha\,\cos\alpha \\ \cos\alpha\,\sin\alpha & -\cos^2\alpha \end{pmatrix}, \qquad (2)$$

where the R's and T's are slightly less than, but approximately equal to 1. Using these expressions instead of the previously used matrices, gives the following transmission expression:

$$T = T_\alpha^{\,4}\, T_\theta^{\,4}\, \cos^2(\theta-\beta) \left\{ \left[1 + \frac{\sin^2\gamma\,(1-R_\alpha^{\,2}R_\theta^{\,2}\cos^2\gamma - T_\theta^{\,2}R_\alpha^{\,2}\sin^2\gamma)}{\cos^2\gamma\,(1-2R_\alpha R_\theta\cos 2\phi_1 + R_\alpha^{\,2}R_\theta^{\,2})} \right] \right.$$

$$\left. + 4T_\theta^{\,2}\, R_\alpha^{\,2}\, \sin^4\gamma \left[\frac{\sin\delta + R_\alpha R_\theta\cos^2\gamma\sin(2\phi_1-\delta)}{\cos^2\gamma\,(1-2R_\alpha R_\theta\cos 2\phi_1 + R_\alpha^{\,2}R_\theta^{\,2})} \right]^2 \right\}^{-1}. \qquad (3)$$

This expression may be simplified by recalling that grid transmission is not difficult to make near ideal so that $T_\alpha = T_\theta \approx 1$. Also let $R_\alpha = R_\theta = R$, since grid reflection is generally nonideal. These substitutions are made for convenience in analyzing a few special cases. If the R's and T's are known exactly, they can be substituted into Equation (3) to determine T for any given case. Figure 6 gives the result of calculating normalized transmission as a function of phase shift for different values of R, showing that losses have a great effect on transmission for this type filter. In this regard, note that R as de-

31
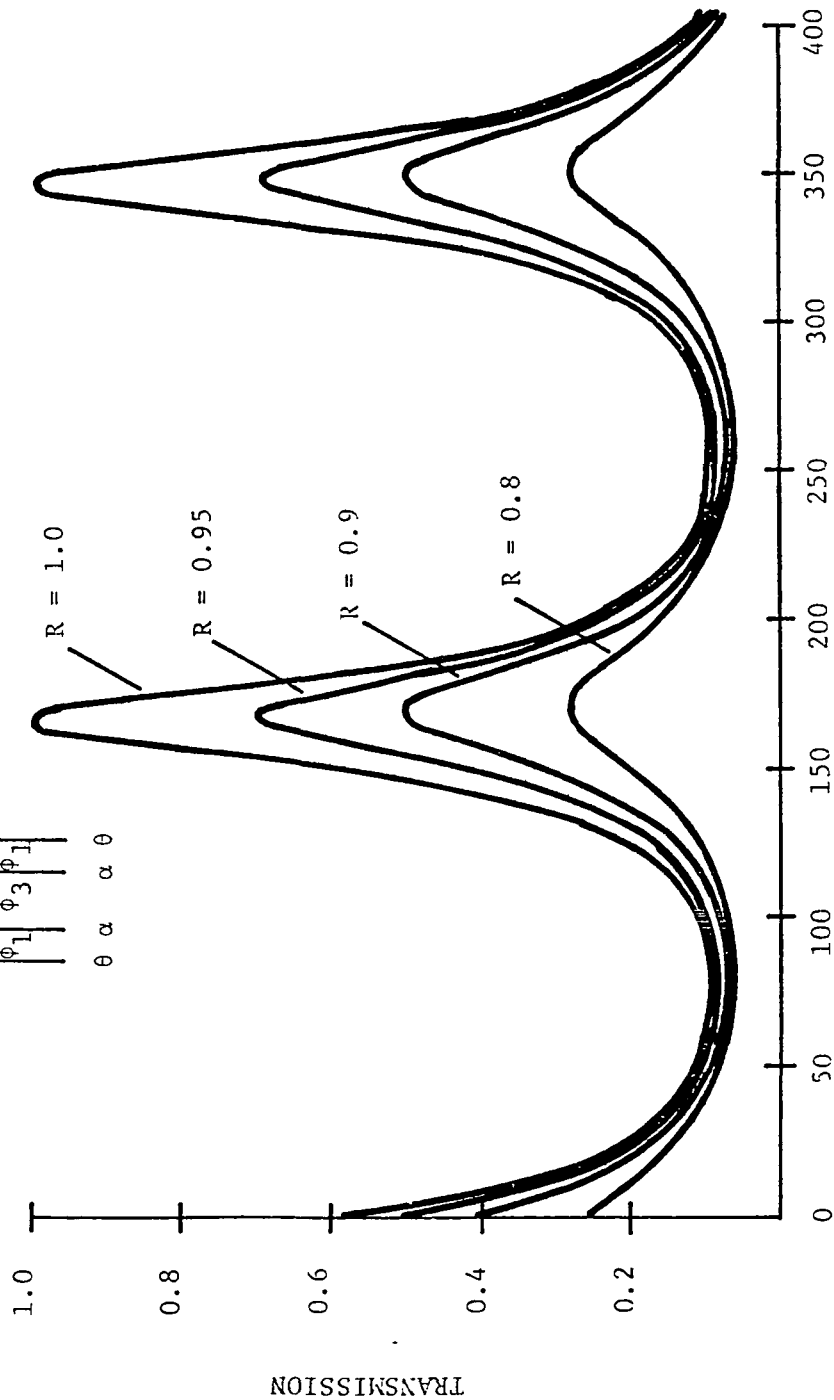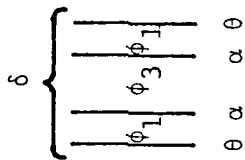
Figure 6. Calculated transmission of grid-reflector interferometer with R as a parameter.

$\theta - \beta = 0$

$\phi_1 = \pi/4$

$\gamma = \theta - \alpha = 60°$

R = 1.0

R = 0.95

R = 0.9

R = 0.8

PHASE SHIFT δ

TRANSMISSION

32

fined herein is an amplitude reflectivity and should be squared to get true power reflectivity. The curve for R = 0.8 then corresponds to reflectivity = 0.64.

By proper choice of the phase δ it is possible to make the second bracketed term of Equation (3) equal to zero, so that the remaining bracketed term corresponds to a maximum transmission for given values of R, γ, and ϕ_1. Figure 7 shows how maximum transmission varies as a function of R with ϕ_1 constant for three different values of γ. Figure 8 shows the same calculation with γ constant for four different values of ϕ_1.

It is also of interest to determine the bandpass characteristics of these filters relative to their center frequencies as functions of grid parameters. Figures 9, 10 and 11 give filter bandpass for three different values of R. Each of these curves in turn gives bandpass for three different values of γ, except Figure 11 in which the transmission for γ = 80° was too low to be of interest. These curves clearly show the effects of loss on performance and also show the effect of changing γ on the center frequency.

Fabry-Perot interferometers in a four-grid array as described in this report have the potential of being very useful devices for both microwave and far infrared spectral regions. The combination of both tunable bandpass and polarization control gives a capability that is not presently available in this portion of the electromagnetic spectrum and is not even available, in a single device, in the visible spectrum.

4.0 PLANS FOR NEXT PERIOD

The Model A subharmonic mixer modification will be completed during this period and some preliminary results on its performance should be available. Modification of the radiometer to include the quasi-optical filter should also be completed and some results should be available if this hardware is finished early in March. A pair of grid mounts to be used with the grids being furnished by Jerry Lamb of NASA/GSFC is
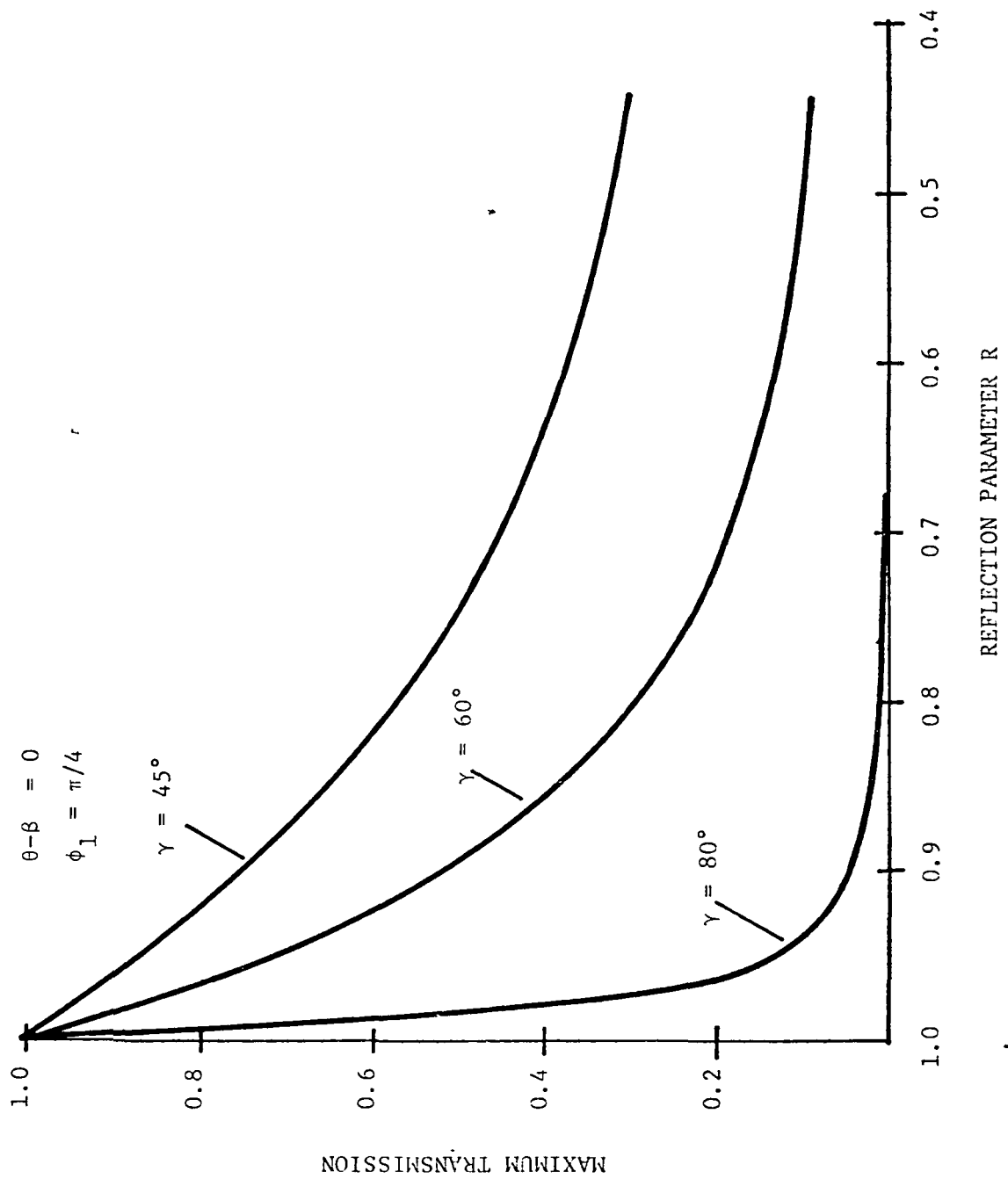
Figure 7. Maximum inteferometer transmission as a function of reflection and grid angle.
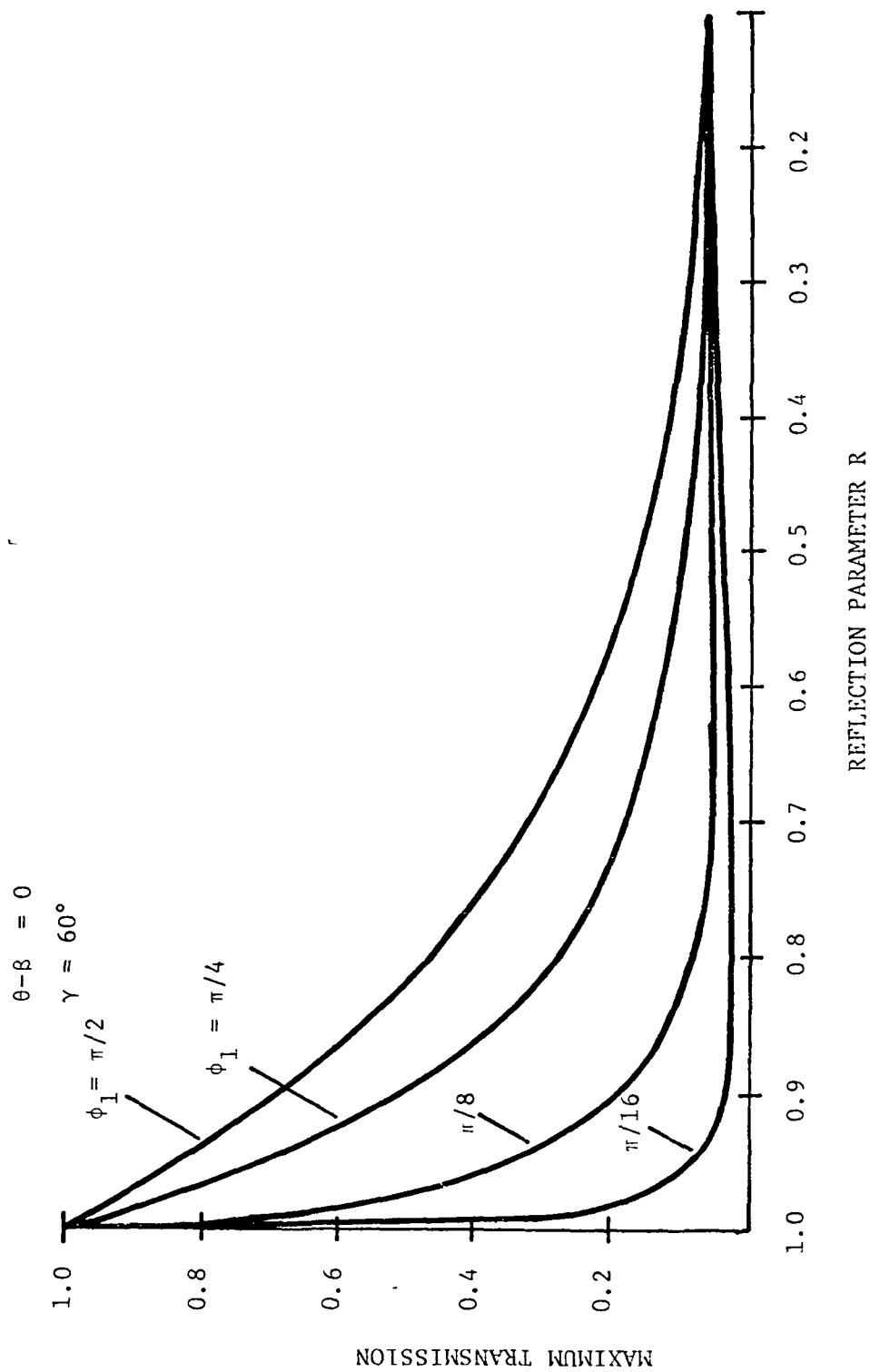
Figure 8. Maximum interferometer transmission as a function of reflection and phase shift.
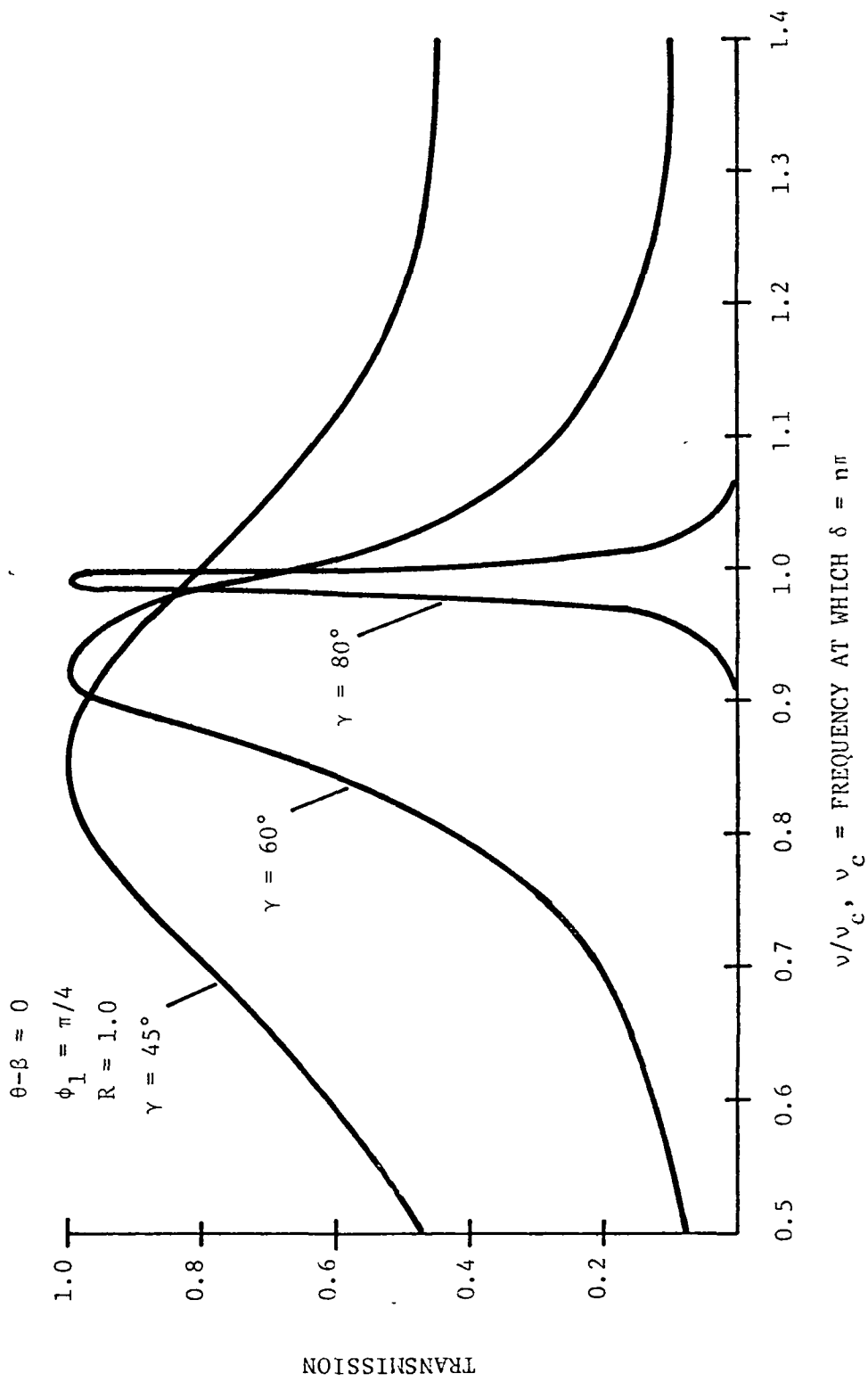
Figure 9. Interferometer bandpass as a function of deviation from center frequency, with grid angle as a parameter, for ideal reflectors.
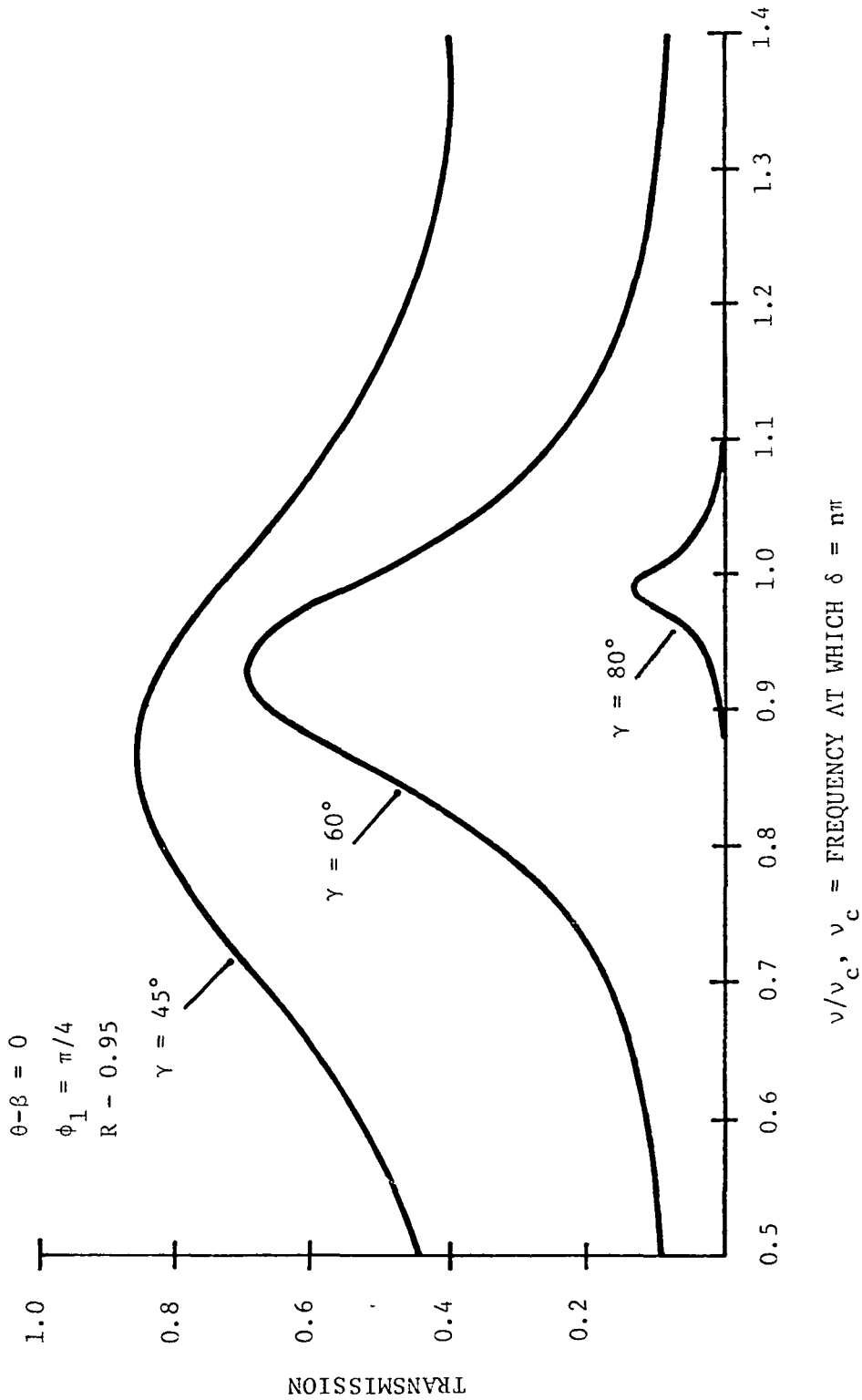
Figure 10. Interferometer bandpass as a function of deviation from center frequency, with grid angle as a parameter, for R = 0.95.
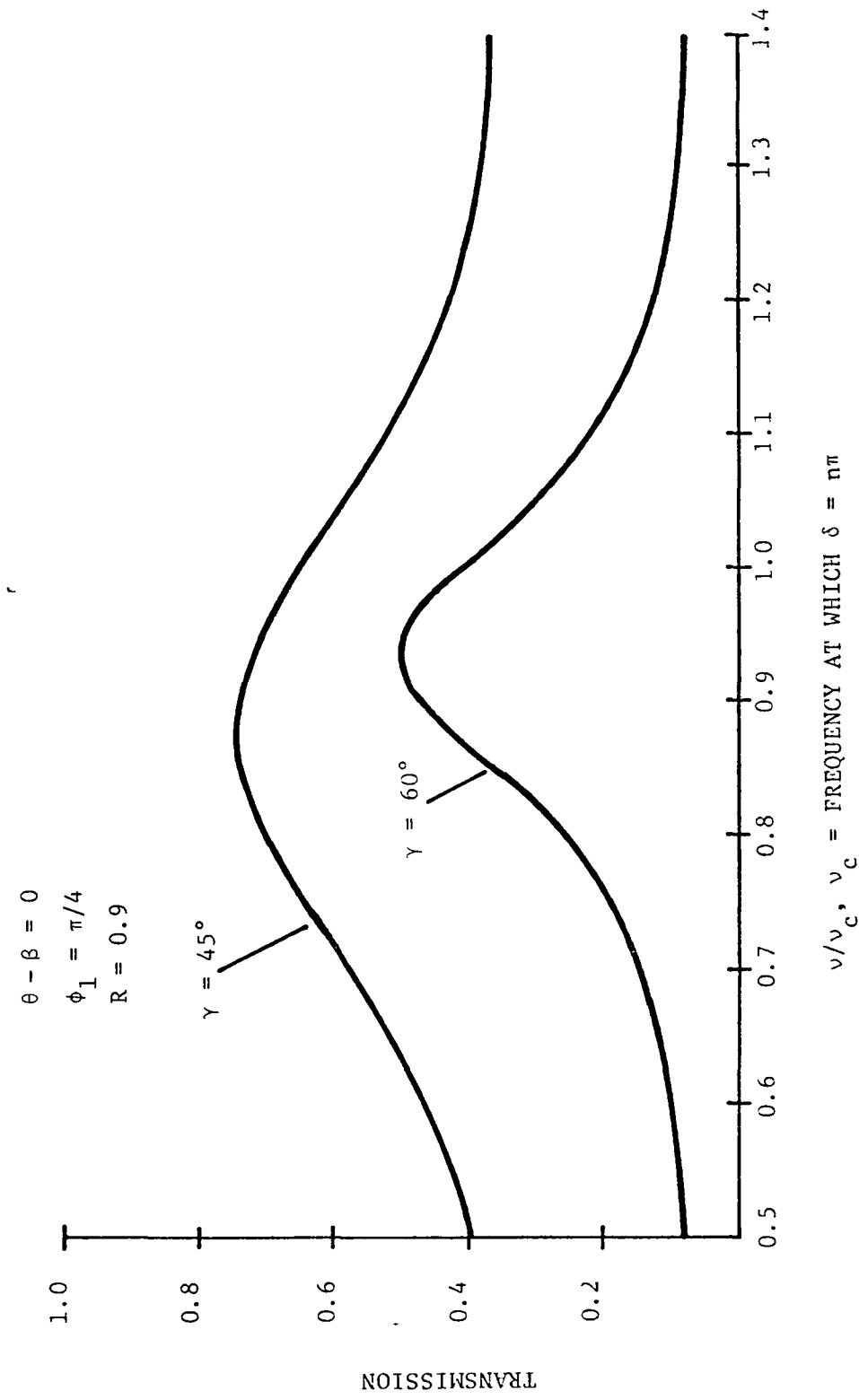
37

Figure 11. Interferometer bandpass as a function of deviation from center frequency, with grid angle as a parameter, for R = 0.9.

ν/ν_c, ν_c = FREQUENCY AT WHICH $\delta = n\pi$

$\theta - \beta = 0$

$\phi_1 = \pi/4$

R = 0.9

$\gamma = 45°$

$\gamma = 60°$

TRANSMISSION

38

also being fabricated and should be finished in 2-3 weeks. If time allows, the grid filter analysis described in this report will be extended to include the effects of totally arbitrary grid angles, with the hope that this configuration will allow polarization rotation for a transmitted signal.

RESEARCH IN MILLIMETER WAVE TECHNIQUES

Thirty-Third Monthly Progress Report

Report Period

15 February to 15 March 1977

NASA Grant No. NSG-5012

GT/EES Project No. A-1642

Project Director: R. W. McMillan
Project Monitor: J. L. King

Engineering Experiment Station
Electromagnetics Laboratory
Georgia Institute of Technology
Atlanta, Georgia 30332

-

SUMMARY OF WORK

1.0 Mixers

The Model A subharmonic mixer has been received from the machine shop and testing of this device has begun. Both of the stripline filters have been installed and the mixer diodes are being mounted. The Model B mixer is also available for test but will not be evaluated until work on the Model A is completed or reaches a logical milestone such that the two mixers can be compared. Artwork for the Model A stripline filters is also complete and a copy is being mailed to Jerry Lamb of GSFC for his use in making these filters for the final version of this mixer.

A 1-2 GHz local oscillator together with its power supply has been received for the mixer test facility. Only the 1-18 GHz mixer and its power supply remain to be received for this facility, and delivery of these items is expected in early April. The noise sources were received from NASA/GSFC on March 9.

Some difficulty has been experienced in contacting additional 183 GHz mixer diodes. On several occasions, diodes with good dc characteristics have been made, but examination by the scanning electron microscope (SEM) has revealed that the whiskers are bent, indicating that mixer performance will be poor. This problem is being studied by Vernon Brady, and a solution is expected during the next monthly reporting period. Dr. Gerry Wrixon, who will be joining us for two weeks beginning March 14, may also be able to help with this problem.

2.0 Radiometric Measurements

Modification to the 183 GHz radiometer to include the quasi-optical filter are complete. Since the 90 GHz klystron has failed, a tube covering the range 80-86 GHz will be used until a replacement can be found. The harmonic mixer used on this radiometer is also in need of repair which will be accomplished when work on the fundamental mixers permits. The new roof lab atop Baker Building on the Georgia

Tech campus is expected to be finished in two weeks, so the radiometer

will be moved to this lab for future measurements.

3.0 Quasi-Optical Calculations

An equation has been derived which gives the resonant transmission of a

series of four wire grids oriented at arbitrary angles and separated by arbitrary

phase shifts, with the exception that the equation cannot be written in closed

form unless the angles of the two interior grids are equal. Tentatively, this

equation shows that input polarization can be changed to any desired directon at

the output by proper choice of phase shifts and grid angles. Such a device would

be very useful because it is both polarization-twisting and bandpass-tunable over

a large part of the millimeter and submillimeter frequency domains. An equation

for reflection is being derived and should be completed during the next reporting

period. A detailed synopsis of the grid calculations made during this program

will be written when time permits. If calculated and measured values of grid inter-

ferometer transmission and reflection show good agreement, this synopsis will form

the basis for a technical paper on this subject.

4.0 Quasi-Optical Measurements

Measurements of transmission and reflection are being made on the wire grids

furnished by Jerry Lamb of GSFC. Figure 1 is a block diagram of the apparatus

used for these measurements. It was found necessary to place an aperture made

of a piece of microwave absorber between the transmitter horn and the grid to

ensure that the rays incident on the grid are normal to its surface. Inconsistent

measurement results were obtained until this step was taken.

A total of ten measurements of each parameter are made for each grid. The

means and standard deviations of these measurements are then determined.
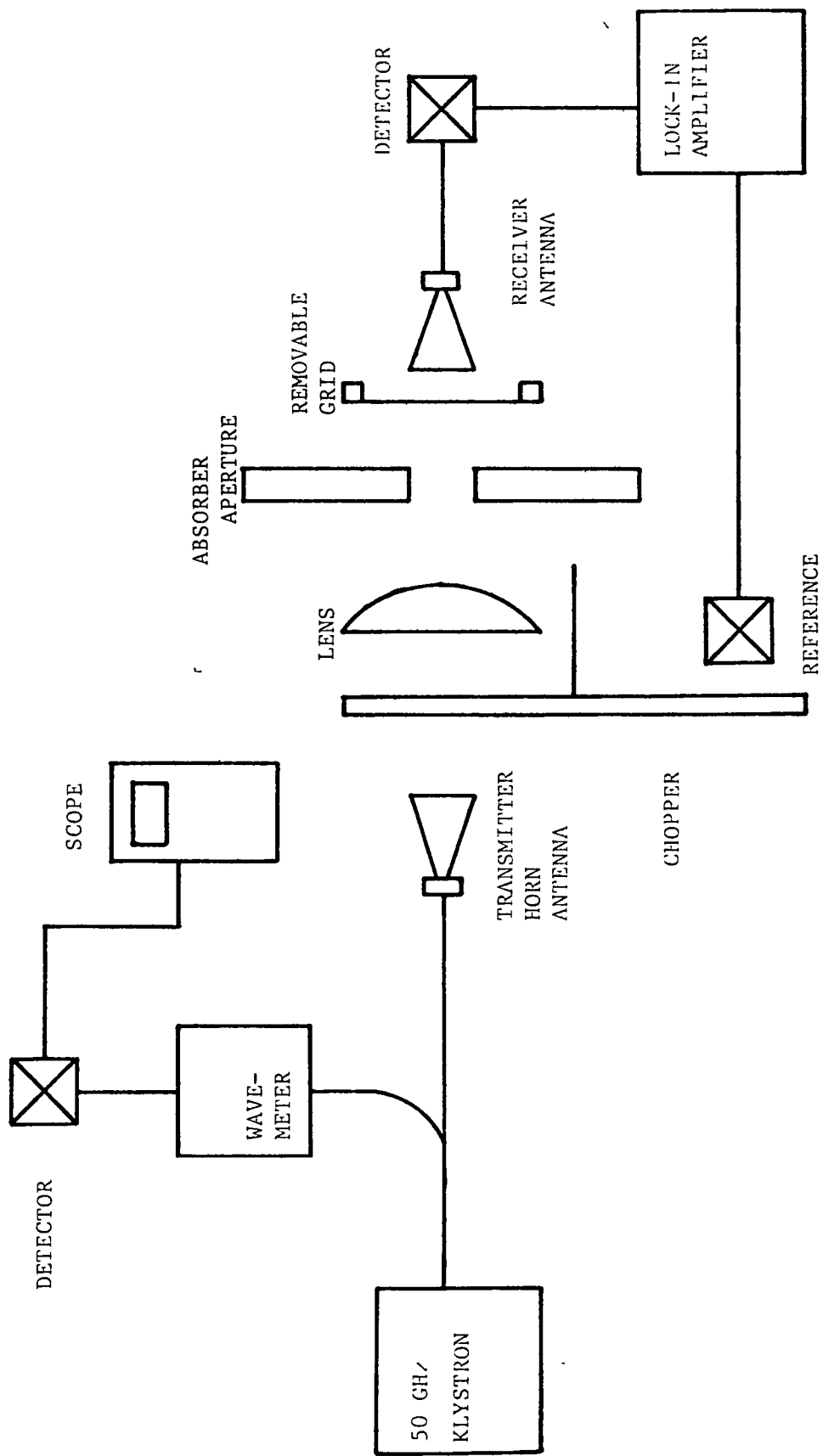
FIGURE 1. Block diagram of apparatus for measuring grid transmission. Signal levels with and without the grid in place are compared to obtain transmission.

These steps are necessary because the equations derived for interferometer transmission given in the last progress report are critically dependent on the losses in individual grids. Table I gives the results of these measurements for transmission of the six grids furnished by Jerry Lamb. Reflection measurements are currently being made.

TABLE I. Transmissivity measurements for wire grids for polarizations perpendicular and parallel to the grid conductors.

	TRANSMISSIVITY			
	Polarization Perpendicular to Wire		Polarization Parallel to Wire	
Grid Number	Mean	Standard Deviation	Mean	Standard Deviation
QO-4	97.44%	1.856%	.5840%	.0568%
QO-5	98.21	0.890	.9935	.0464
QO-6	97.80	1.937	.9234	.0640
QO-7	97.67	1.350	.3706	.0342
QO-8	98.03	1.080	.8458	.0530
QO-9	97.40	1.851	.2250	.0304

5.0 Plans for Next Period

During the next report period it is expected that testing of the Model A subharmonic mixer will be essentially complete and that testing of the Model B mixer will begin. The stripline quartz for the 183 GHz versions of the mixers will also be available early in April, and scale drawings for the machining of these devices will be started.

Radiometric measurements in the range 160-172 GHz will begin from
the new roof laboratory. The calculations of grid interferometer transmission
and reflection, including losses, will be essentially finished and characteriz-
ation of the wire grids furnished by Jerry Lamb will be completed. If time
permits, a preliminary design of a polarization-twisting, bandpass-tunable
Fabry-Perot interferometer will be made.

RESEARCH IN MILLIMETER WAVE TECHNIQUES

Thirty-Fourth Monthly Progress Report

Report Period

15 March to 15 April 1977

NASA GRANT No. NSG-5012

GT/EES Project No. A-1642

Project Director: R. W. McMillan

Project Monitor: J. L. King

Engineering Experiment Station
Electromagnetics Laboratory
Georgia Institute of Technology
Atlanta, Georgia   30332

SUMMARY, OF WORK

1.0 Mixers

The Model A subharmonic mixer is being tested. Initially, difficulty was experienced in maintaining a stress-free mounting of the fragile beam lead Aertech diodes, and as a result, several of these diodes were destroyed. Better methods of mounting these devices are being investigated and additional spare diodes have been ordered.

A preliminary report describing the stripline filter work done to date as part of the Model A mixer development is included as an appendix to this report. This report presents detailed results for the design of the suspended substrate stripline filter for $\omega_s/2$ LO pumping.

At the time that the Model A mixer was designed and built, provision was also made for pumping this mixer with a local oscillator frequency of $\omega_s/4$ in addition to the basic $\omega_s/2$ frequency, where ω_s is the signal frequency. A low pass stripline filter has been designed and built for this application which has attenuation of 0.1 dB at 1.7 GHz and greater than 50 dB at 6.8 GHz. This filter is designed to pass the local oscillator frequency and reject the signal frequency to prevent loss of signal through the LO input. Filter art work for the actual size Model A filters will be sent to Jerry Lamb of GSFC when the Model A mixer assembly details are finalized.

With regard to the problem of contacting additional 183 GHz fundamental mixer diodes encountered during the last reporting period, Dr. Gerry Wrixon suggested that our contacting whiskers are too long and narrow, so that they are easily bent on contact. He suggests that the whiskers be made with sharper taper to avoid this problem. This approach will be tried on the current subharmonic and radiometer mixers.

2.0 Radiometric Measurements

All of the usable contact points on the previously used Schottky barrier diode chip for the 183 GHz radiometer have been used, so that it has been necessary to replace this chip. A diode has been contacted on the replacement chip and noise figure measurements are currently being made. The new roof lab atop the Baker Building is complete, and the radiometer will be moved to this lab when noise figure measurements are finished. It is also expected that meteorological data from the instrumented tower will be available for correlation with radiometric data when the radiometer is put into operation.

3.0 Quasi-Optical Calculations

An expression for reflected amplitude for a four-grid interferometer has been derived. This expression is valid for arbitrary grid angles and phase shifts, with the exception that the equation cannot be written in closed form unless the angles of the two interior grids are equal, a limitation which does not affect the usefulness of the device. Equations for power transmission and reflection must now be derived. This task has been completed for some special transmission cases as described in the Thirty-Second MPR.

4.0 Quasi-Optical Measurements

Reflectivity measurements have been completed on the six grids furnished by Jerry Lamb. The results of these measurements, which were made at 50 GHz, are summarized in Table I. Note that some of the measurements show reflectivities greater than 1, which is an indication of the errors inherent in this type measurement. These results also indicate that the grids are virtually lossless at this frequency, and that it should be possible to construct very high Q filters using them.

Grids 4, 5, 7 and 9 were used to build a four-grid filter, as described in the Thrity-Second MPR, and characterization of this device at 50 GHz is being accomplished. Resonant peaks and valleys of transmission have been observed, and the polarization-twisting capability has been verified. If the capabilities of these devices, as indicated by the transmission and reflection equations, can be realized, they will be very useful as polarization-twisting, bandpass-tunable filters.

TABLE I

Reflectivities of Wire Grids at 50 GHz

Grid	Mean Reflectivity (10 Measurements)	Standard Deviation
Q0-4	0.995	0.024
Q0-5	0.995	0.034
Q0-6	1.011	0.032
Q0-7	1.004	0.031
Q0-8	1.031, 1.039	0.024, 0.024
Q0-9	0.995	0.024

5.0 Plans for Next Period

An improved diode mounting technique for the Model A mixer will be devised, so that testing of this device can be completed. Noise figure characterization of the 183 GHz radiometer mixer diode will be completed and measurements with this device will begin from the new roof laboratory. Characterization of the four-grid interferometer for various grid angles will continue.

APPENDIX

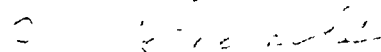Preliminary Test Report

SUSPENDED SUBSTRATE
STRIPLINE FILTERS
FOR MIXER APPLICATIONS

Part I Individual Scale Model Filter Data

March 1977

Prepared By

Ron Forsythe

Reviewed by:

James M. Schuchardt

ABSTRACT

Suspended substrate stripline filters were designed, fabricated, and tested. These filters will be used in a scale-model version of a subharmonically pumped mixer to couple local oscillator power into the mixer and the intermediate frequency out of the mixer. The scaling is by 26.9:1 down in frequency from 183.3 GHz (up in size). The filters were built on a 0.084" thick quartz substrate using copper tape (3-M #1181). A computer program [1] was utilized to establish design curves for the evaluation of the impedances and phase velocities as functions of strip width for the suspended substrate configuration.

In this report, the RF test results of these filters are compared to the theoretical frequency responses of the filters.

INTRODUCTION

A subharmonically pumped mixer utilizing an antiparallel diode pair is desired at 183.3 GHz using a 91.65 GHz local oscillator (LO).

The Model A mixer configuration* is shown in Figure 1. This design requires two low pass filters. The LO filter connects the LO and signal waveguides. Its function is to inject the LO power into the diodes for mixing; it must pass 91.65 GHz with low loss. This filter must also reject 183 GHz to prevent loss of the signal through leakage. The 3 dB cutoff frequency of the LO filter should then be about 108 GHz. The IF filter must pass all frequencies less than 10 GHz with low loss but reject 91.65 GHz by about 30 dB. The cutoff frequency for the IF filter is placed at 48 GHz. Table I shows the filter design parameters for a scaling factor of 26.9. This scaling factor is chosen for testing the mixer because of the availability of standard waveguides and frequency sources.

The suspended substrate configuration is used because it has low loss characteristics. Suspended substrate stripline circuits have been built and operated in the 30 to 100 GHz range by Schneider [2,6]. These circuits have shown good results for mixer applications in these frequency ranges. This configuration reduces the amount of dielectric in the channel and consequently decreases the effect of the dielectric loss tangent on the total dielectric attenuation of the circuit. Quartz substrate is used because of its low loss tangent ($tan\delta \sim 0.0001$) and because it may be made as thin as 0.002" [3], as would be required when scaling these filters up in frequency. An analysis of the losses of these filters is given in the section on losses.

---

*Model A is nomenclature utilized by G. T. Wrixon for this particular mixer design utilizing low pass filters in both the LO and IF paths. Model B (not discussed here) utilizes a band pass filter in the LO path.

IF Output

IF Filter

LO Waveguide

Waveguide-to-
Stripline
Transition

LO Filter (91.65 GHz)

Anti-Parallel
Mixer Diodes

Signal Waveguide
(183.3 GHz)
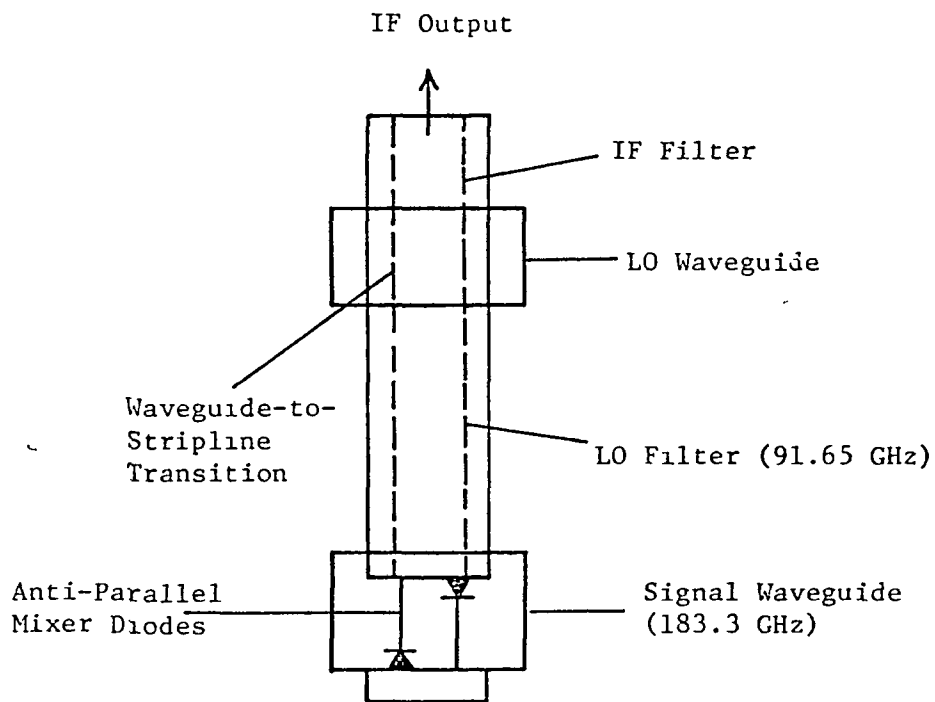
Figure 1.   Model A Mixer Cross Section Schematic
Showing Filters Under Discussion.

TABLE I

FILTER PARAMETERS AND DATA

filter	scaled f_{cs}	actual f_c	Design curves $IL_{Sig.}$	IL_{LO}	Filter Prototype
IF	1.8 GHz	48 GHz	0 dB	39 dB	Butterworth
LO	4.0 GHz	108 GHz	46 dB	0.1 dB	0.1 dB Chebyschev
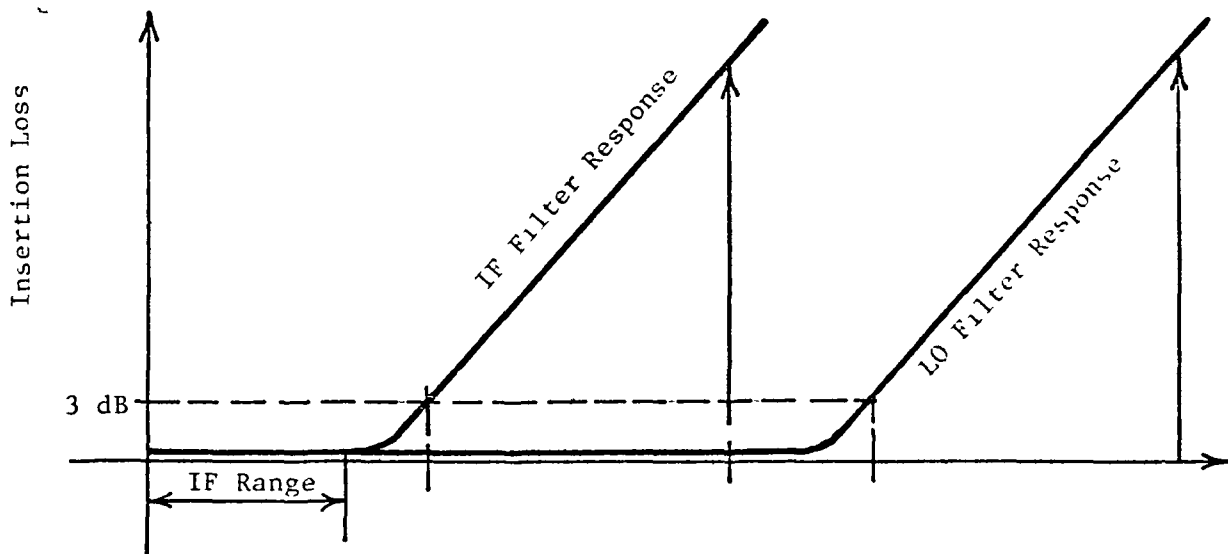
Actual Frequency	10	48	91.65	108	183.3
Scale Model Frequency	(0.37)	(1.8)	(3.4)	(4.0)	(6.8)
			(LO)		(Signal)

Frequency (GHz)

SUSPENDED STRIPLINE DESIGN DATA

Computer generated impedance and phase velocity data are shown in Figure 2. Shown are characteristic impedance Z_o and phase velocity as a function of normalized strip width. The actual wall configuration used in the experimental work shown in Figure 3 has a notch structure to support the quartz substrate. To account for this in the selection of various strip widths, two calculations were run: first for a = 0.672" (the nominal structure width) and then for a = 0.77" (an average width in the vicinity of the quartz support notch). This average width was used to account for electric field fringing in the notch.

As can be seen, the effect of small variations in structure width on the impedance-stripwidth relationship is small; only significant when w/b is around 1.5. When wide strip widths (low Z_o) were required in the design described below, an average value from these two curves was selected.

LO Filter

The LO filter cutoff frequency (-3 dB response) is desired to be 4.0 GHz. Previous experience has shown that about a 10% error exists between the experimental and theoretical cutoff frequencies with the measured value being less than the theoretical value. Therefore, a cutoff frequency of 4.5 GHz was used in the calculations with an anticipated measured cutoff frequency of 4.0 GHz.

A high-impedance/low-impedance filter design is used. [See Reference 4]. A sketch of a generalized filter is shown in Figure 4

Let Z_{high} = 125 ohms,

and Z_{low} = 18 ohms.

Then w_{high} = 0.08", (v/c = 0.9)

w_{low} = 0.64", (v/c = 0.88) .

Using a Chebyschev design with n = 7 and 0.1 dB ripple, the line widths are determined to be

$$\ell_1 = \ell_7 = 0.14",$$
$$\ell_2 = \ell_6 = 0.18",$$
$$\ell_3 = \ell_5 = 0.243",$$

and $\ell_4 = 0.195",$

$\varepsilon_r = 3.78$

$b = 0.416"$

$c = 3.10^{10}$ cm/sec

$$\lambda_g = \left(\frac{v}{c}\right) \cdot \frac{c}{f}$$

Phase Velocity (v/c)

0.94
0.92
0.90
0.88

Z_o
(ohms)

200

100

a = 0.77"

a = 0.68"

0   0.5   1.0   1.5

$\frac{w}{b}$
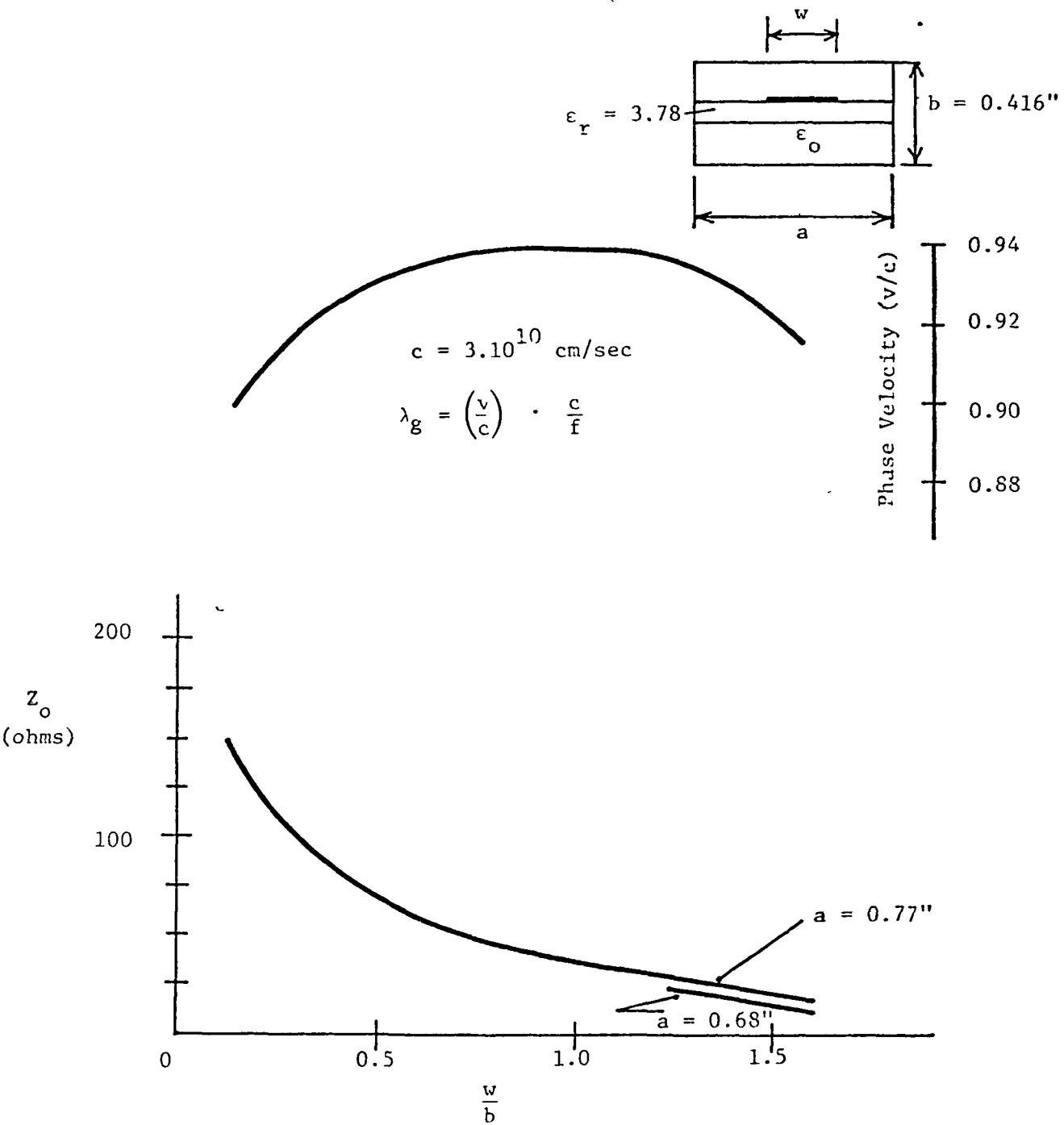
Figure 2.   Suspended Stripline Design Curves – Characteristic
Impedance and Phase Velocity.

56
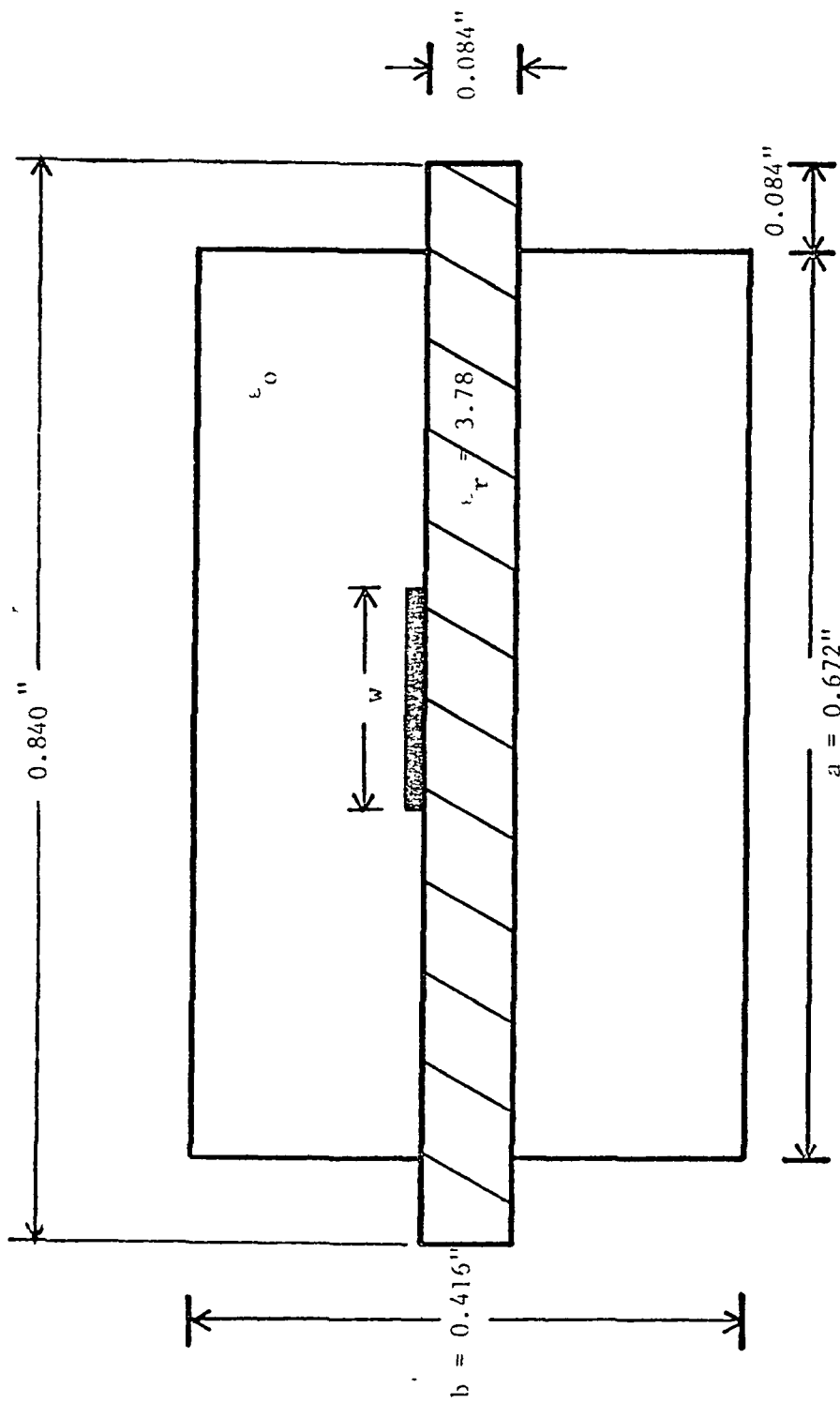
Figure 3.   Suspended Stripline Cross Section. (Dimensions Shown Are 26.9:1 Larger Than Needed For Operation At 183.3 GHz.)

$$\ell_L \ (K) = \left[\frac{v_p}{\omega}\right] \text{arctan} \left[\frac{G(K) \ Z_o}{Z_L}\right]$$

$$\ell_c \ (K) = X_{cc} \ (K) \ Z_o \left[\frac{v_p}{\omega}\right]$$

$$X_{cc} \ (K) = \frac{G(K)}{Z_o} \left[C_\pi(K-1) + C_-(K-1)\right]$$
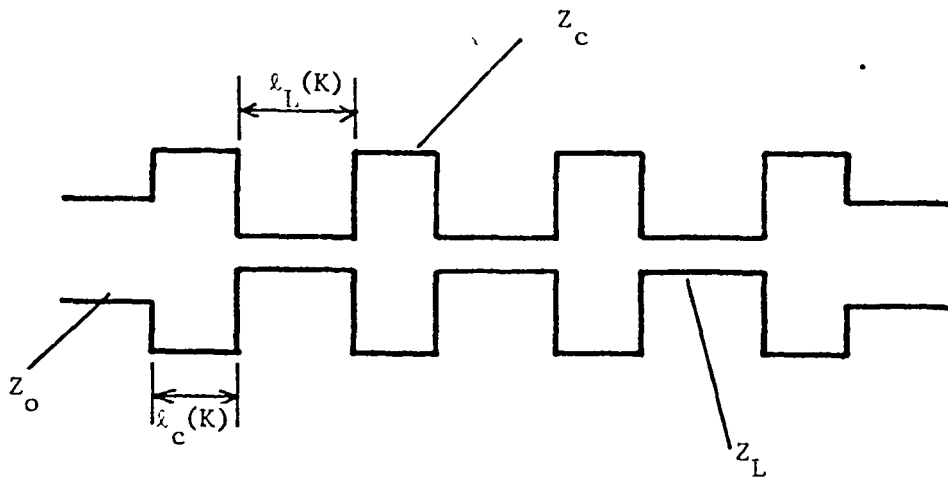
$$C_\pi(K) = \frac{\omega \ell_K}{2v_p \ell_K}$$

v_p = phase velocity

Z_o = characteristic impedance of K-th section

X_{cc} = wanted capacitive susceptance of the low impedance line

ℓ_K = length of K th section

C_π = unwanted capacitive susceptance of the high impedance lines

$G(K)$ = normalized element value from tabulated data [4]

ω = cut off frequency in radians = $2\pi f_c$

Figure 4. Generalized Stripline Low Pass Filter Geometry and Design
    Equations.

58

where ℓ_1, ℓ_3, ℓ_5 and ℓ_7 are low impedance lines and ℓ_2, ℓ_4 and ℓ_6 are high impedance lines. These parameters are shown in Figure 5. A photograph of an LO filter model used for testing is shown in Figure 6.

LO Scaling

The LO filter when scaled up in frequency and down in size would fit in a channel that is 0.0155" long and 0.025" wide. The dimensions of the filter elements would be

$$\ell_1 = \ell_7 = 0.0052",$$
$$\ell_2 = \ell_6 = 0.0067",$$
$$\ell_3 = \ell_5 = 0.009",$$

and $\qquad \ell_4 = 0.00725",$

where ℓ_1, ℓ_3, ℓ_5, and ℓ_7 are 0.0238" wide and ℓ_2, ℓ_4 and ℓ_6 are 0.003" wide.

IF Filter

The IF filter is a low pass Butterworth filter design with seven elements having a scale model 3 dB cutoff frequency at 1.8 GHz. From a high-impedance/low-impedance design, the circuit lengths are

$$\ell_2 = \ell_6 = 0.314",$$

and $\qquad \ell_1 = \ell_7 = 0.134"$

where ℓ_1 and ℓ_2 are low impedance (18 ohms) lines and ℓ_2 and ℓ_6 are high impedance lines with

$$Z_{high} = 175 \text{ ohms},$$
$$w_{high} = 0.054", (v/c = 0.9) .$$

The fourth element was increased in length by decreasing its characteristic impedance to help separate the low impedance sections (ℓ_3 and ℓ_5).

Let $\qquad \ell_4 = 0.62"$

with $\qquad Z_{high} = 125 \text{ ohms},$
$$w_{high} = 0.08", (v/c = 0.9) .$$

The ends of ℓ_3 and ℓ_5 were broadened as shown in the layout of Figure 7. This method gives the required low impedance needed for these lengths in the
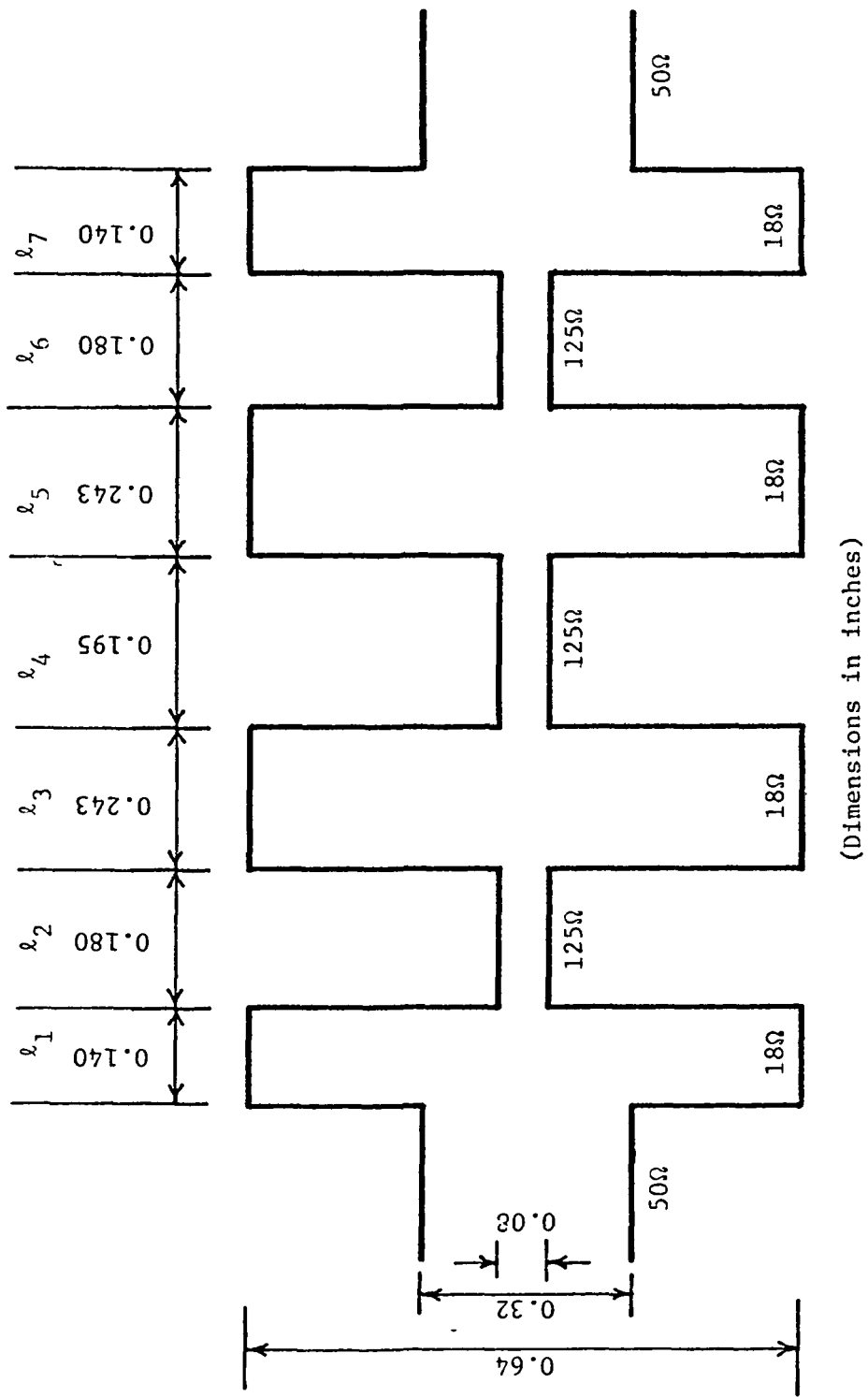
Figure 5. Printed circuit Layout of the Scale Model LO Filter
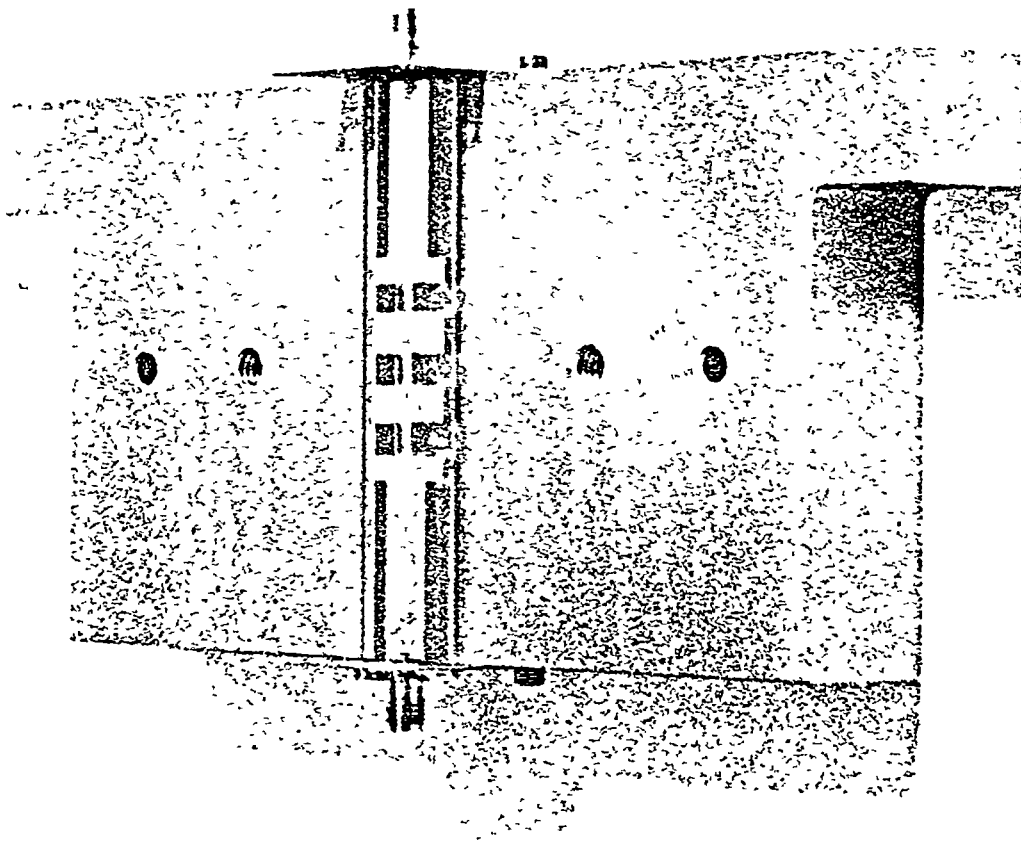
Figure 6. LO Low-Pass Filter Model – Photograph.
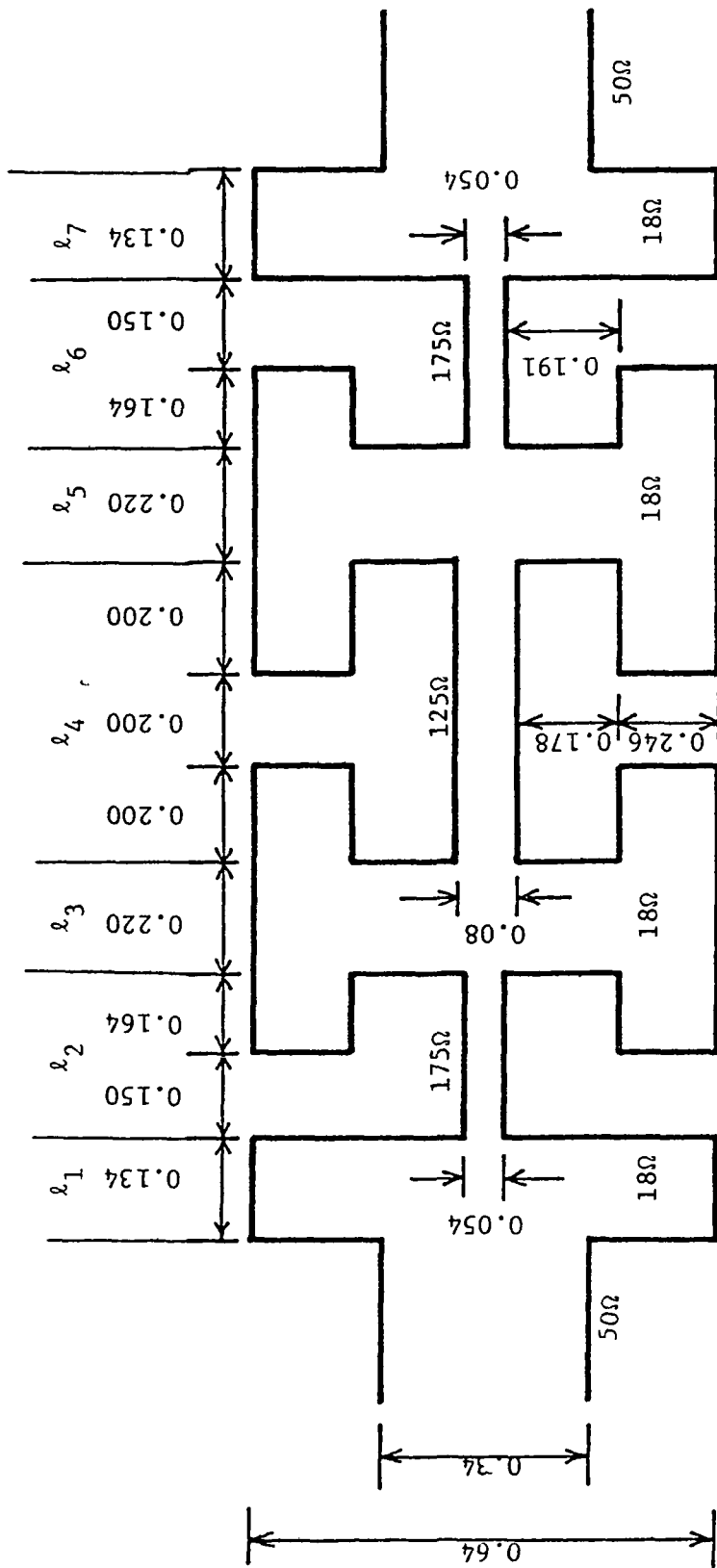
Figure 7. Printed Circuit Layout of the Scale Model IF Filter.

(Dimensions in inches)

size structure desired. The size of the ends is determined by a cut and try method. The excessive size of these elements necessitates the use of a long ℓ_4 to get some separation between ℓ_3 and ℓ_5 and reduce coupling. These steps are taken to reduce overall filter length and to broaden the stop band. Figure 8 is a photograph of an IF filter model used for testing.

IF Scaling

All dimensions shown in the IF filter layout and the broadside view of the stripline configuration will be reduced by 26.9:1 for the final mixer.

Testing Procedure

The filters were tested using an Alfred or an HP network analyzer and an HP sweep oscillator as shown in Figure 9.

COMPARISON AND ANALYSIS OF DATA

The graphs of measured insertion loss of the LO filter are given in Figures 10 and 11. They show about a 10% error in the cutoff frequency. This is acceptable since this error is considered in the design of the LO filter and the measured response is very close to the response desired for the mixer application.

The measured IF filter response data are given in Figures 12 and 13. These data correspond very well to the theoretical values up to about 5 GHz. Variations from the theoretical plot are within experimental error up to this frequency. Above 5 GHz the largest element (ℓ_4) is no longer less than a quarter wavelength which is the basic assumption behind the design of the filter elements.

Any variation from the theoretical response can be attributed to conductor losses and coax-to-stripline conversion. Possible waveguide modes propagating above 4 GHz may have been responsible for the large error in the response of the LO filter.

All measured filter losses are summarized in Table II.
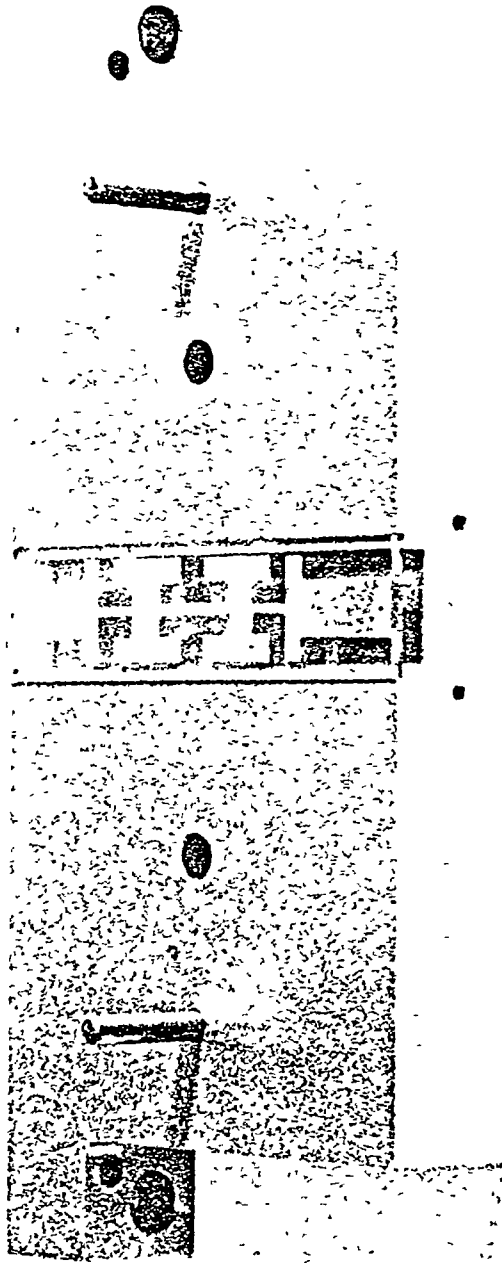
Figure 8. IF Low-Pass Filter Model – Photograph.
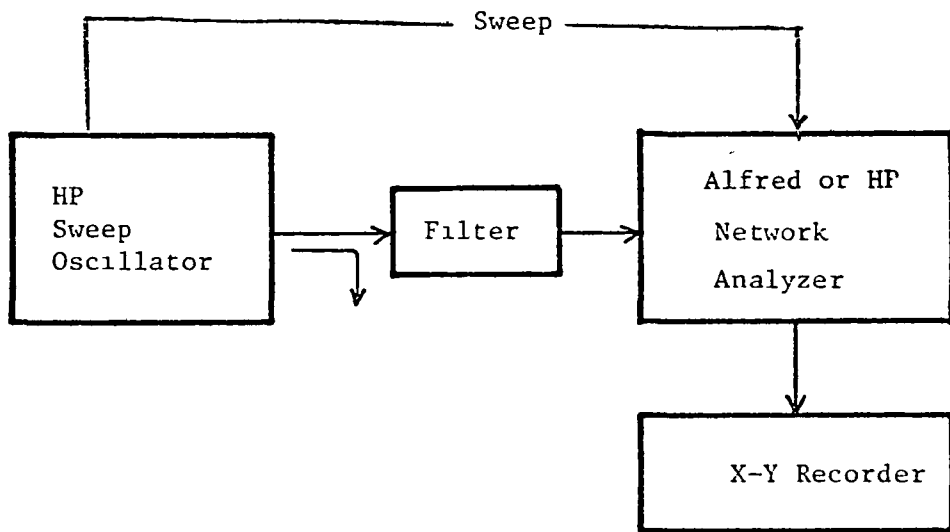
Figure 9.   Scale Model Filter RF Test Setup.
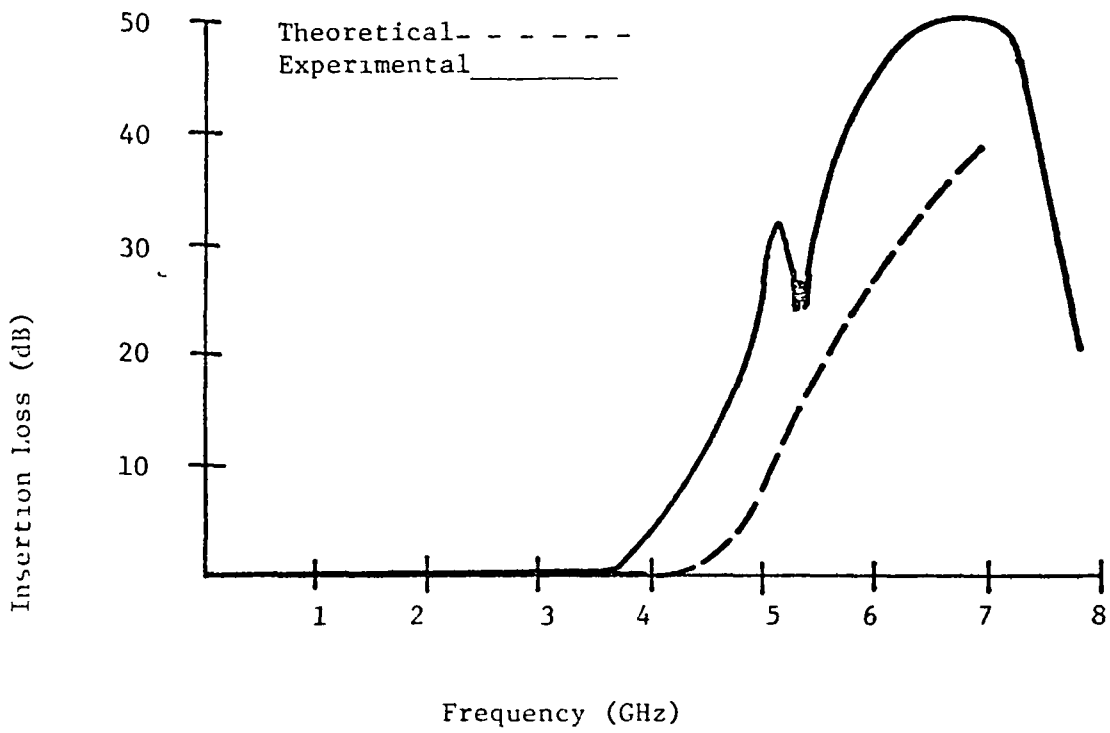
Figure 10. Measured Insertion Loss of the Scale Model LO
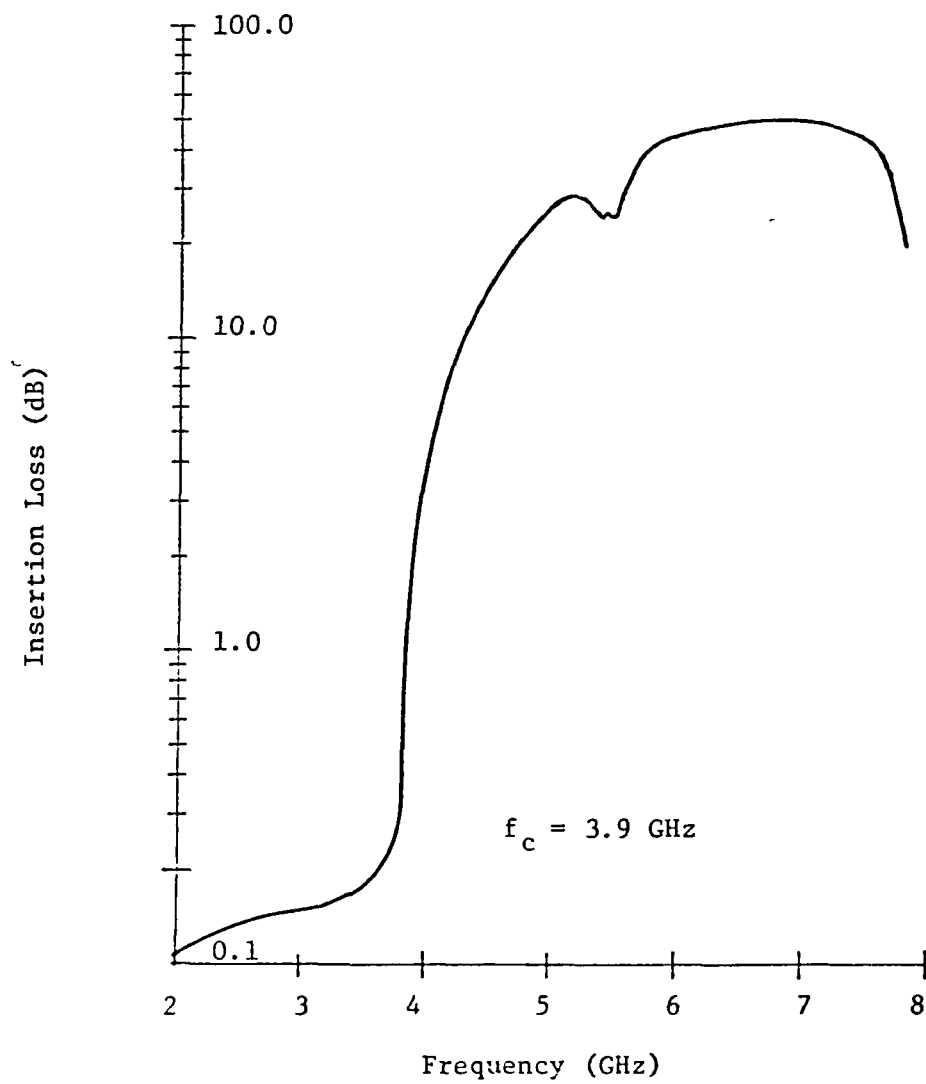Filter (Linear dB Scale)

Figure 11.   Measured Insertion Loss of the Scale Model LO
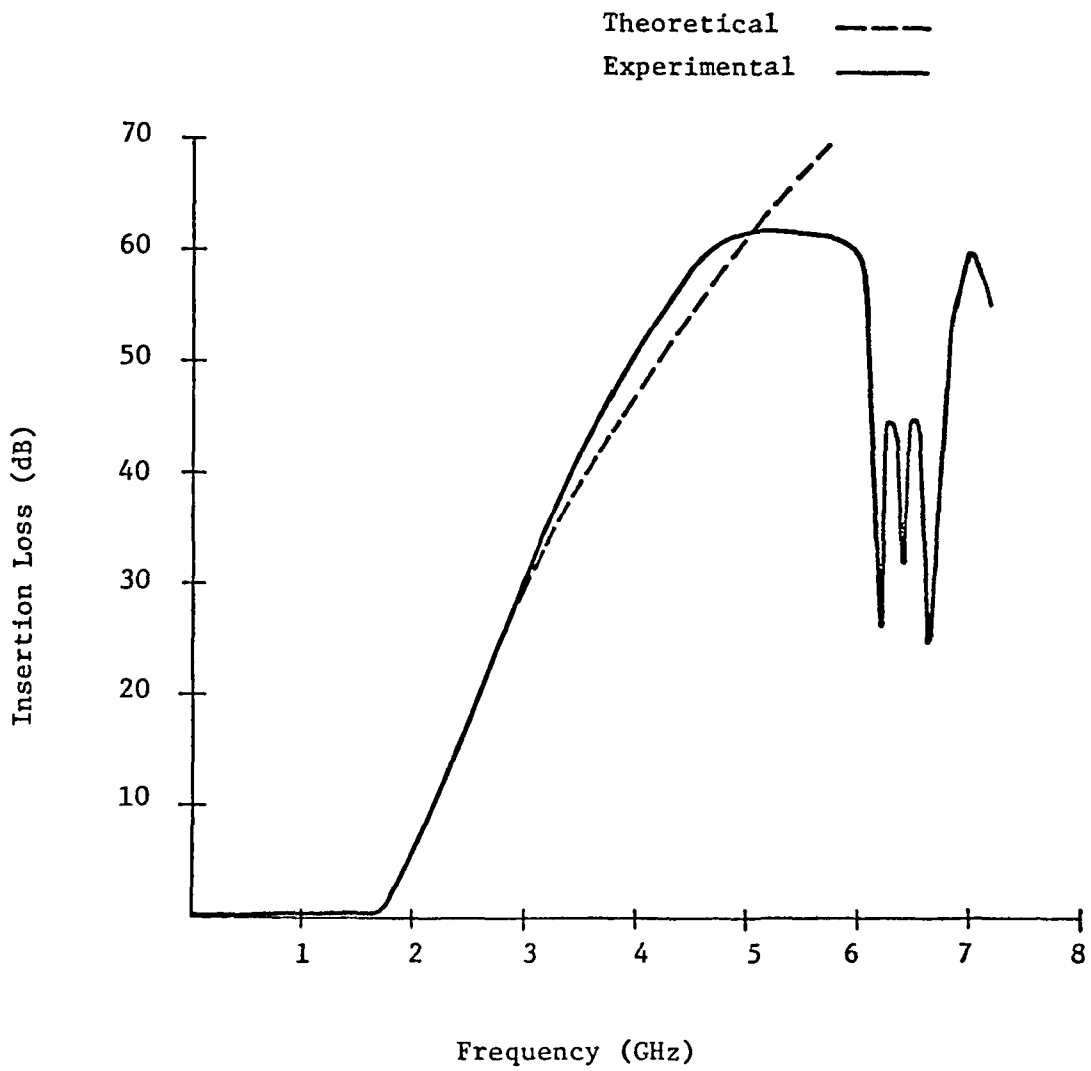Filter (Logarithmic dB Scale)

Figure 12. Measured Insertion Loss of the Scale
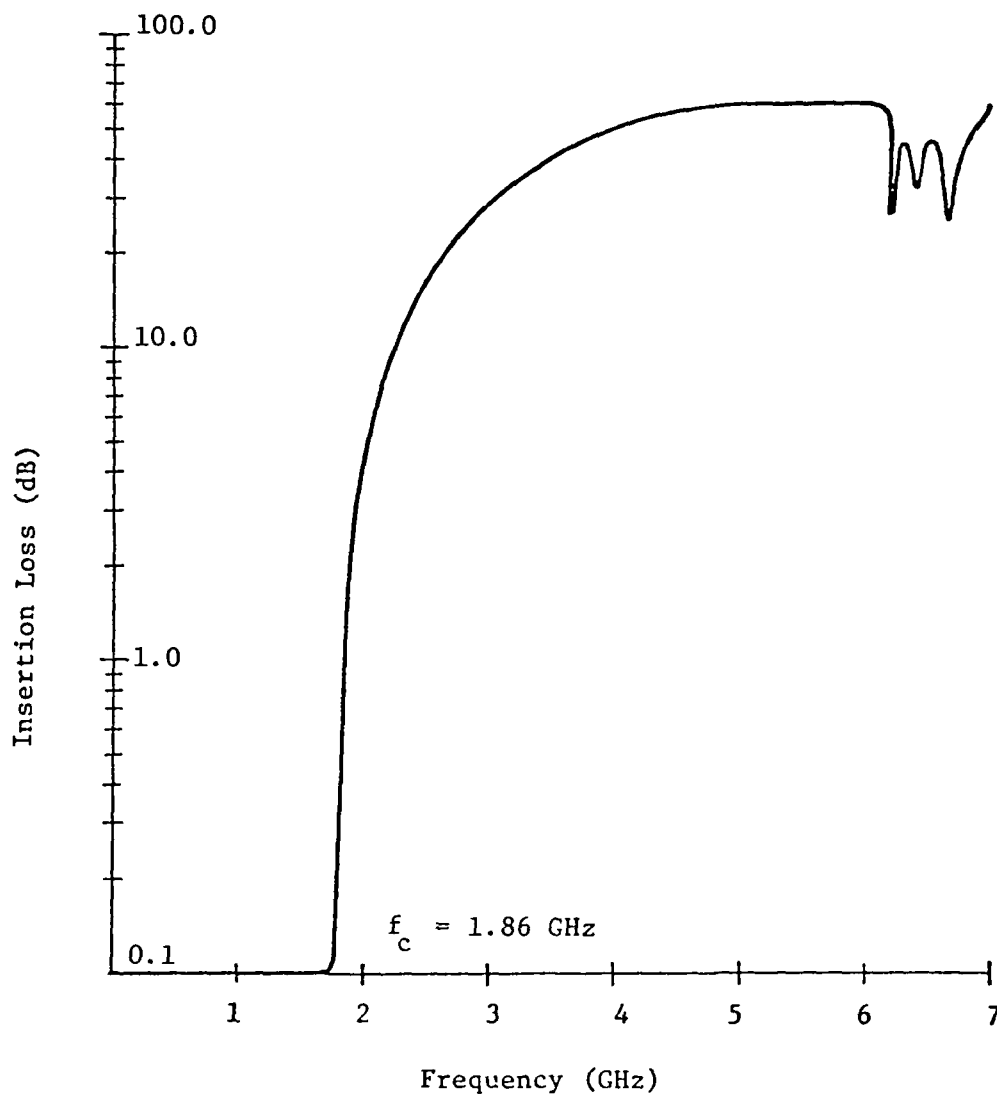Model IF Filter (Linear dB Scale)

Figure 13. Measured Insertion Loss of the Scale Model IF
Filter (Logarithmic dB Scale)

TABLE II

MEASURED SCALE MODEL FILTER LOSSES

FILTER	f_c (des)	f_c (meas)	f = 3.4 GHz	f = 6.8 GHz
IF	1.8 GHz	1.9 GHz	Loss ≃ 40 dB	Loss > 40 dB
LO	4.0 GHz	4.0 GHz	Loss < 0.1 dB	Loss > 40 dB

All dimensions are to be reduced by a factor of 26.9 in scaling up in frequency to 183 GHz. Losses do not scale linearly and are detrimental to the filter. Therefore, some approximate values for the conductor and dielectric losses are determined to get some feel for the amount of losses to be expected.

The dielectric properties for quartz are:

$$\tan \delta = 0.0001 \text{ and } \varepsilon_r = 3.78.$$

The attenuation due to dielectric losses is then [5]

$$\alpha_d \simeq \frac{27.3 \sqrt{\varepsilon_r} \tan \delta}{\lambda} \quad x \quad \frac{\text{Area of Dielectric}}{\text{Area of Channel}}$$

$$\simeq 0.011 \text{ dB/inch} \qquad \text{at } f = 91.65 \text{ GHz.}$$

The conductor losses are dependent on strip width. Using an average relative dielectric constant of 1.5 and copper conductor, the attenuation for a 125 ohm impedance line, α_{c125}, is given by [5].

$$\frac{\alpha_{c125} b}{\sqrt{f_{GHz} \varepsilon_r}} = \text{a constant} \equiv 0.0013 \text{ from Figure 5.04-3 of Reference 5.}$$

Therefore $\quad \alpha_{c125} \simeq \dfrac{\sqrt{1.5 \times 91.5}}{0.0155} \quad x \quad 0.0013$

$$\simeq 0.98 \text{ dB/inch} .$$

For an 18 ohm line the attenuation α_{c18}, is [2]

$$\alpha_{c18} \simeq \frac{\sqrt{f_{GHz}\varepsilon_r}}{0.0155} \; 0.00045 = 0.34 \text{ dB/inch.}$$

The constant 0.00045 is obtained from Reference 5, Figure 5.04-3.

Therefore, most of the attenuation will be due to conductor losses and occurs primarily in the high impedance sections of the filter. While this loss may seem high, the lengths of each element are very short and the total loss due to losses is not great. For instance, the largest inductor in the LO filter is

$$\ell_4 = 0.00725".$$

The attenuation due to this element is then

$$\ell_4 = (\alpha_c + \alpha_d) \; \ell_4$$

$$= (0.98 + 0.011) \; (0.00725) = 0.00718 \text{ dB.}$$

The total attenuation based on the above type calculation at the actual frequencies of operation is thus estimated to be about 0.03 dB for the LO filter.

SUMMARY

Suspended stripline design curves were developed during the implementation and fabrication of test scale model filters for the model A mixer. Data obtained from measurements of filters designed using these curves were in close agreement with the experimental data both in the passband and the reject band.

These filters can now be scaled up in frequency and down in size by dividing all dimensions by 26.9 for use in the final version of the subharmonically pumped mixer. The current filters will be used in the low frequency mixer model now under construction.

In the future, high frequency tests at the actual operating frequency should be made on the stripline circuits. Specifically, the transmission losses at 91.65 GHz through a final LO filter designed to pass this frequency should be measured. This will require using several waveguide to stripline transitions, two waveguides, at both 91.65 and 183 GHz, and a power meter. Insertion loss may be determined by substituting a 50 ohm line in the channel and measuring the relative power transmitted at the two frequencies. This way stripline losses may be taken into account and some determination of the utility of the transition from waveguide to stripline can be made. The complexity of this actual frequency measurement should not be underestimated.

REFERENCES

1) Brenner, H. E., "Use a Computer to Design Suspended Substrate ICs," Microwaves, pp. 38-45, Sept. 1968.

2) Schneider, M. V., "Millimeter Wave Stripline Circuits", Microwave Journal, pp. 51-52, Dec. 1976.

3) Rubin, D. and Saul D., "MM Wave MICs Use Low Value Dielectric Substrates," Microwave Journal, pp. 35-39, Nov. 1976.

4) Howe, H.,Stripline Circuit Design, Aertech House, 1974.

5) Matthai. Young, and Jones, Microwave Filters. Impedance-Matching Networks, and Coupling Structures, New York, McGraw Hill, 1964.

6) Schneider, Glance, and Bodtmann, "Microwave and Millimeter Wave Hybrid Integrated Circuits for Radio Systems", BSTJ, pp. 1703-1726, July-August 1969.

RESEARCH IN MILLIMETER WAVE TECHNIQUES

Thirty-Fifth Monthly Progress Report

Report Period

15 April to 15 May 1977

NASA GRANT NO. NSG-5012

GT/EES Project No. A-1642

Project Director: R.W. McMillan

Project Monitor: J.L. King

Engineering Experiment Station
Electromagnetics Laboratory
Georgia Institute of Technology
Atlanta, Georgia 30332

SUMMARY OF WORK

1.0 MIXERS

Some progress has been made in devising mounting and assembly
techniques for the final versions of the subharmonic mixers. Several
usable dummy glass stripline substrates have been gold plated, scribed
and cut. Dummy diodes have been successfully butt soldered to the ends
of these substrates. This work is being done as practice for devising
the techniques and improving the skills needed for assembling the final
subharmonic mixers. The appendix shows in detail how this assembly will
be accomplished.

In the area of subharmonic mixer modeling, the LO and IF stripline
filters have been changed slightly to improve performance and ease
fabrication requirements. The change involved decreasing the width of the
low impedance sections to give more distance between these sections and
the side walls. An LO filter was made with a cutoff frequency of 2.7 GHz
for the fourth harmonic mixer. This filter will pass the LO of 1.7 GHZ
and block the 2nd and 4th harmonics from leaking out around the diodes.

The filters have to be placed correctly in order to function
properly in the mixer body. The IF filter is to act as a diplexer, and
the LO power reflected from it must add in phase to the power going
directly to the diodes from the waveguide-to-stripline transition.
Measurements were taken of the insertion loss of the combination of the
IF filter and waveguide-to-stripline conversion by placing the IF filter in
the LO stripline channel and measuring the power out of the IF port with
a 50 ohm line connecting the combination to the IF port. Insertion loss
of about 0.1 dB was measured at 3.4 GHz.

Measurements are currently being made to determine proper LO filter
placement. The LO filter is placed in different positions inside the
stripline channel and the conversion loss is measured. The minimum
conversion loss then dictates the optimum LO filter placement. This work
is tedious because of the fragile nature of the beam lead diodes and the
large size of the Model A mixer. The development of better diode mounting

procedures has resulted from this effort. This is discussed in detail in the appendix. Chromium-gold plating and etching techniques were used to accomplish the diode mounting.

The Aertech beam lead diodes used in the mixer have proven to be very fragile and therefore difficult to mount in the mixer. Also, the diodes have an unusually high series resistance of 30 ohms. Nevertheless, the iterations of LO stripline placement have resulted in the measurement of a preliminary double-sideband mixer conversion loss of 8.8 dB, with the possibility of further slight improvement with another iteration. Additional diodes have been ordered from Aertech and other companies which will hopefully have lower series resistance (6-8 ohms), resulting in an improved mixer conversion loss.

Drawings for the scale-down (actual size) subharmonic mixer are complete. Machining of this mixer will begin when an acceptable conversion loss measurement is made on the model. At that time, art work for the scaled down stripline filters will be sent to Jerry Lamb of GSFC.

2.0 RADIOMETRIC MEASUREMENTS

The radiometer has been installed in the new roof lab atop the Baker Building. The harmonic mixer used in this instrument was rebuilt and a conversion loss of 16 dB was measured, which is comparable to the best performance achieved for this mixer. Unfortunately, the roof lab was found to be poorly shielded against radiation from nearby TV Channel 17, and it has not yet been possible to obtain any radiometric data. Shielding material has been placed over the windows of the building and cables are being shortened on the experimental set-up. It may also be necessary to improve circuit bypass techniques and to use a power line filter. These modifications are expected bo be completed during the next reporting period, but in the meantime, the Fabry-Perot interferometer bed used on this radiometer can be used for additional grid filter measurements.

3.0 QUASI-OPTICAL MEASUREMENTS

A four-grid Fabry-Perot interferometer filter has been built using grids furnished by Jerry Lamb of GSFC. During the last reporting period, losses in these grids were measured and they were found to be essentially

77

lossless at 50 GHz, as was reported in the last monthly report. In
an earlier report, the lossless transmission of a four-grid interfero-
meter was given as

$$T = \frac{\cos^2(\Theta-\beta)}{1 + \dfrac{\tan^4\gamma}{4}\left[\dfrac{\sin\delta + \cos^2\gamma\sin(2\phi_1-\delta)}{\sin^2\phi_1}\right]^2} \qquad (1)$$

where:

Θ = angle of first and fourth grids,

β = polarization angle of input,

γ = $\Theta - \alpha$,

α = angle of second and third grids,

ϕ_1 = phase shift between first and second grids and between third and fourth grids,

δ = $2\phi_1 + \phi_3$,

φ_3 = phase shift between second and third grids.

This equation is shown plotted as a function of δ in Figure 1 with
$\Theta - \beta = 0$, $\gamma = \pi/3$ and $\phi_1 = \pi/2$. The transmission of this filter
was also measured and the results are shown as circles superimposed
on the calculated curve. The filter was essentially lossless. The
disagreement between theory and experiment in the skirts of the filter
is probably caused by ϕ_1 being slightly greater than $\pi/2$. It will be
recalled from an earlier report that the bandpass of this filter may be
tuned by changing ϕ_1.

The transmission of this filter was also plotted as a function
of deviation from center frequency. In this case, the theoretical
transmission for $\phi_1 = \pi/2$ becomes

$$T = \frac{\cos^2(\Theta-\beta)}{1 + \dfrac{\tan^4\gamma}{4}\left[\dfrac{\sin(n+1)\pi\frac{\nu}{\nu_0} - \cos^2\gamma\sin(n\pi)\frac{\nu}{\nu_0}}{\sin^2\frac{\pi}{2}\frac{\nu}{\nu_0}}\right]^2} \qquad (2)$$
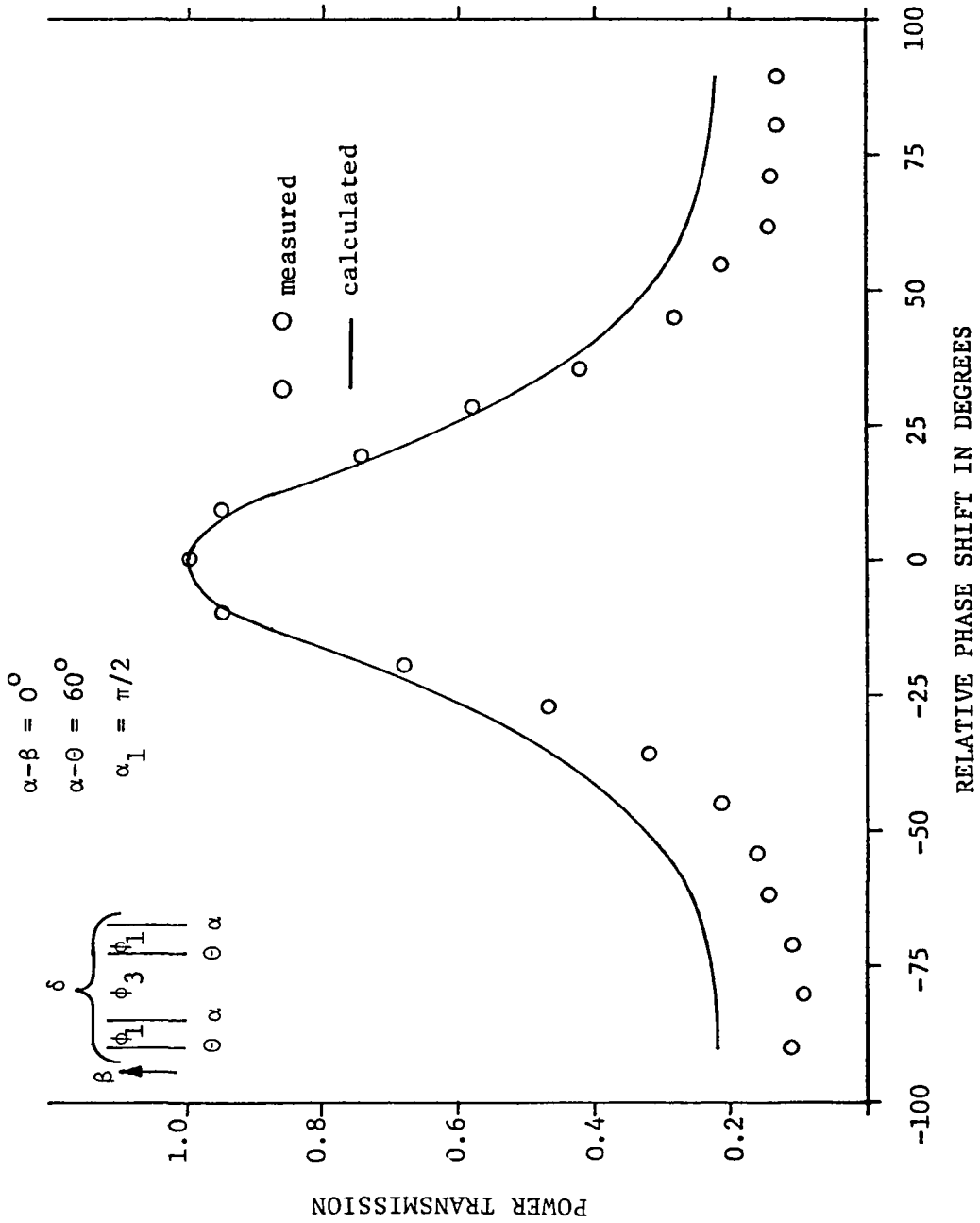
Figure 1 – Grid Interferometer Transmission vs. Phase
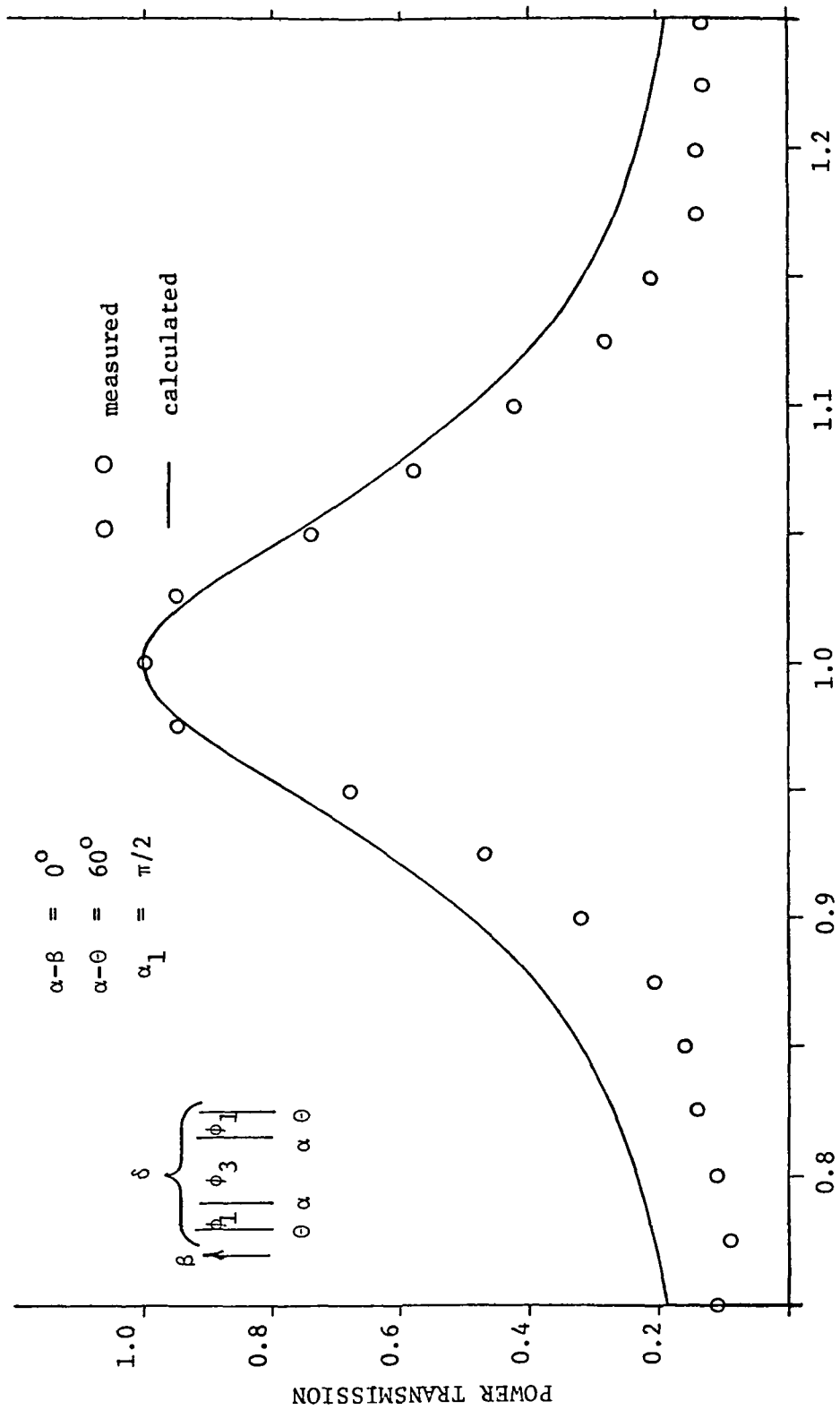
Figure 2 - Grid Interferometer Transmission vs. Frequency

where ν is frequency and ν_0 is center frequency. This expression is plotted in Figure 2 as a function of ν/ν_0 for the same parameters as those of Figure 1. The circles represent measured data inferred from the measurements of transmission as a function of phase.

In Equation (2), it is interesting to note that transmission goes to zero whenever ν/ν_0 is an even integer because $\sin \pi\nu/2\nu_0$ goes to zero, causing the denominator of T to approach infinity. This fact suggests that such a filter would reject all even harmonics of its center frequency, unlike other Fabry-Perot interferometers. This feature might be useful in some filter applications.

4.0 PLANS FOR NEXT PERIOD

During the next reporting period, the new subharmonic mixer diodes should be available so that the conversion loss for this device can be measured under optimum conditions. The radiometer shielding problem should also be solved and some radiometric data obtained. Since the Fabry-Perot interferometer bed from the radiometer is available, quasi-optical measurements will be continued on filters of higher Q.

RESEARCH IN MILLIMETER WAVE TECHNIQUES

Thirty-Sixth Monthly Progress Report

Report Period
15 May to 15 June 1977

NASA GRANT NO. NSG-5012
GT/EES Project No. A-1642

Project Director: R. W. McMillan
Project Monitor: J. L. King

Engineering Experiment Station
Electromagnetics Laboratory
Georgia Institute of Technology
Atlanta, Georgia 30332

1.0 MIXERS

New beam lead Schottky-barrier diodes have been received from
Aertech, for the subharmonic mixer model, which more nearly approxi-
mate those diodes which will be used in the final version of this
mixer. Also, these new diodes are more rugged and therefore easier
to mount without damage. Unfortunately, the first pair used in the
mixer model were rather poorly matched, so that optimum noise figures
were still not obtained, but measurements made on the mixer model
using these diodes are still considered good enough to conclude that
the stripline filter designs are optimized, and to begin fabrication
of the final 183.3 GHz filters based on these designs. Drawings of
these filters are being made to be sent to Jerry Lamb of GSFC for fabri-
cation.

Table I gives the results of a series of measurements of double-
sideband conversion loss made on the subharmonic mixer model using these
improved diodes. In making these measurements, the back short tuners
were optimally matched for an IF of 100 MHz. Column 1 is the RF input
level, and Column 2 is the IF output level at 100 MHz. The difference
between these numbers is the mixer conversion loss. Columns 3, 4, 5 and
6 give IF output levels at several other intermediate frequencies for RF
inputs of -60 and -70 dBm. The local oscillator power for all of these
measurements was held constant at +7 dBm.

TABLE I

SUBHARMONIC MIXER MODEL

CONVERSION LOSS MEASUREMENTS

RF INPUT dBm	IF = 100 MHz	IF = 30 MHz	IF OUTPUT IN dBm IF = 60 MHz	IF = 100 MHz	IF = 300 MHz
0	-8				
-10	-17				
-20	-27				
-30	-37				
-40	-47				
-50	-56				
-60	-66	-68	-66	-65	-67
-70	-76	-77	-76	-75	-77

These measurements show that conversion loss varies from 5 to 8 dB over the decade of IF frequencies between 30 and 300 MHz and over a range of signal inputs from 0 to -70 dBm. It is possible that further improvement can be made when the mixer diodes are replaced with devices that are more nearly matched. Measurements using these better matched diodes are planned for the next reporting period.

The .003 inch x 1 inch quartz disks for the 183.3 GHz stripline circuits have been received. Some of these disks will be sent to Jerry Lamb along with the stripline art work when the art work drawings are complete. Also, machine work on the 183.3 GHz mixer, delayed until the model stripline filters are optimized, has begun and will be completed in about 4 weeks.

2.0 RADIOMETRIC MEASUREMENTS

Since the last reporting period, when it was found that radiation from TV Channel 17 was causing erratic radiometer outputs, the radiometer has been extensively modified. The mixer bias box has been rebuilt,

using a recessed panel meter and carefully shortening leads and by-passing inputs and outputs. A single-point grounding scheme was also used. All of the IF cables were replaced by semi-rigid coaxial cable, and other signal cables were shortened to a length of less than two (2) feet.

As a result of these modifications, and the shielding earlier placed over the windows, the interference problem has been eliminated. No further erratic behavior has been observed as a result of persons moving around the room, and the calibrations are repeatable. However, it has been necessary to re-contact the mixer, which apparently lost contact shortly after these modifications were completed. Additional losses present in the Fabry-Perot interferometer impose more stringent requirements on mixer performance. It is expected that data will be obtained with this radiometer during the next reporting period.

3.0 RADIOMETRIC CALCULATIONS

Measurements made with the airborne 183.3 GHz radiometer during the period 8 March to 5 April, 1977 showed some rather interesting and unexpected results. For example, a difference in radiometric temperature was measured in the Arctic, depending upon whether the NASA Convair 990 aircraft was flying over open water or over ice, indicating that the radiometer can "see" the ground when water vapor density is low.

Because of these observations, a series of calculations of expected antenna temperatures, observed from 20,000 feet, as a function of frequency were made. Subarctic winter water vapor density and temperature distributions, obtained from Air Force Cambridge report AFCRL-71-0279, were used in these calculations. Figure 1 shows the result of calculating antenna temperature under these conditions for earth reflectivities of 0.1 and 0.3, corresponding to ice and water, respectively. These curves indeed show that the earth can be seen in the 5 GHz channel of this radiometer, because the difference in antenna temperature due to ice and water is shown to be about 5 °K in this channel. Figure 2 shows total attenuation between 20,000 feet and ground level, calculated near the 183.3 GHz water vapor absorption line.

EARTH REFLECTIVITY
= 0.10 (ICE)

EARTH REFLECTIVITY
= 0.30 (WATER)

$*\rho_o$ H_2O = 1.2 g/m^3
$*T_o$ = 257.1 °K
LOOKDOWN ANGLE = 45°
PRESSURE = 760 mm
INCLUDES 325.2 GHz H_2O LINE

*DISTRIBUTIONS OF THESE PARAMETERS CORRESPONDING
TO SUBARCTIC WINTER WERE USED

FREQUENCY GHz
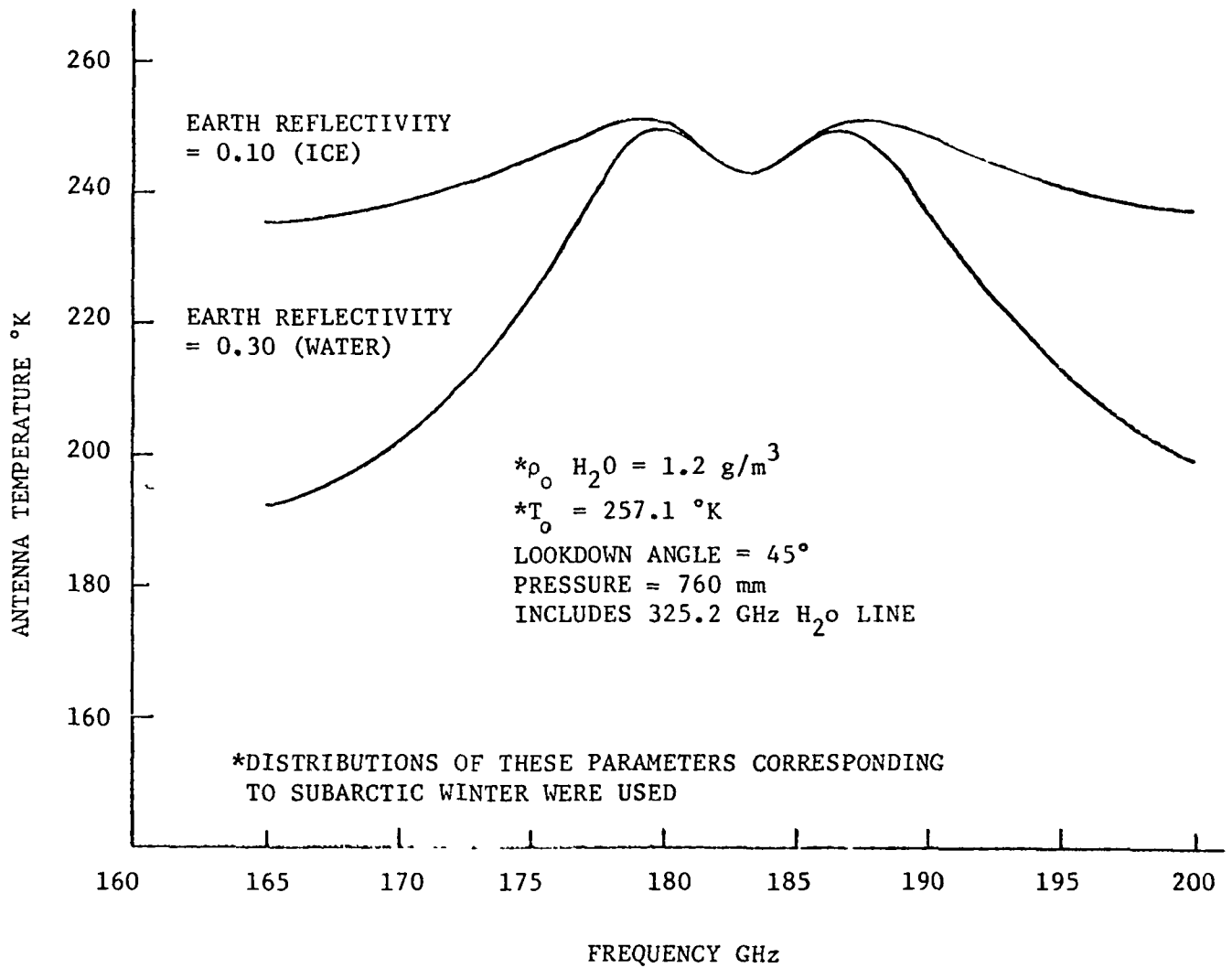
FIGURE 1. ANTENNA TEMPERATURE LOOKING DOWN FROM 6.1 km (20,000 FT.)
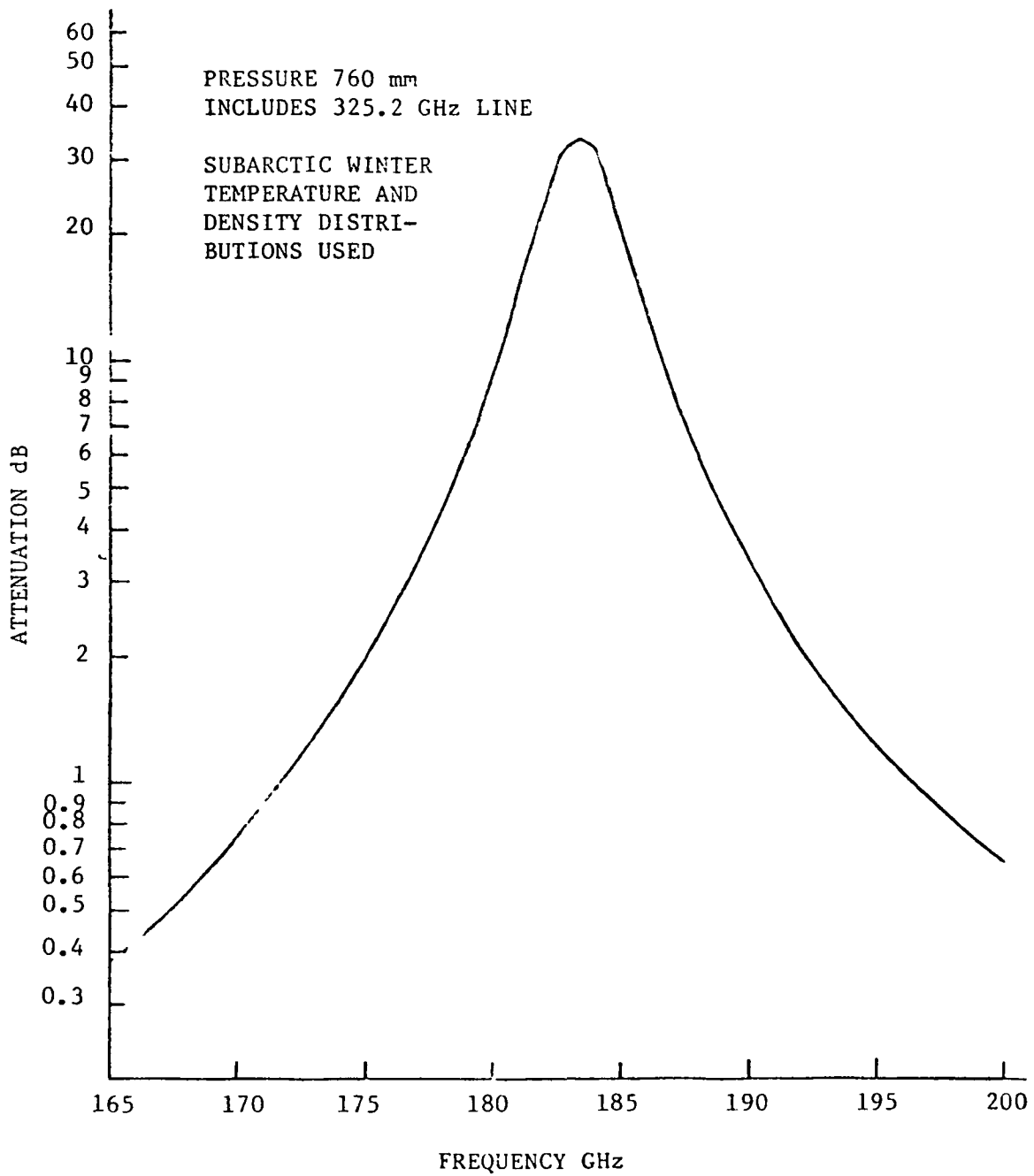
FIGURE 2. TOTAL ATTENUATION TO 6.1 km AT 45° ANGLE

The radiometer was also used several times to look upward. Figure 3 shows the results of calculating antenna temperature looking upward from 11.9 km (20,000 ft.). Two different Zenith angles were used in this calculation. Note in this case that the 5 GHz channel should see the cold sky, which has a temperature of about 3°K, giving an additional check on radiometer calibration. It would be of great interest to make an extensive comparison of calculated results and data measured during this recent series of Convair 990 flights.

4.0 QUASI-OPTICAL MEASUREMENTS

The grids were re-oriented in their mounts to an angle of 80°, which should give a fairly sharp transmission bandpass. Some preliminary measurements were made, but the losses were higher than expected because the interferometer mounts caused the grid substrates to wrinkle slightly due to slight extra pressure on the grid ring. The mounts have been changed to correct this problem, and additional grid interferometer data will be obtained when the interferometer mount can be spared from the radiometer experiments.

5.0 PLANS FOR NEXT PERIOD

During the next reporting period, subharmonic mixer model measurements will be continued with better matched diodes to determine optimum conversion loss for this device. Drawings of art work for the 183.3 GHz stripline circuits will be sent to Jerry Lamb and machining of the 183.3 GHz mixer should be almost complete. Radiometric measurements using the interferometer filter will continue, and grid measurements will resume when the interferometer bed is available.
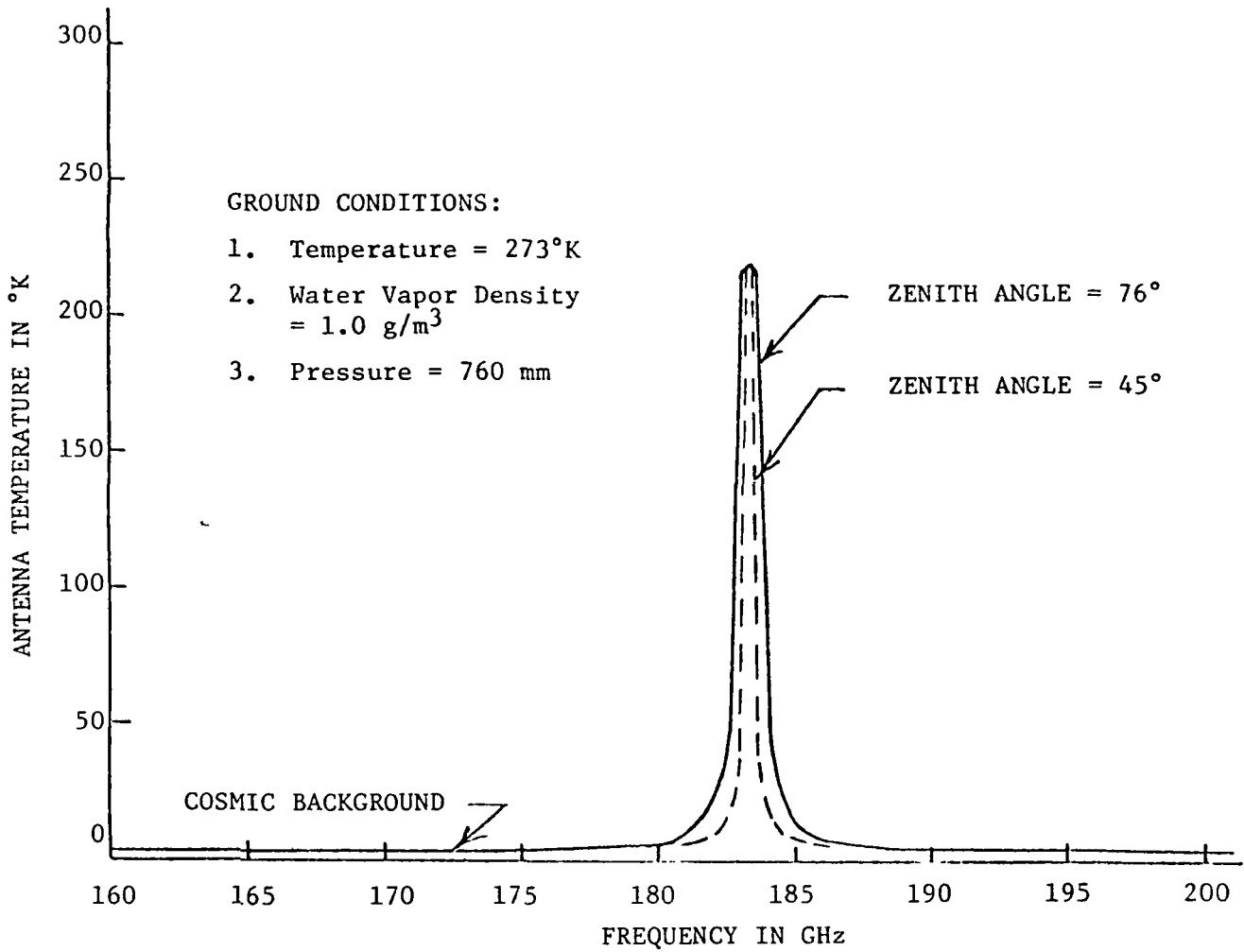
FIGURE 3. CALCULATED ANTENNA TEMPERATURE LOOKING UPWARD FROM 11.9 km

APPENDIX A-2

Preliminary Test Report

SUSPENDED SUBSTRATE
STRIPLINE FILTERS
FOR MIXER APPLICATIONS

Part II

Finalized Scale Model Filter Data
Waveguide to Stripline Conversion

and

Mixer Measurements

June 1977

Prepared by

Ron Forsythe

Reviewed by:

James M. Schuchardt

ABSTRACT

This report presents further progress achieved in the development of
a 183 GHz subharmonically pumped mixer using an antiparallel diode configur-
ation (Model A). It contains finalized individual data on the Model A
filters and some test results on the mixer applications of these filters
which were introduced in Part I.

The types of tests performed include insertion loss measurements of the
IF and the LO model filters, IF filter diplexing properties of the LO input
power with a unique waveguide to stripline transition and some conversion
loss data and noise figure measurements.

LO AND IF FILTERS

The LO and IF filters for the model A subharmonically pumped mixer have been finalized. Plots of insertion loss versus frequency are shown in Figures 14 and 15. Sketches giving the dimensions of the filters are shown in Figures 16 and 17.

These filters represent further refinements on the filters reported on in Part I. Refinements were necessary to ease fabrication tolerances on the stripline channel.

IF FILTER PLACEMENT

The first step in integrating the mixer stripline circuits is determining the placement of the IF filter with the waveguide to stripline transition in place. The mixer geometry is shown in Figure 18. Correct placement of this filter insures that the power reflected by the IF filter adds in phase to the power directed to the diodes. This would maximize the power delivered to the diodes and minimize the required pumping power. The IF filter has been designed to block (reflect) the LO frequency. However, improper placement of this filter may cause the power to add out of phase and the purpose of the filter would be defeated. The waveguide to stripline transition must be in place because additional phase changes will be caused by the shape of the transition.

The filter was placed at different distances from the waveguide wall in the stripline channel where the LO filter would normally go. Different shapes for the transition section were tried at each placement of the filter. The insertion loss was then measured from the LO input to the IF output. The IF output was connected to the transition by a 50 ohm stripline section where the IF filter would normally go. This method was used because of the symmetric properties of the circuit and because of the availability of the IF output port. The best transition was two triangular shaped sections as shown in Figures 19 and 20. The measured insertion loss was 0.4 dB from the input of the LO port to the IF port. Some insertion loss ($\sim$ 0.2 dB) is due to the coax to waveguide adapter. The best response (minimum insertion loss) was found when the IF
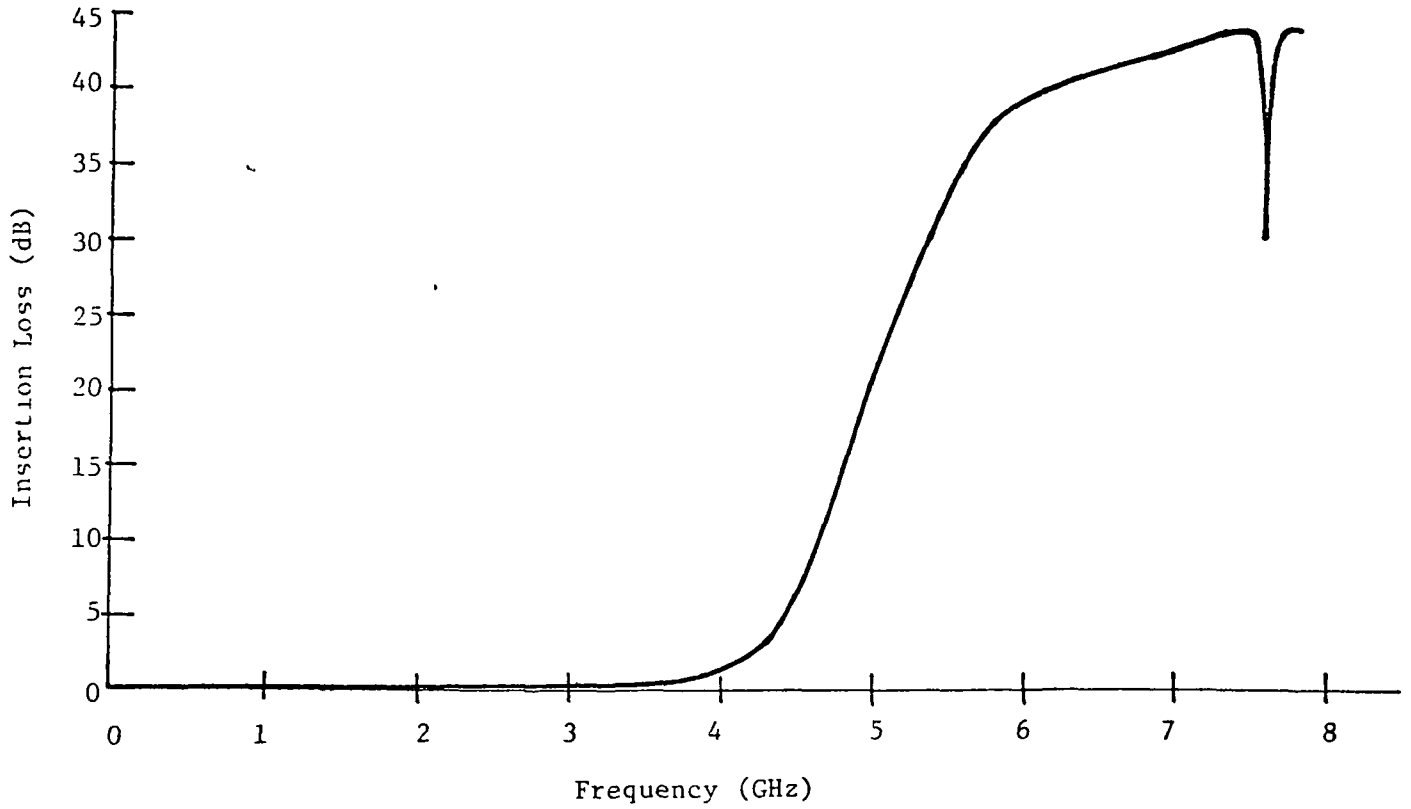
Figure 14. Measured Insertion Loss of the Scaled Model LO Filter (Linear dB Scale)
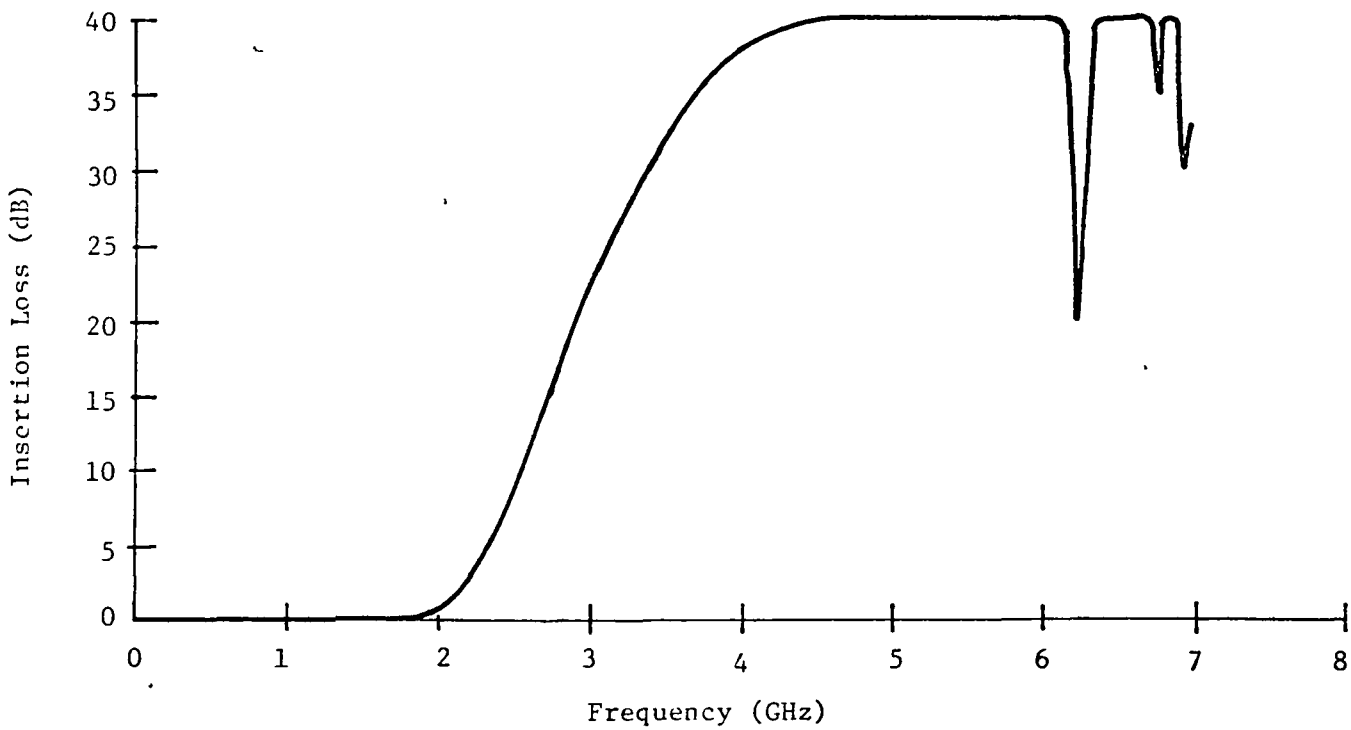
Figure 15 . Measured Insertion Loss of the Scaled Model IF Filter (Linear dB Scale)
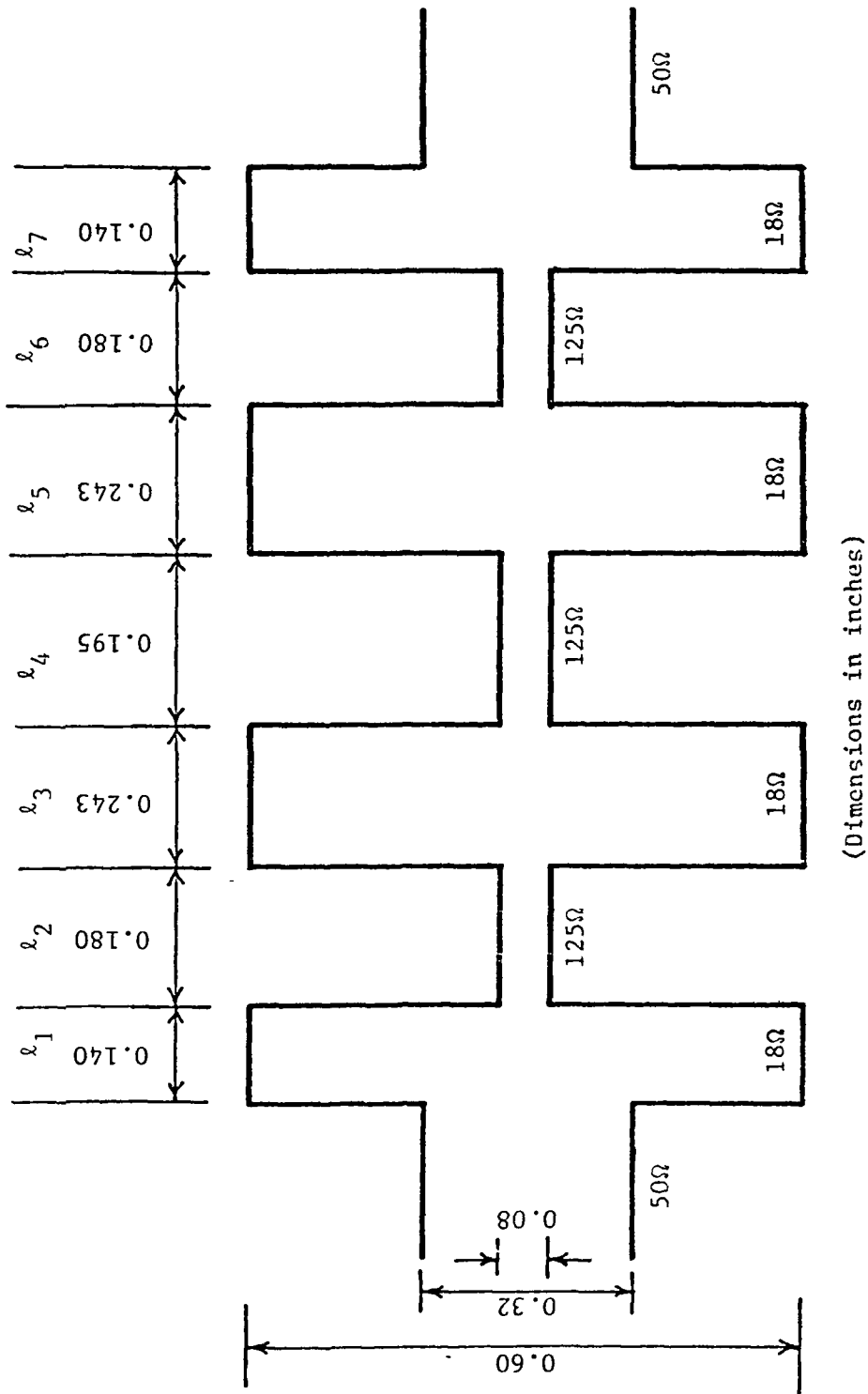
Figure 16. Printed Circuit Layout of the Scale Model LO Filter (Finalized)

(Dimensions in inches)

95
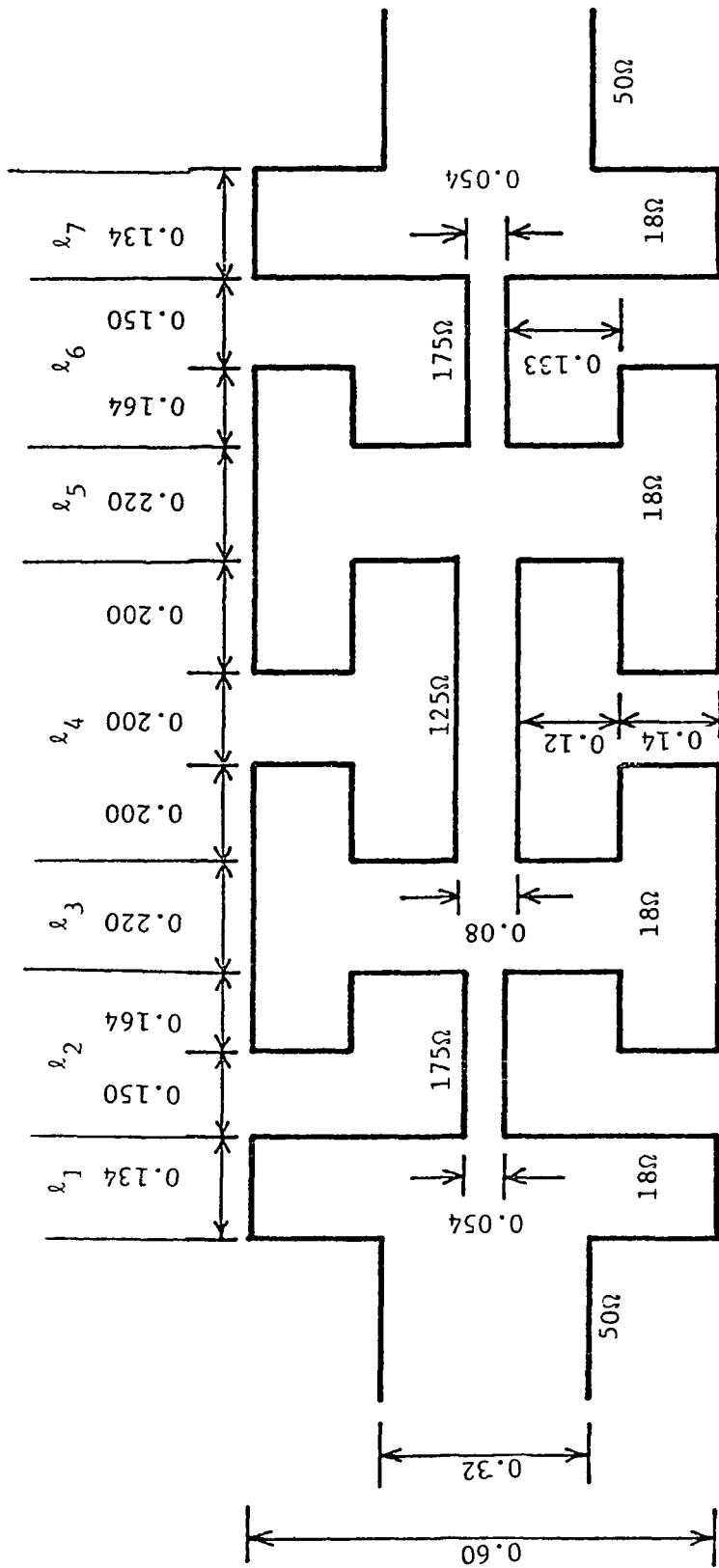
Figure 17. Printed Circuit Layout of the Scale Model IF Filter (Finalized)

(Dimensions in inches)

96
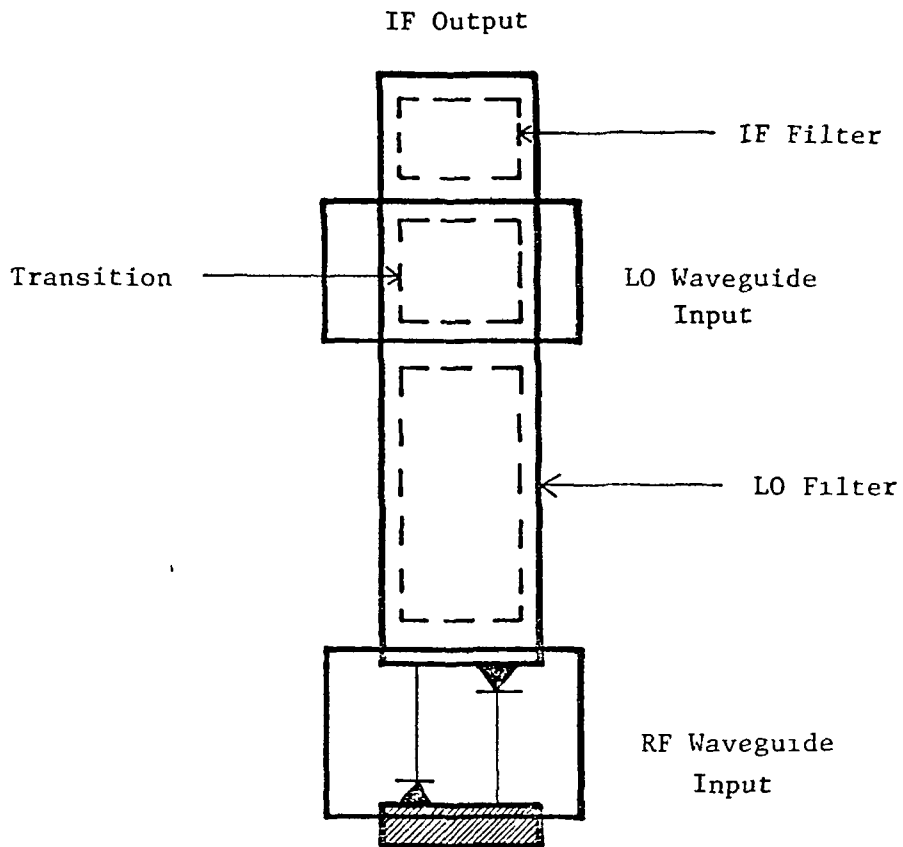
Figure 18. Schematic of Subharmonic Mixer (Model A)

97
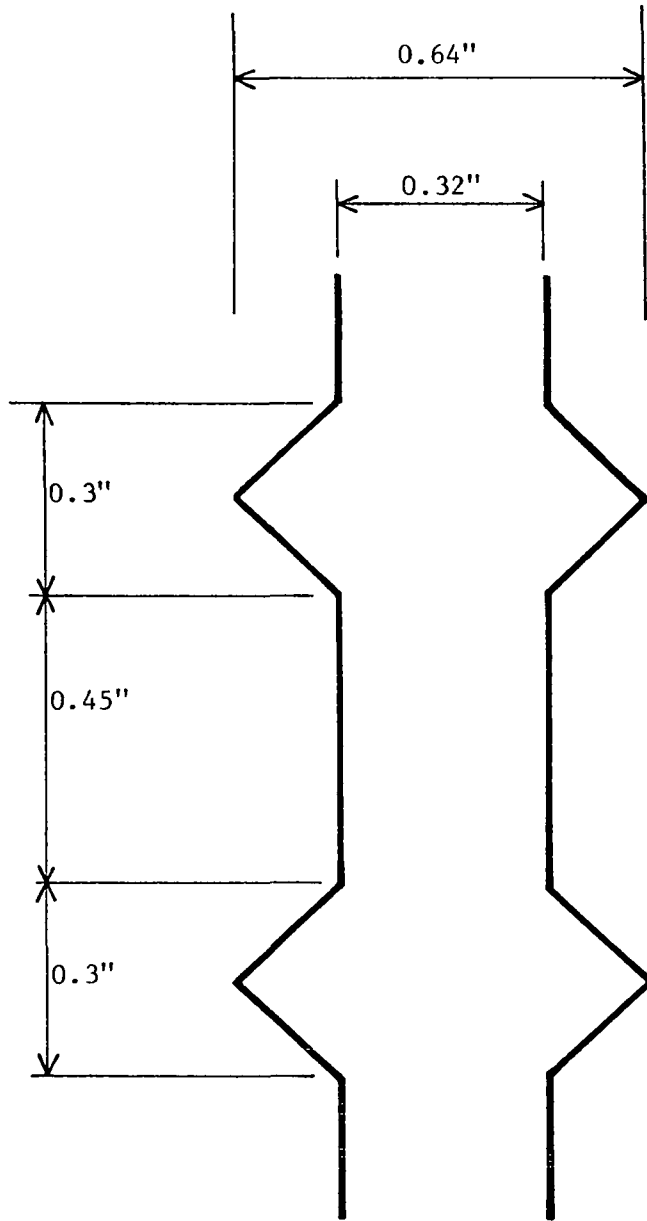
Figure 19. Waveguide to Stripline Transition
            (Located in Center of LO Waveguide)
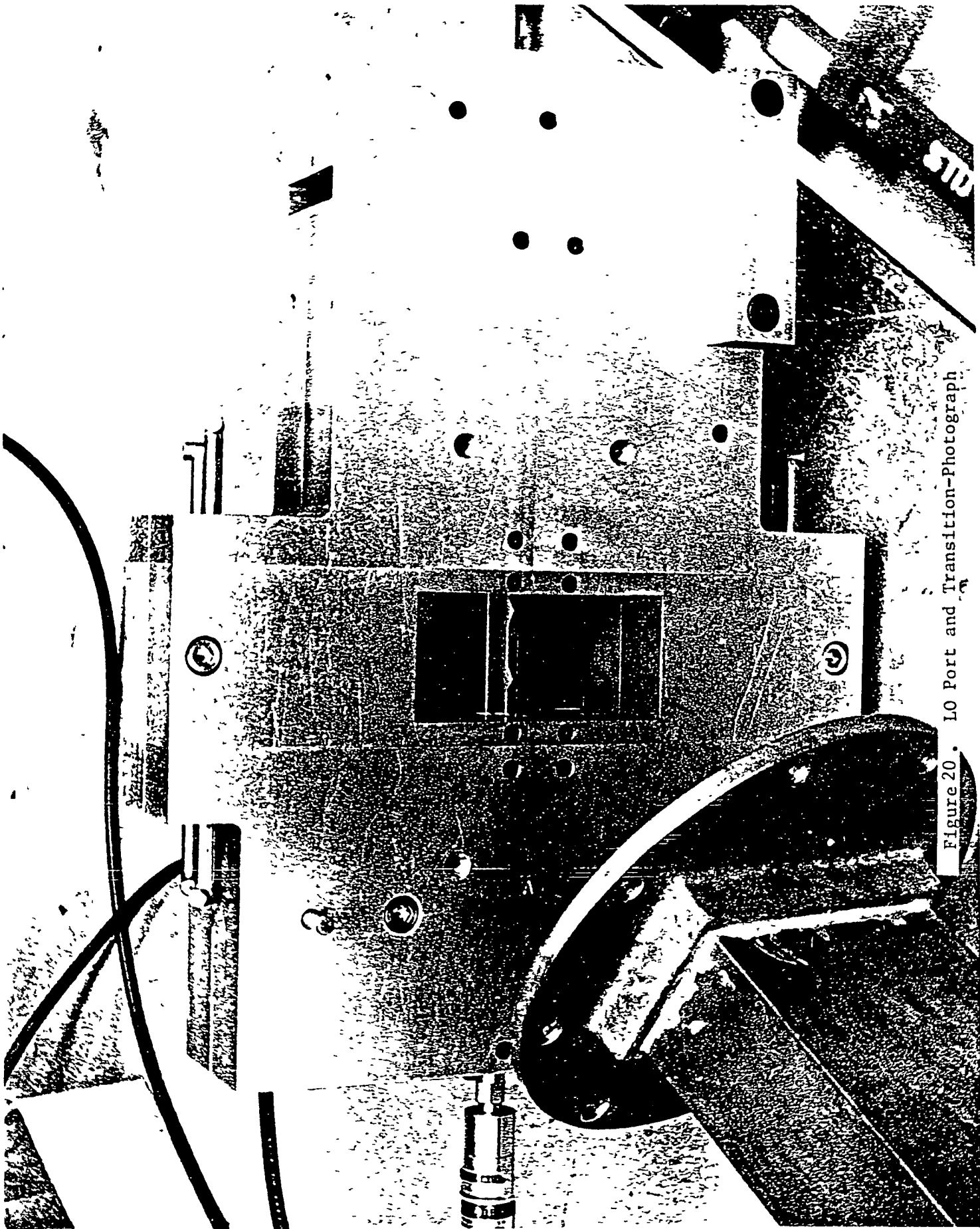
Figure 20. LO Port and Transition—Photograph

99

filter was placed about 1" in from the waveguide wall with a double triangle transition.

A plot of insertion loss versus frequency for two backshort positions is given in Figure 21. The test setup used in these measurements is shown in Figures 22 through 24.

LO FILTER PLACEMENT

The placement of the LO filter affects the conversion loss and noise figure of the diode pair. The diodes must see a short circuit at the signal frequency where the diodes are contacted to the stripline circuit. The LO filter was moved up and down the stripline channel with the other portions of the circuit (the IF filter and transition) in their proper place for mixer operation. The conversion loss was measured at each placement of the LO filter. The reflected power at the IF, LO and RF ports was monitored during this process. Optimum placement of the LO filter was found to be right at the edge of the signal waveguide wall. Plots of mixer data are shown in Figures 25 through 36. The final mixer circuit is shown in Figures 37 and 38.

Typical conversion loss measurements were around 6-8 dB. An 8 dB single sideband total system noise figure was measured at 30 and 60 MHz IF frequency with a preamp having a 2 dB noise figure. Return loss at the RF port was typically 8-13 dB. Return loss at the IF port was about 6-9 dB. Return loss measured at the LO port was 12 dB. LO power was between +10 to +23 dBm. The data varied between these limits depending on the diodes used and the signal frequency.

CONVERSION LOSS MEASUREMENTS

The incident RF (signal) power was measured using the power meter shown in the experimental set-up of Figure 39. The RF reflected power could be monitored with the spectrum analyzer to determine the best RF matching positions of the RF and LO backshorts and optimum LO power for minimum reflected signal. The IF power was measured to determine conversion loss. The data shown in Figures 25 through 34 do not take IF or RF mismatch into account.
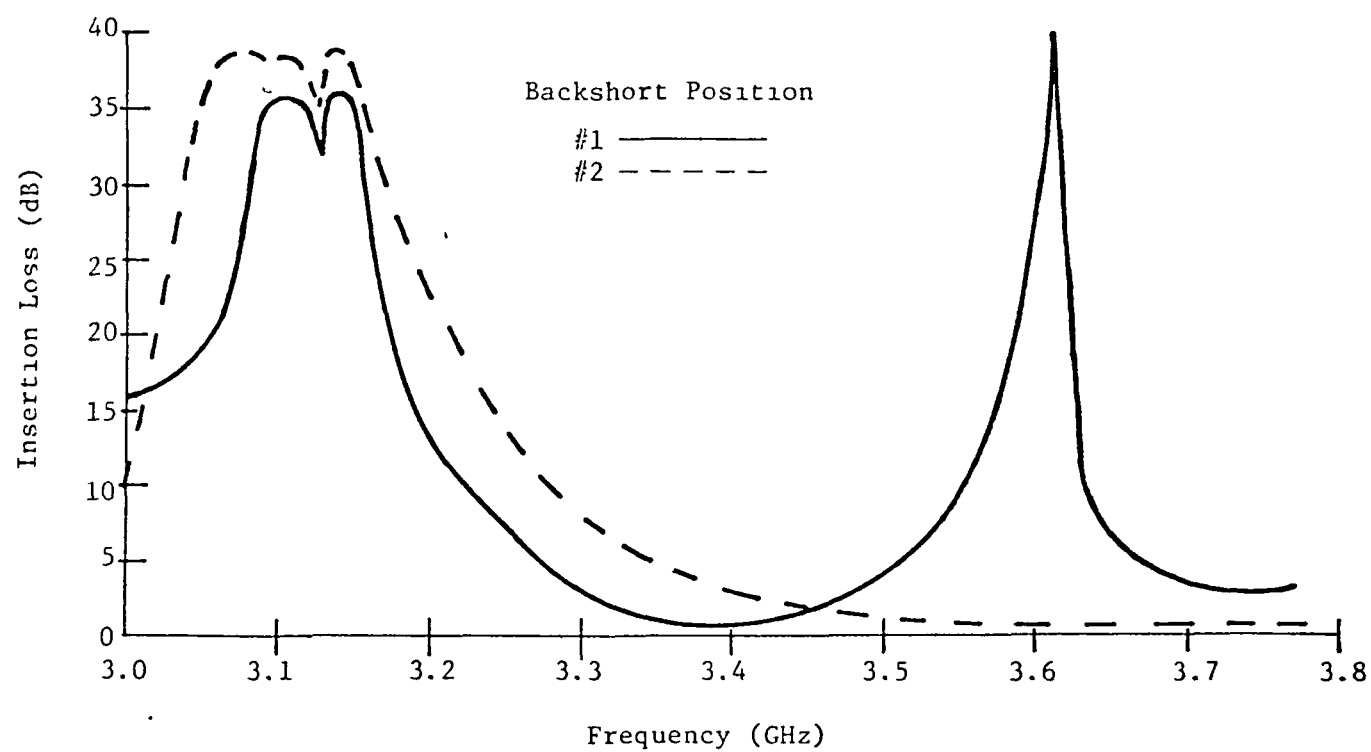
Figure 21. Measured Insertion Loss of Scaled Model LO Power Using a Waveguide to Stripline Transition and the IF Filter as a Diplexer
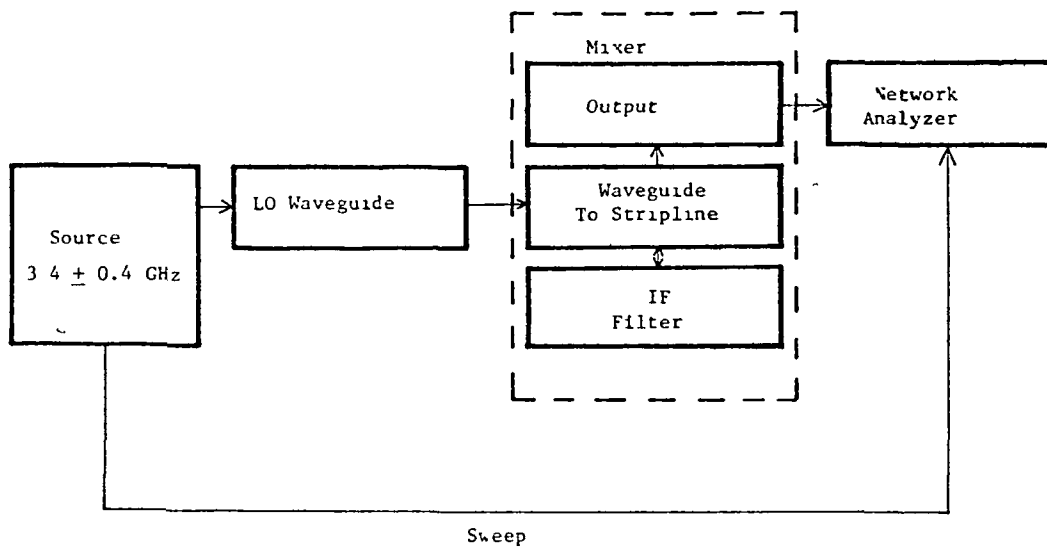
Figure 22. Test Set-up for Measurement of IF Filter Diplexing and Waveguide to Stripline Transition Properties
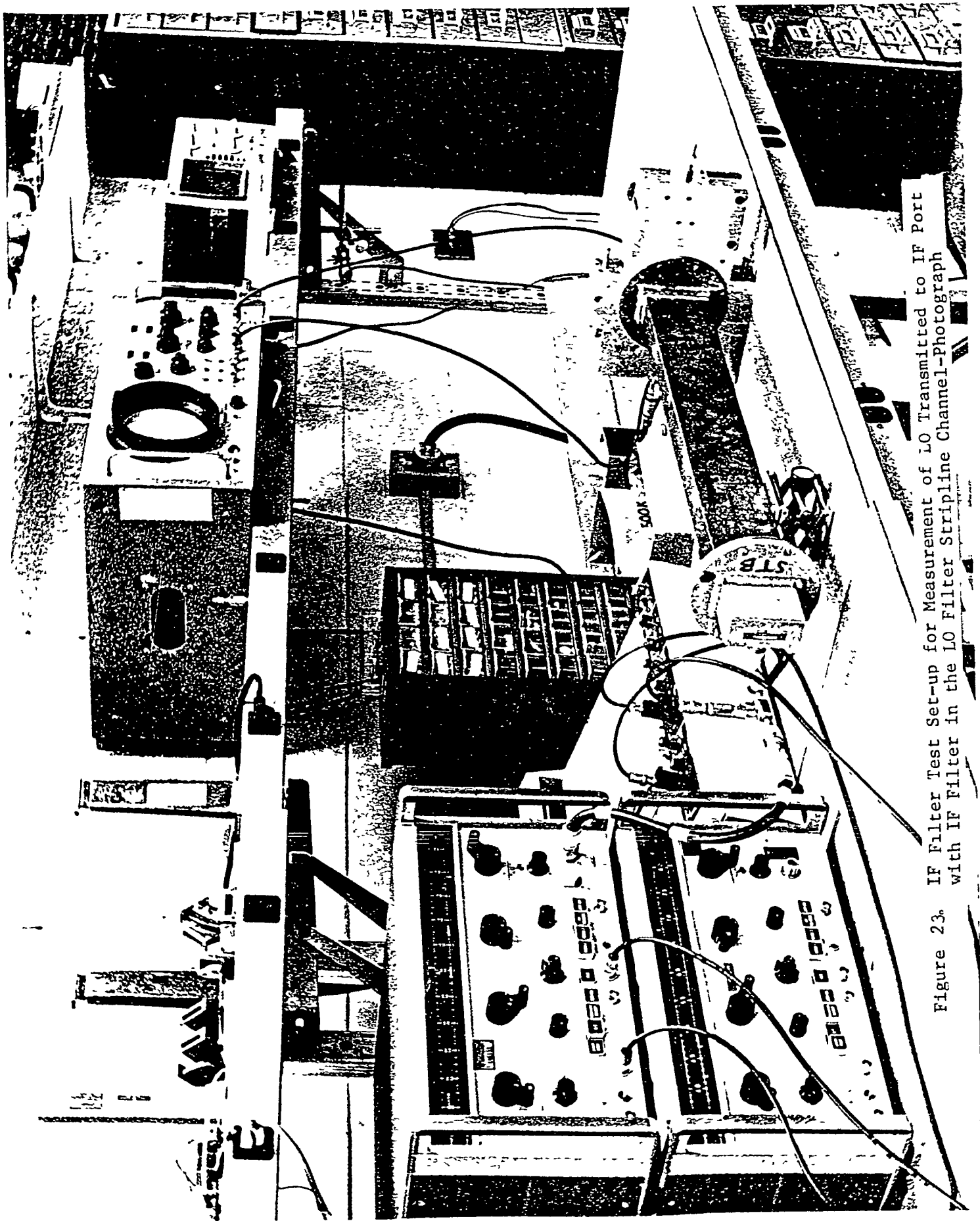
Figure 23. IF Filter Test Set-up for Measurement of LO Transmitted to IF Port with IF Filter in the LO Filter Stripline Channel–Photograph

103
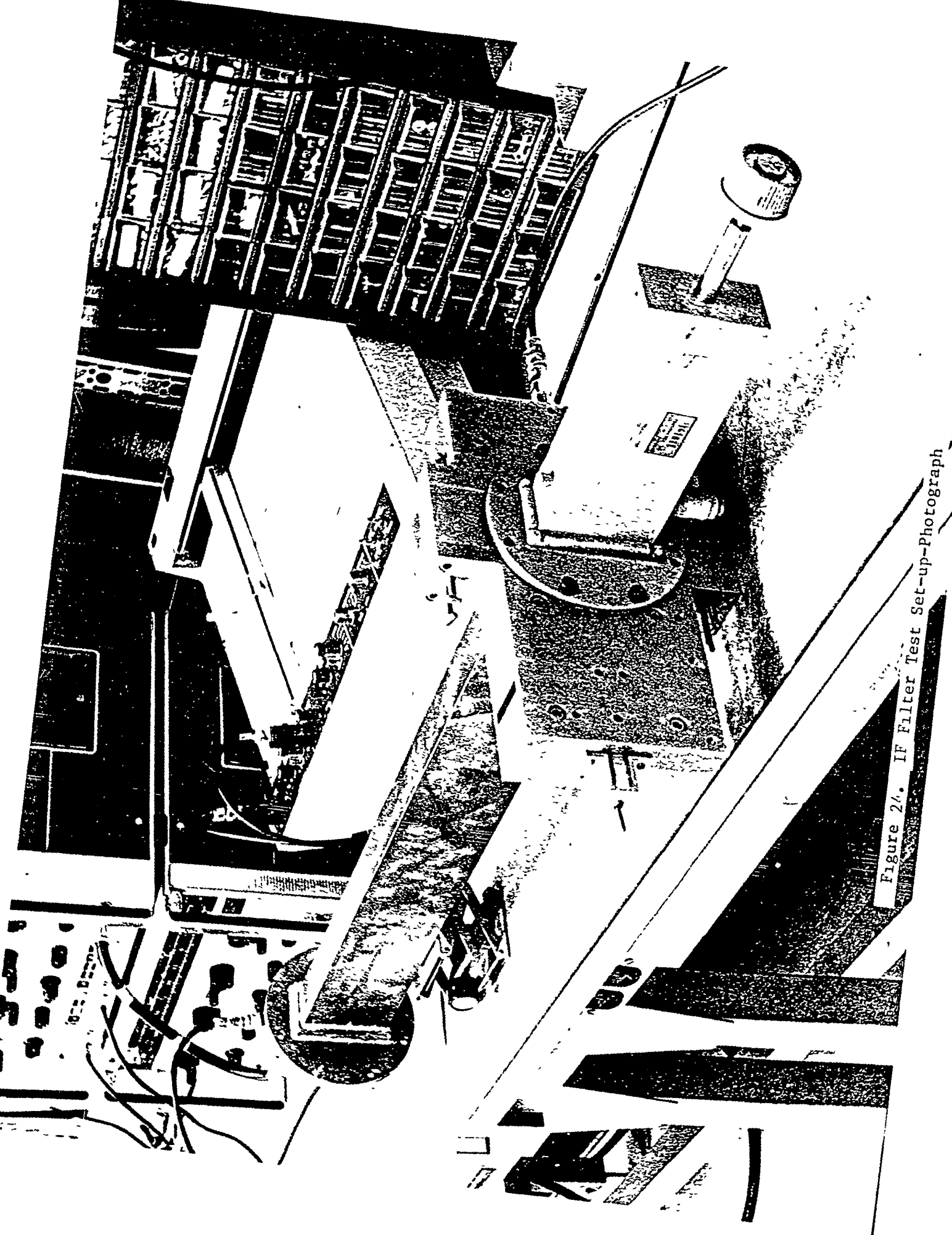
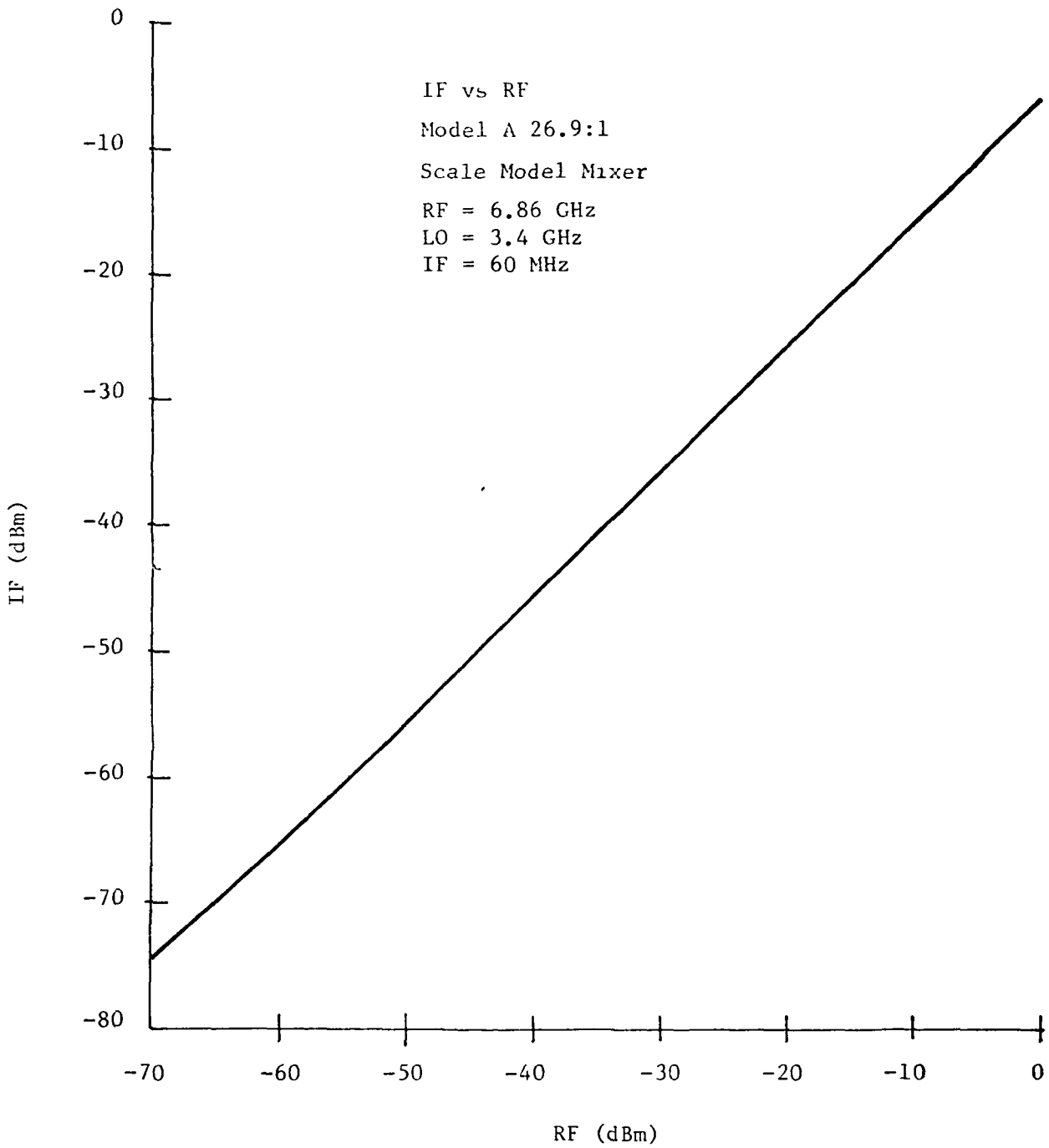Figure 24. IF Filter Test Set-up—Photograph

104

IF vs RF

Model A 26.9:1

Scale Model Mixer

RF = 6.83 GHz
LO = 3.4 GHz
IF = 30 MHz
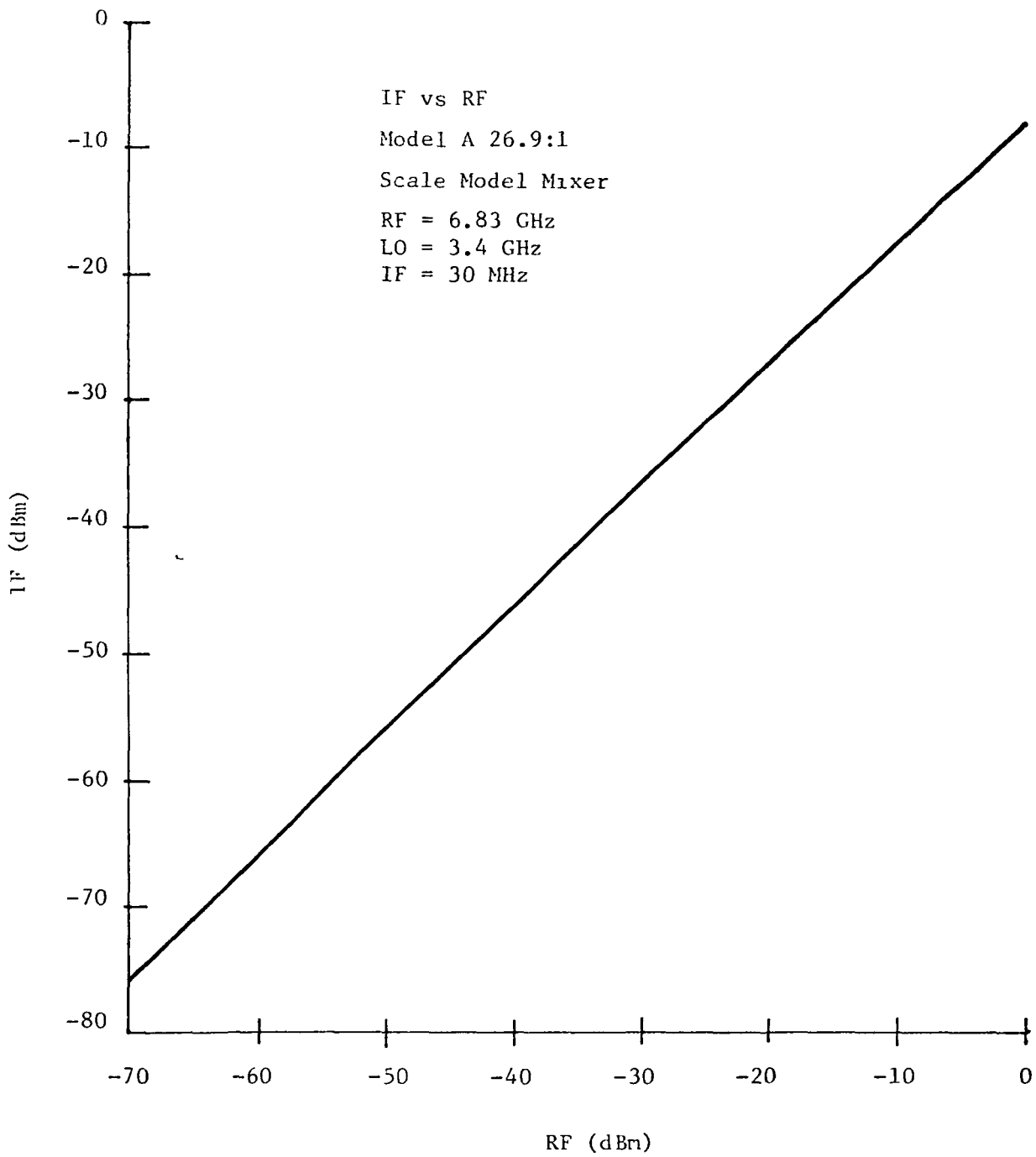
Figure 25. IF vs.RF (30 MHz)

105

Figure 26. IF vs RF (60MHz)

IF vs RF

Model A 26.9:1
Scale Model Mixer

RF = 6.9 GHz
LO = 3.4 GHz
IF = 100 MHz
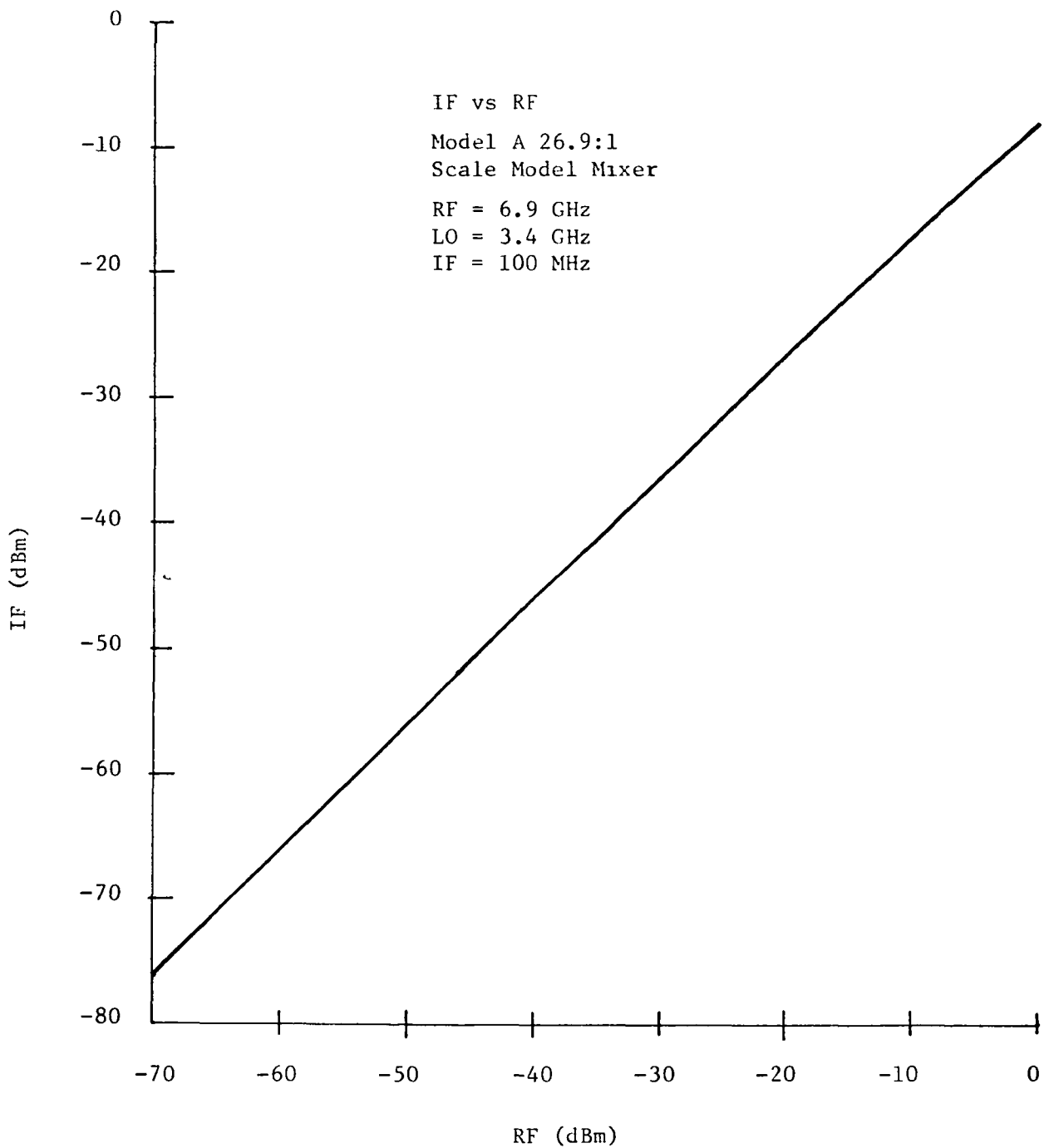
Figure 27. IF vs. RF (100MHz)
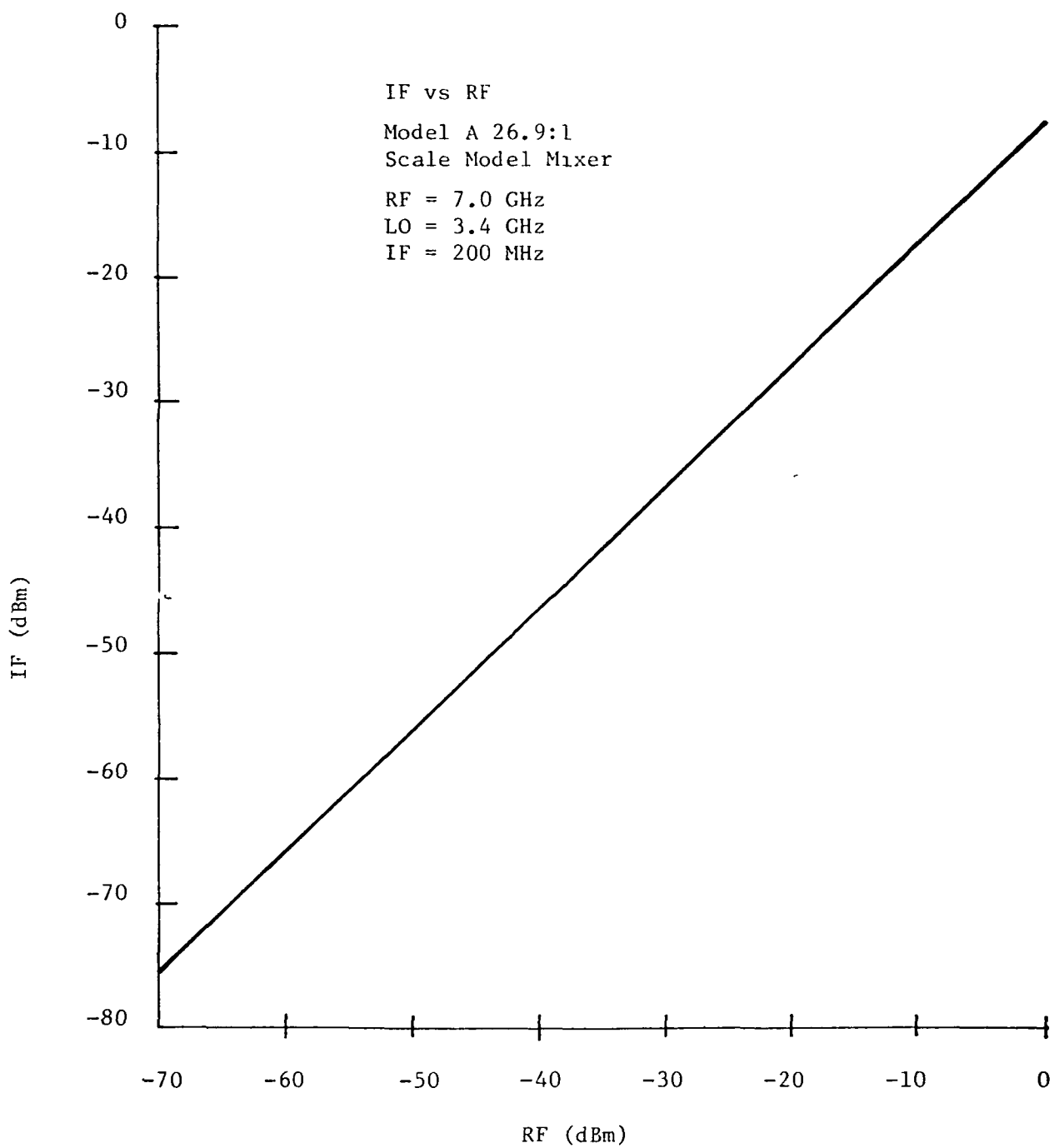
Figure 28. IF vs. RF (200MHz)
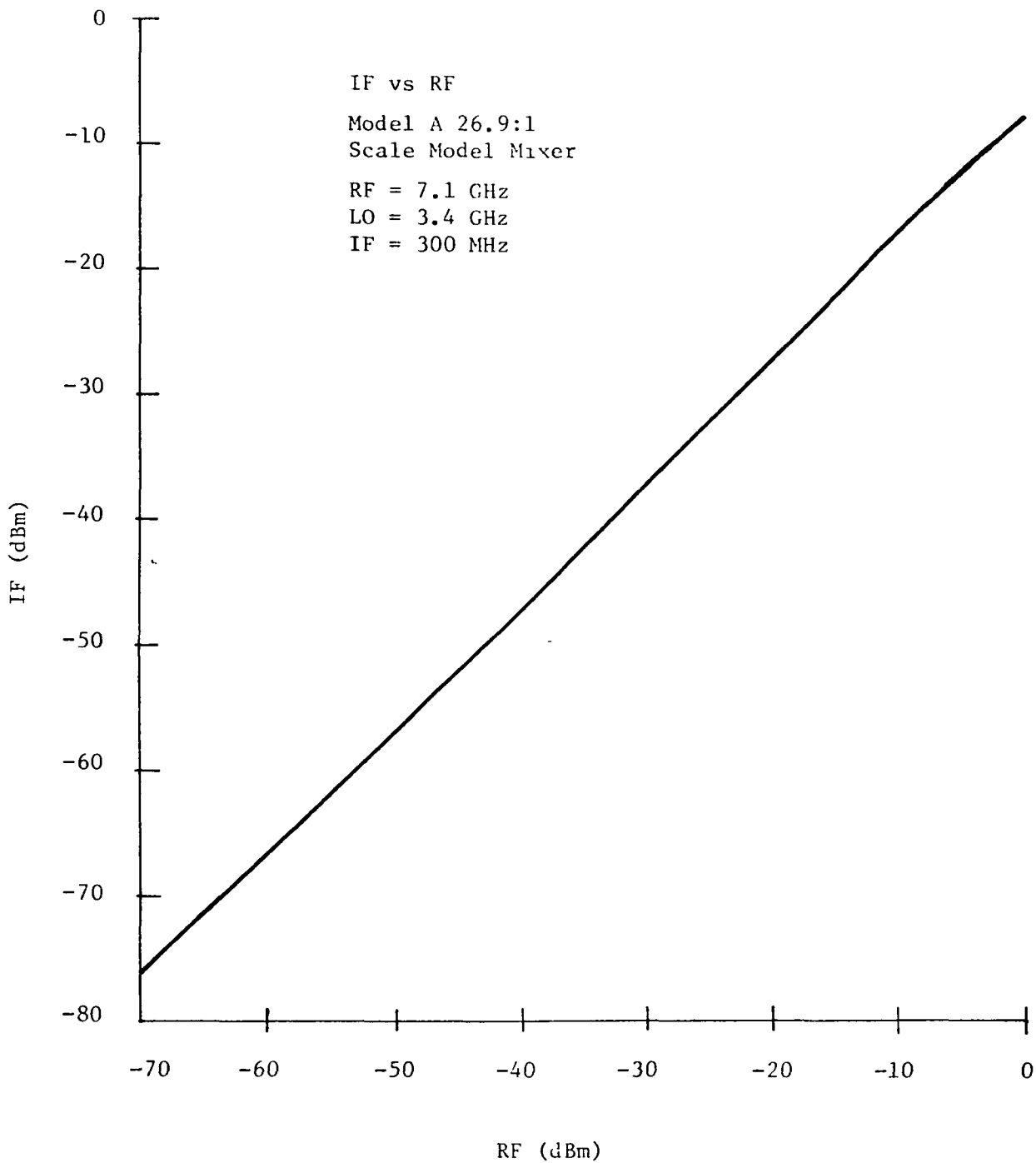
Figure 29. IF vs. RF (300MHz)

109

Converson Loss vs RF Frequency

Model A 26.9:1
Scale Model Mixer

RF power = -60 dBm
Case 1:   Mixer Tuned for Best Con-
          version Loss at Each Frequency
LO Frequency = 3.4 GHz
LO Power ≈ 20 dBm
IF Frequency = RF -2 x LO
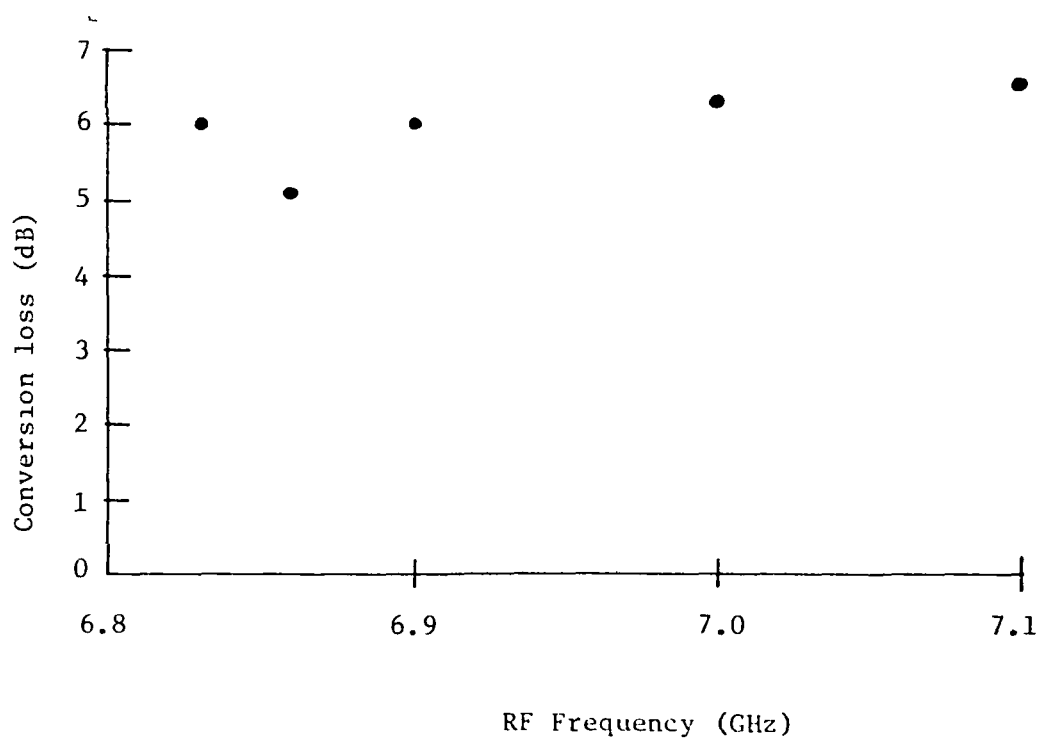
Figure 30. Conversion Loss vs. Frequency (Case 1)

Conversion Loss vs RF Frequency

Model A 26.9:1
Scale Model Mixer

RF power = -60 dBm
Case 2: Mixer Tuned for Optimum
         Operation at f = 6.86 GHz
LO Frequency = 3.4 GHz
LO Power $\sim$ 20 dBm
IF Frequency - RF -2 x LO
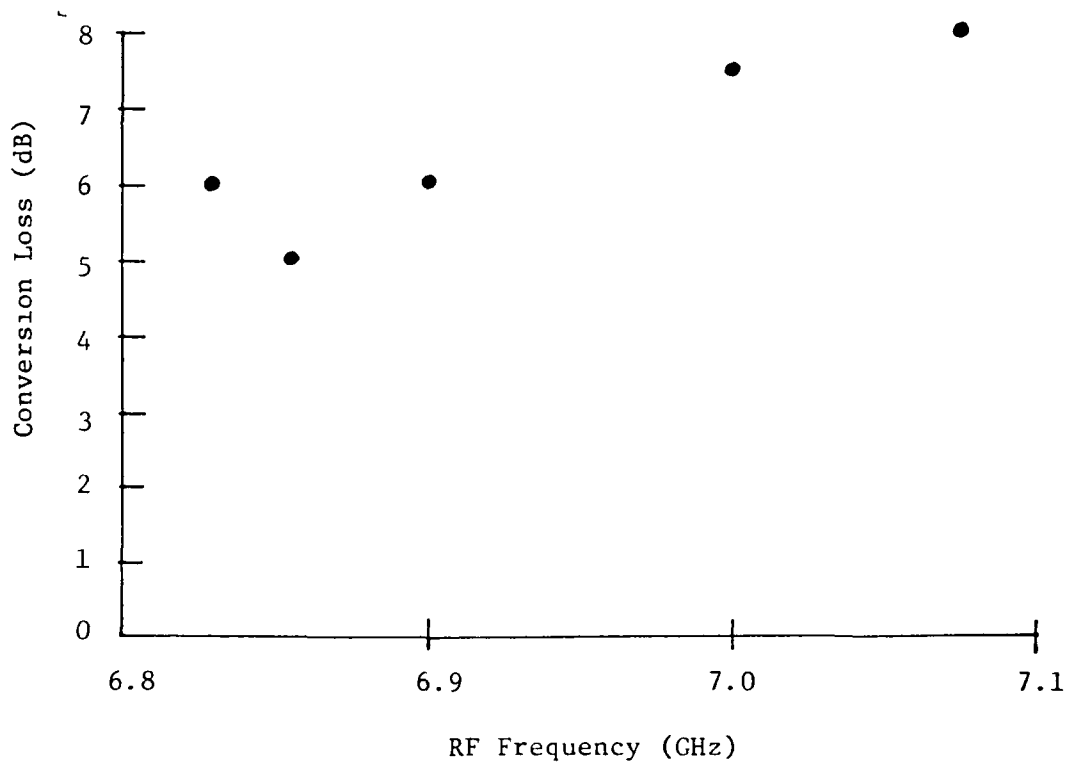
Figure 31. Conversion Loss vs. Frequency (Case 2)

Conversion Loss vs RF Frequency

Model A 26.9:1
Scale Model Mixer

RF Power = -60 dBm
Case 3: Mixer Tuned for Optimum
         Operation at 6.9 GHz
LO Frequency = 3.4 GHz
LO Power $\sim$ 20 dBm
IF Frequency - RF -2 x LO
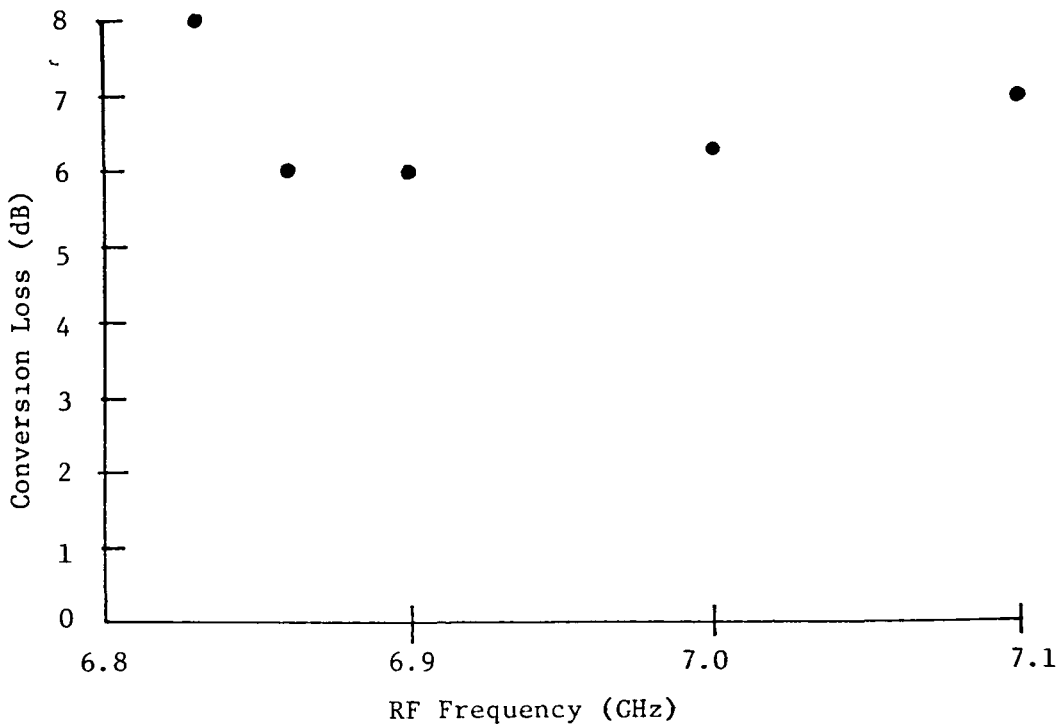
Figure 32. Conversion Loss vs. Frequency (Case 3)

Figure 33. Noise Figure and Conversion Loss vs. LO
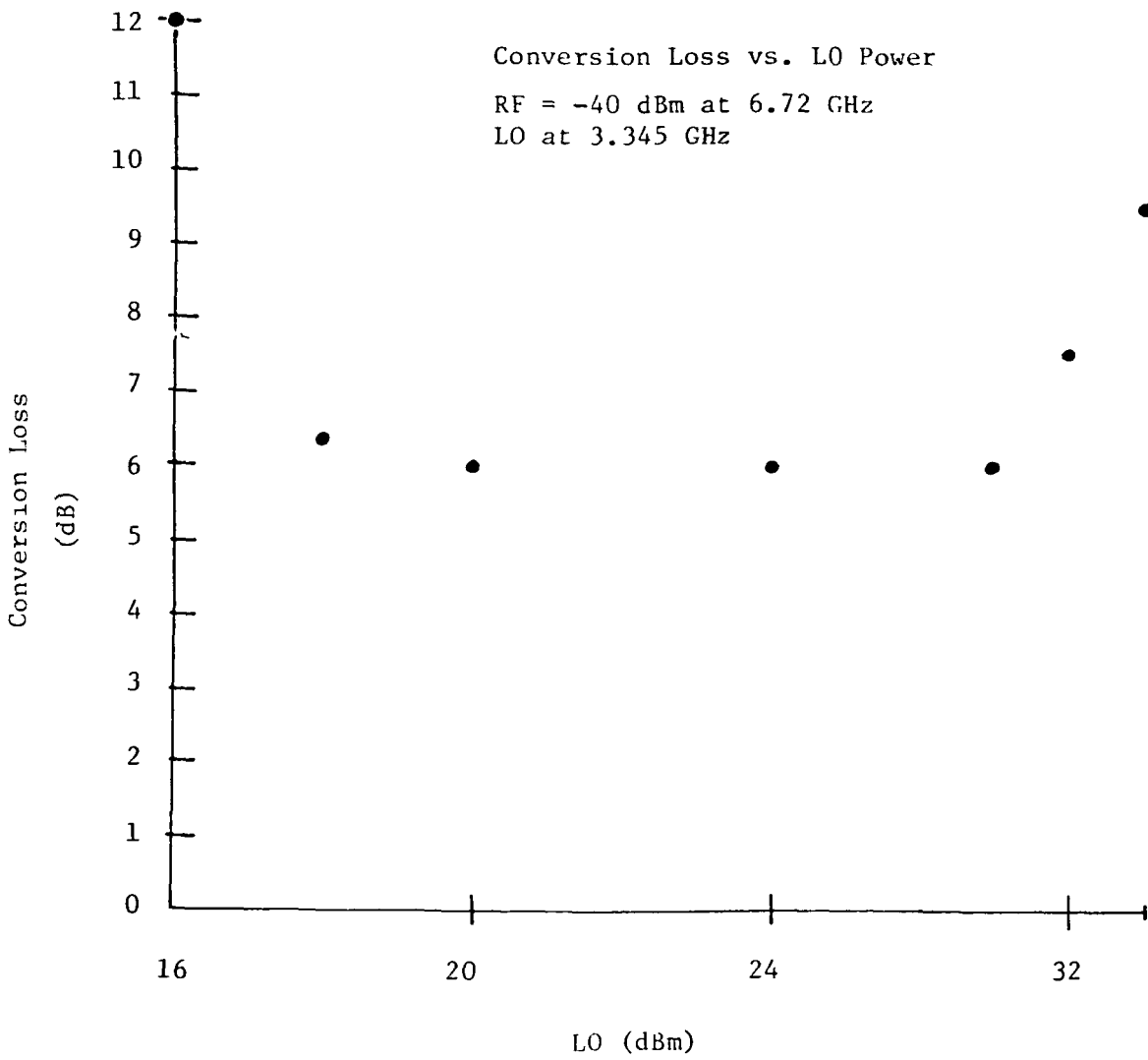
Figure 34. Conversion Loss vs. LO Power

114
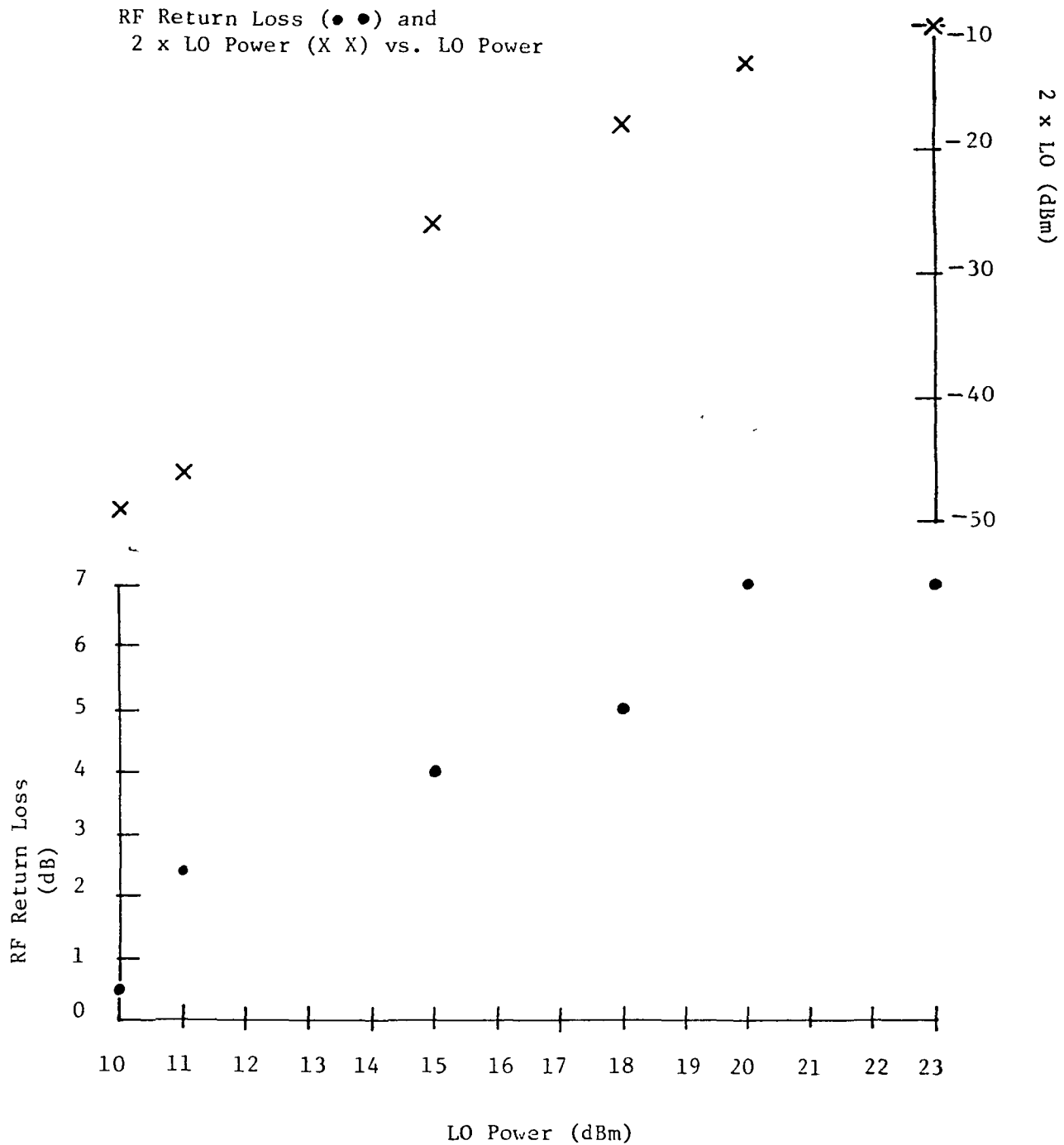
Figure 35. RF Return Loss and 2 x LO Generated
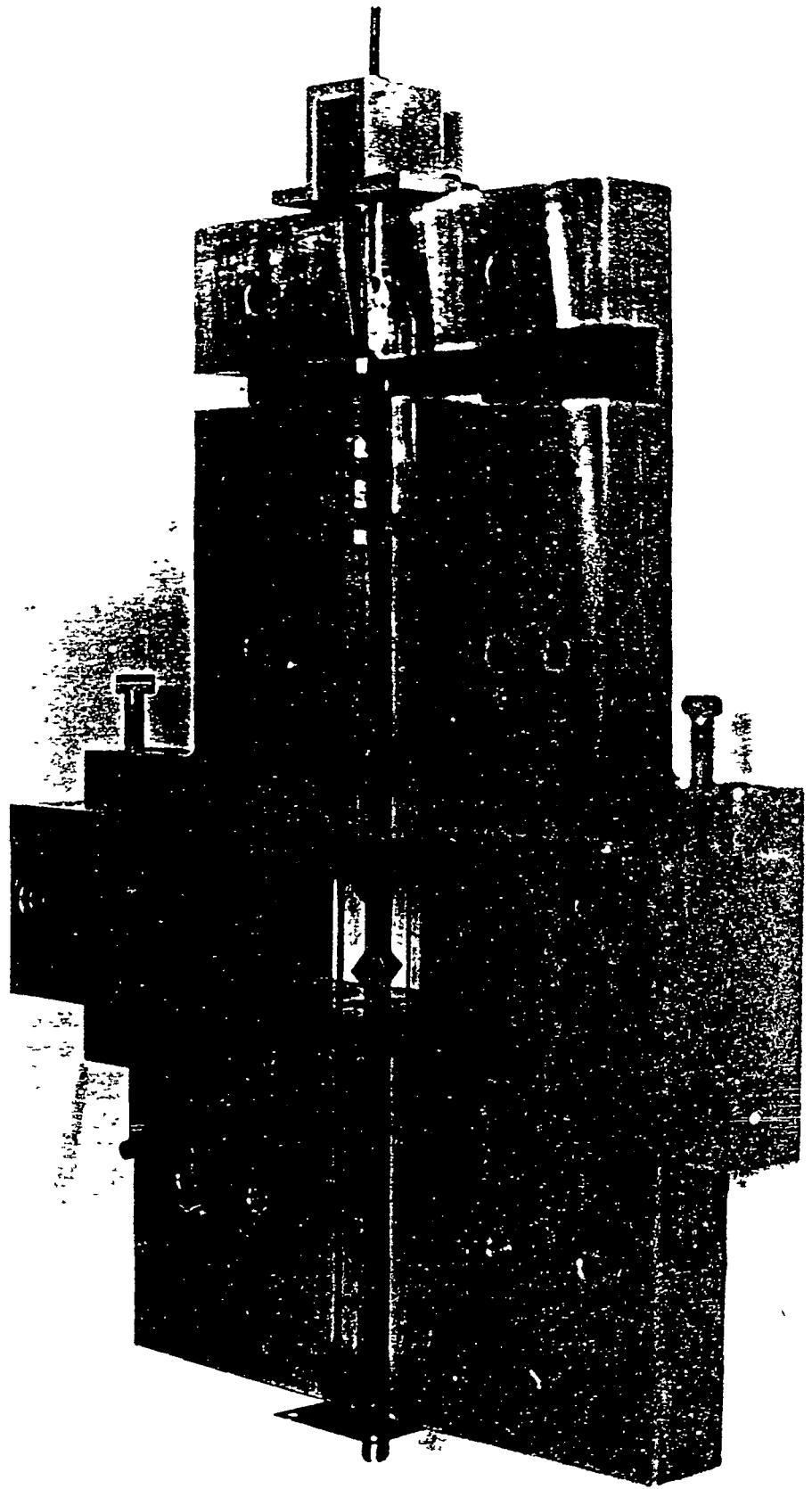(Measured at RF Port) vs. LO Power.

IF Return Loss vs. LO Power at
30 MHz and -40 dBm IF Power
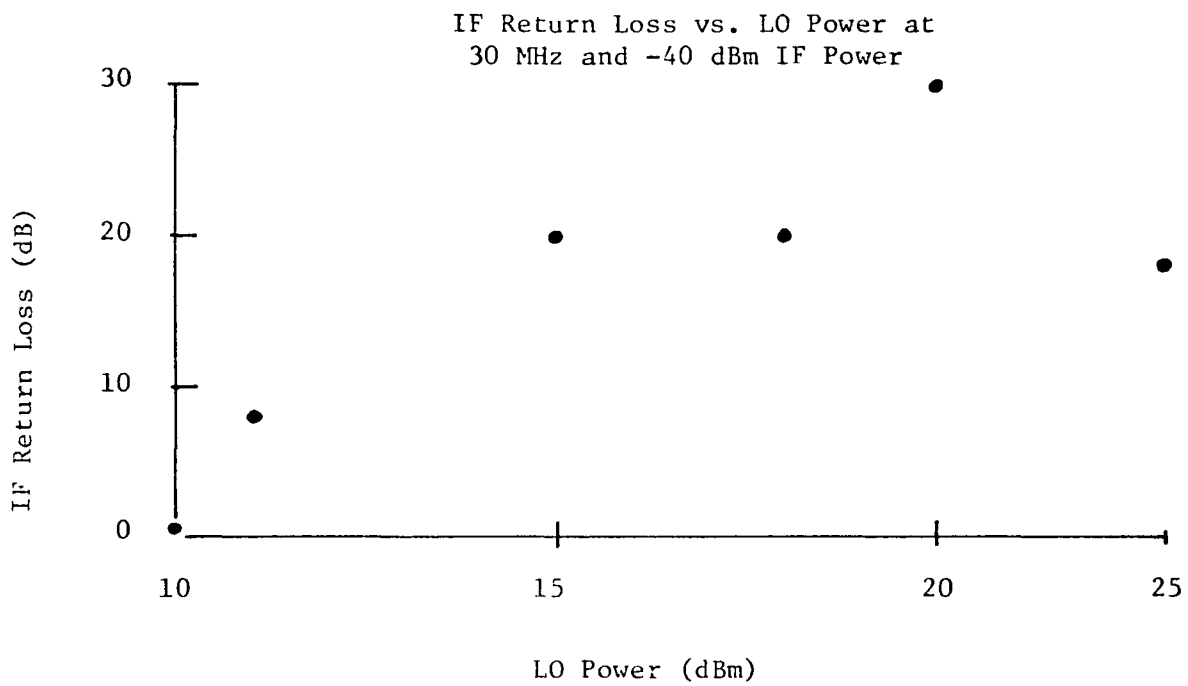
Figure 36. IF Return Loss vs. LO Power

116

Figure 37. Stripline Circuit in Mixer Body-Photograph
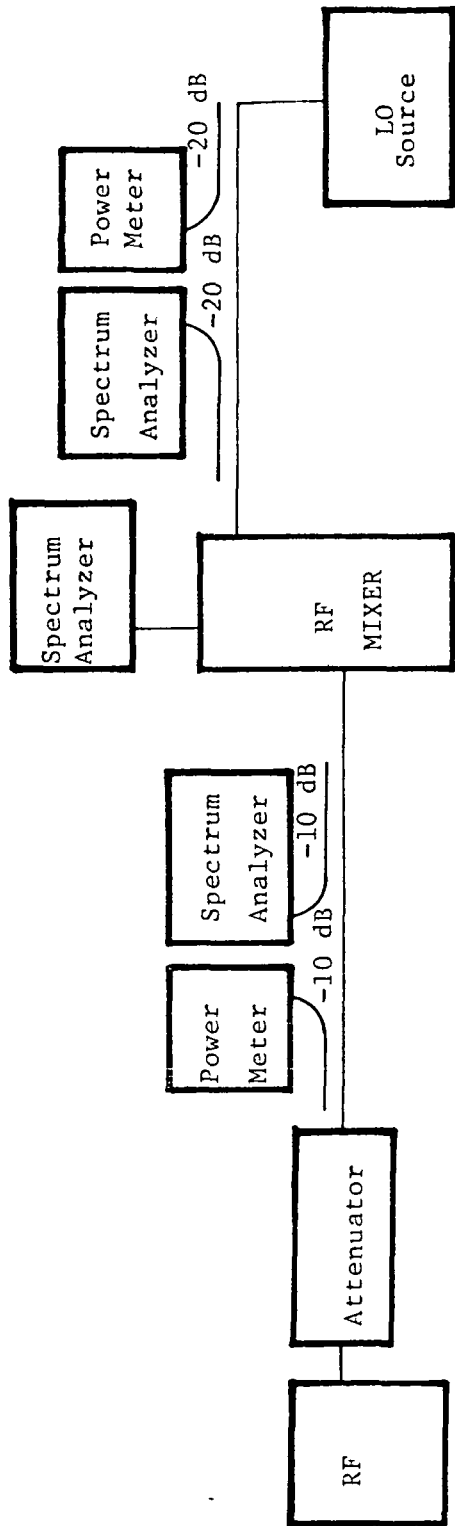
117
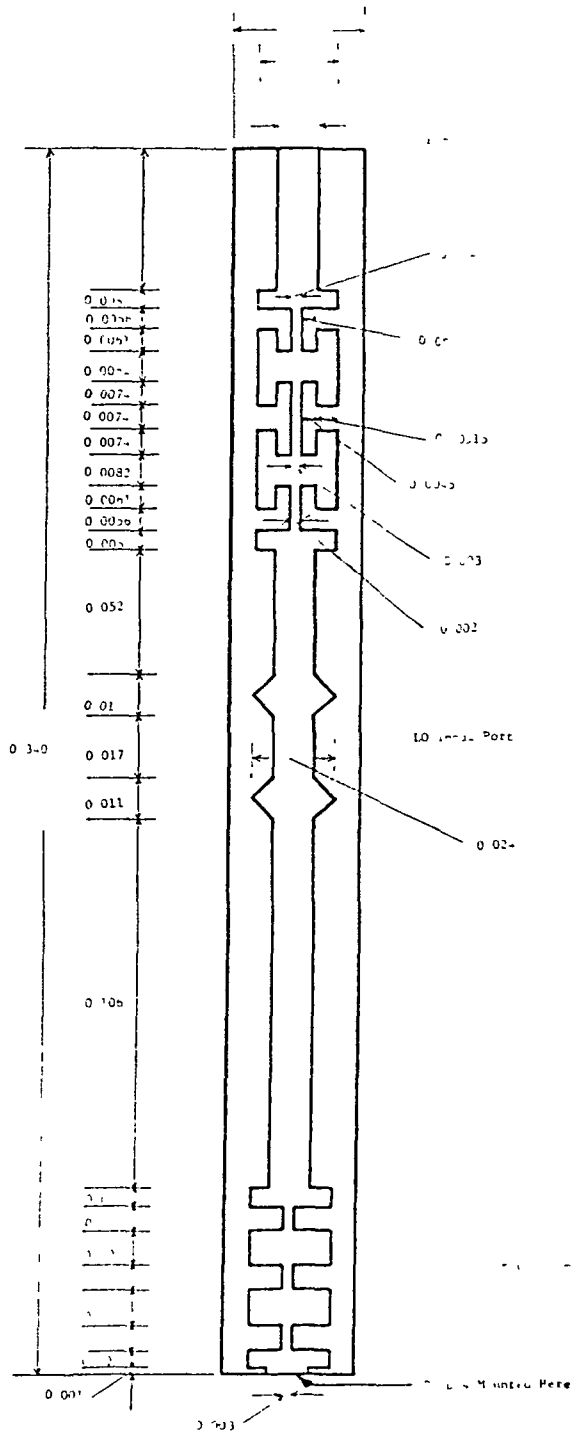
Figure 38. 183 GHz Mixer Network

Figure 39. Conversion Loss Test Set-up.

Conversion loss could be improved to typically 5.0 to 5.5 dB via IF or RF mismatch. The mismatch of the signal and IF frequencies was found to vary according to the diodes used and their placement in the waveguide as well as LO power.

NOISE FIGURE MEASUREMENTS

Noise figure measurements were made using a 34.5 dB ENR diode noise source. The test set-up is shown in Figures 40 through 44. Conversion loss (L_c) at both upper and lower sidebands was measured. The Y factor (difference between IF power with the noise on and the noise off) was measured using the spectrum analyzer. The single sideband total system noise figure was then calculated as below.

Sample Calculation:

$$ENR_{dB} = 34.5$$

$$Y_{dB} = 28.7 \text{ dB} \qquad L_{c\ im} = 7 \text{ dB}$$

Measured Data $\qquad Y_{ratio} = 741 \qquad L_{c\ sig} = 6 \text{ dB}$

The double sideband noise figure F_T is calculated from:

$$F_{T\ dB} = ENR_{db} - 10 \log (Y_{ratio} - 1)$$

$$= 5.8 \text{ dB}$$

$$F_T = 3.806 \text{ (ratio)}$$

$$F_{TSSB} = F_T \left(1.0 + \frac{G_{im}}{G_{sig}}\right)$$

$$F_{TSSB} = 3.806 \left(1.0 + \frac{3.98}{5.0}\right) = 6.85$$

$$= 8.36 \text{ dB} \simeq 8 \text{ dB},$$

where:

F_{TSSB} = Single Sideband Noise Figure,

$L_{c\ im}$ = Image Conversion Loss,

$L_{c\ sig}$ = Signal Conversion Loss,

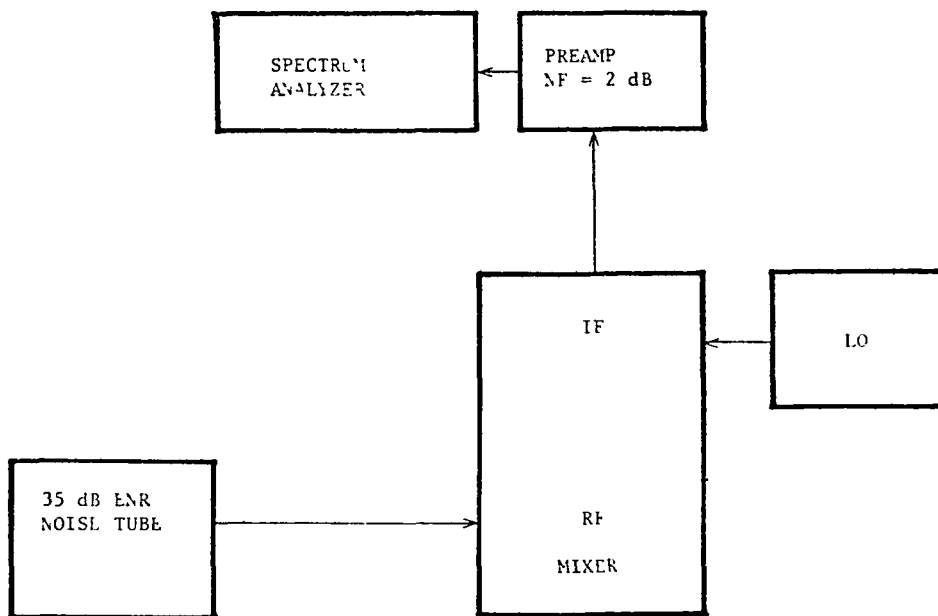G_{im} = Image Gain,

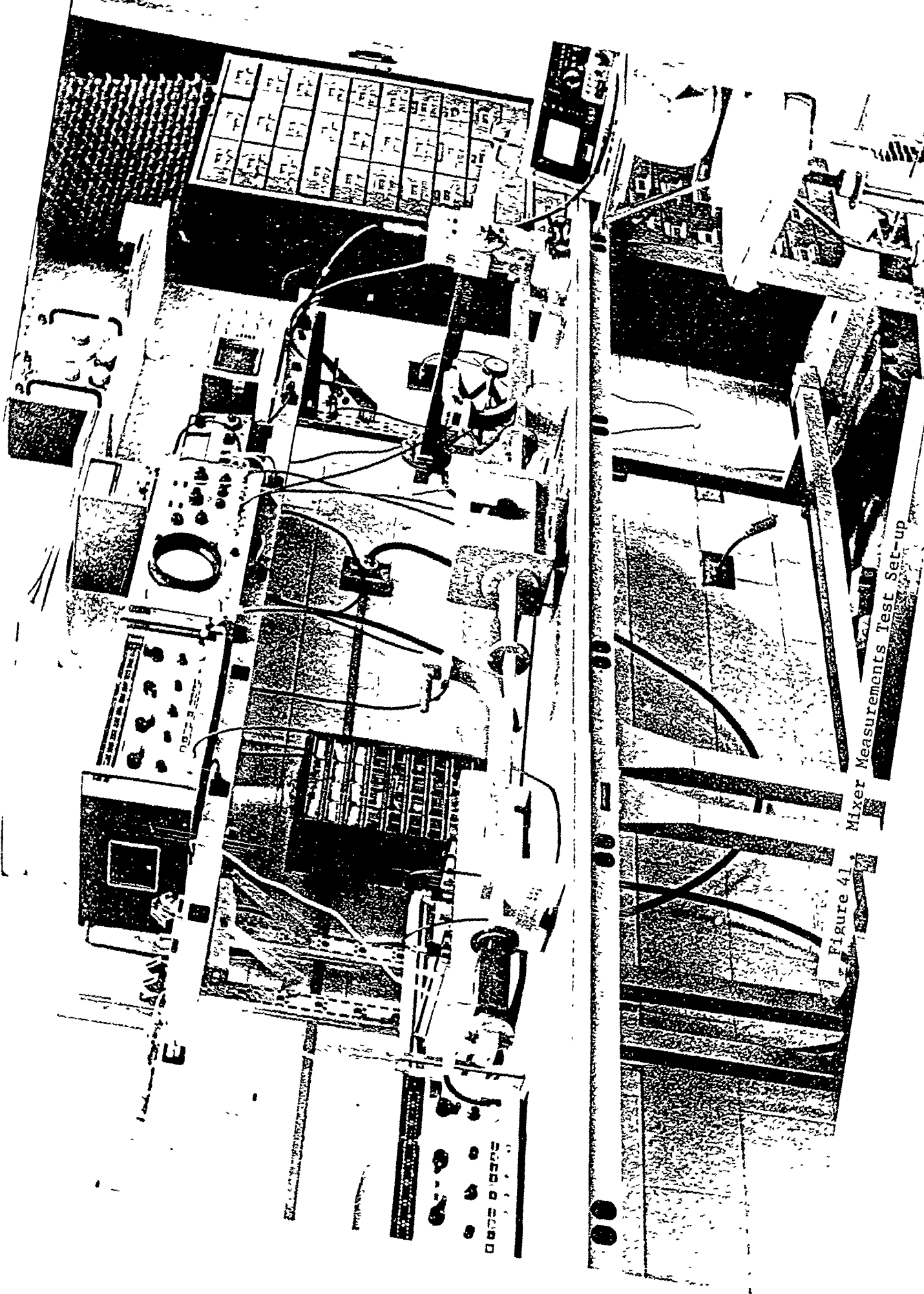G_{sig} = Signal Gain.

Figure 40. Noise Figure Test Set-up
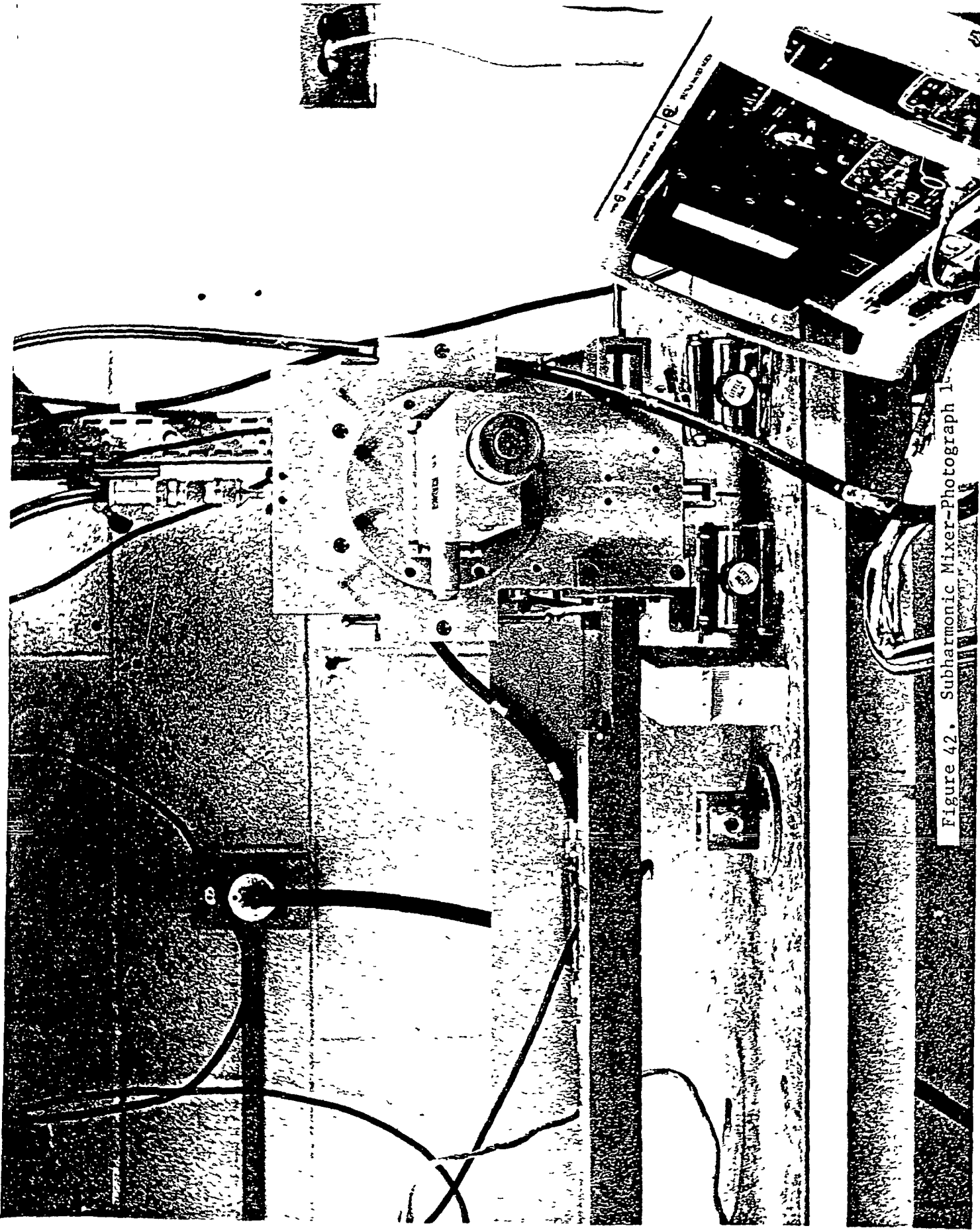
Figure 41. Mixer Measurements Test Set-up
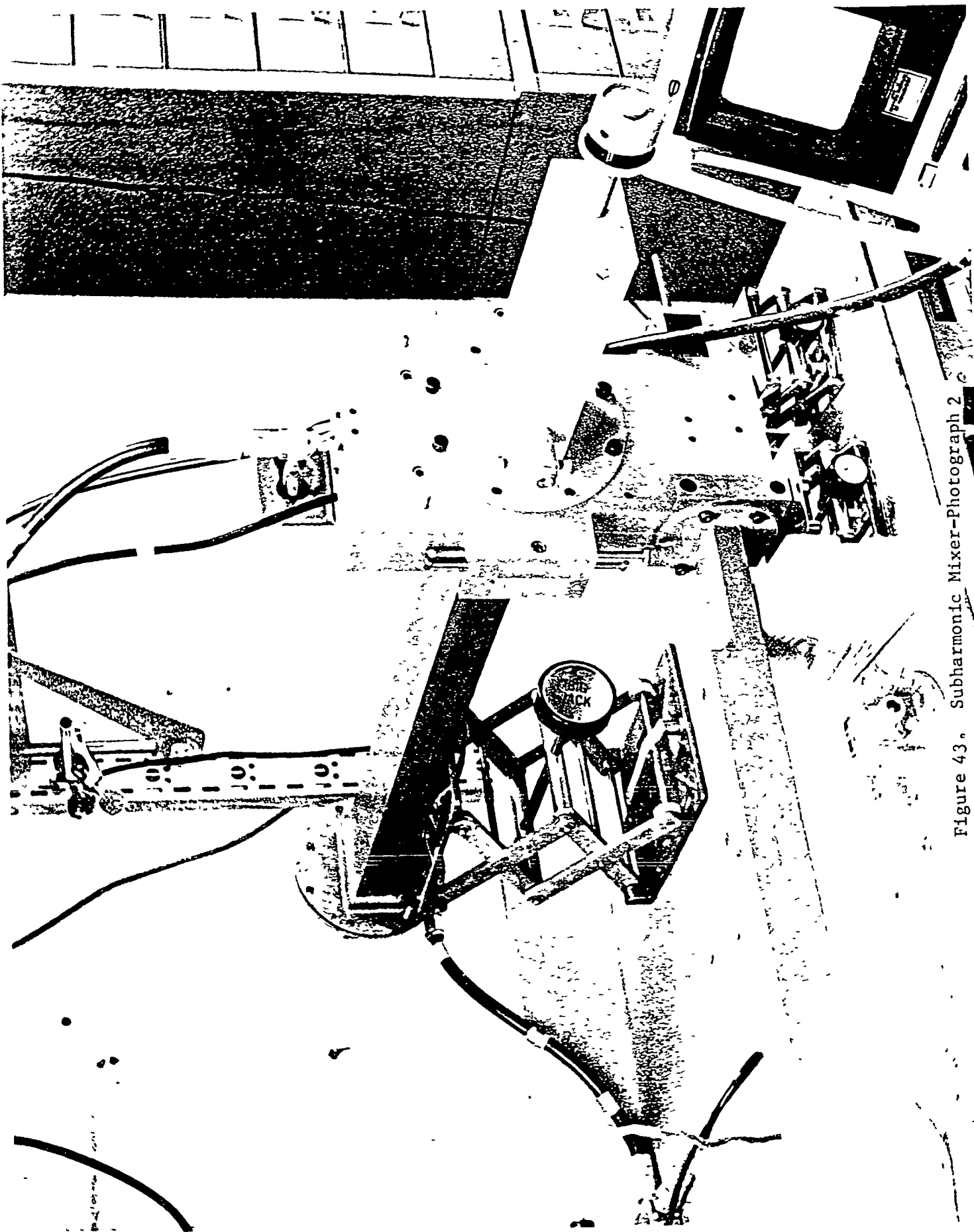
Figure 42. Subharmonic Mixer–Photograph 1.
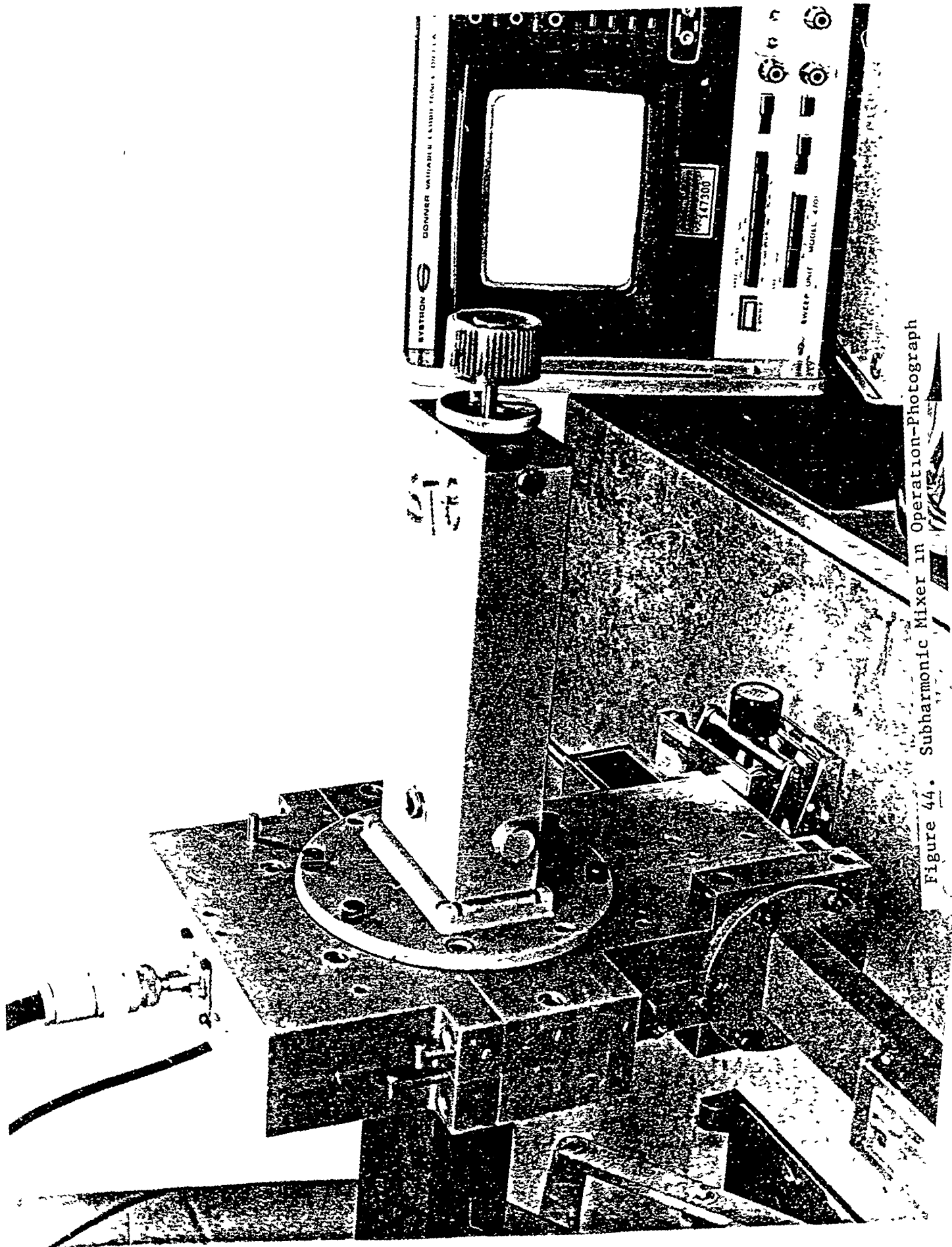
Figure 43. Subharmonic Mixer–Photograph 2

Figure 44. Subharmonic Mixer in Operation—Photograph

MIXER DIODES TYPE AND MEASURED DATA

The diodes were scaled by considering both capacitance and size. These diodes had a series resistance of about 2 ohms, a junction capacitance of about 0.15 pF with a case capacitance of about 0.1 pF and quality factors close to the values of the mm-wave mixer diodes. Diode pills (Alpha-DMK 6601) were mounted on brass blocks which were cut to the scaled size of the actual diodes and contacted by whiskers which were also scaled appropriately. The diodes are shown in Figure 45.

These diodes were chosen to help model the mixer as closely as possible for optimization of the filter circuit. Diode selection* was also aided prior to the mixer assembly by choosing a pair that had a symmetrical I/V curve as is shown in Figure 46. The actual conversion loss and noise figure measurements may be different in the final mixer due to the difficulties in properly scaling the diode properties. The large amounts of LO power (> 20dBm) are required to drive the diodes into an operating point which has a good match for both the RF and IF networks. Loss power would be required if the IF port were matched properly.

The LO rectified current was measured by disconnecting one of the whiskers and replacing it by a wire leading out of the transformer section of the waveguide. The circuit was completed by running the current through an ammeter and back to the body of the mixer (ground). This data is shown in Figure 47. Mixing still occurred in this configuration and a degraded minimum conversion loss of 10dB was measured at a rectified current value of 1.8ma (15dBm LO power).

---

*Proper diode selection using measured I/V curve data is very important since actual data varies significantly from vendor data sheets in many cases.
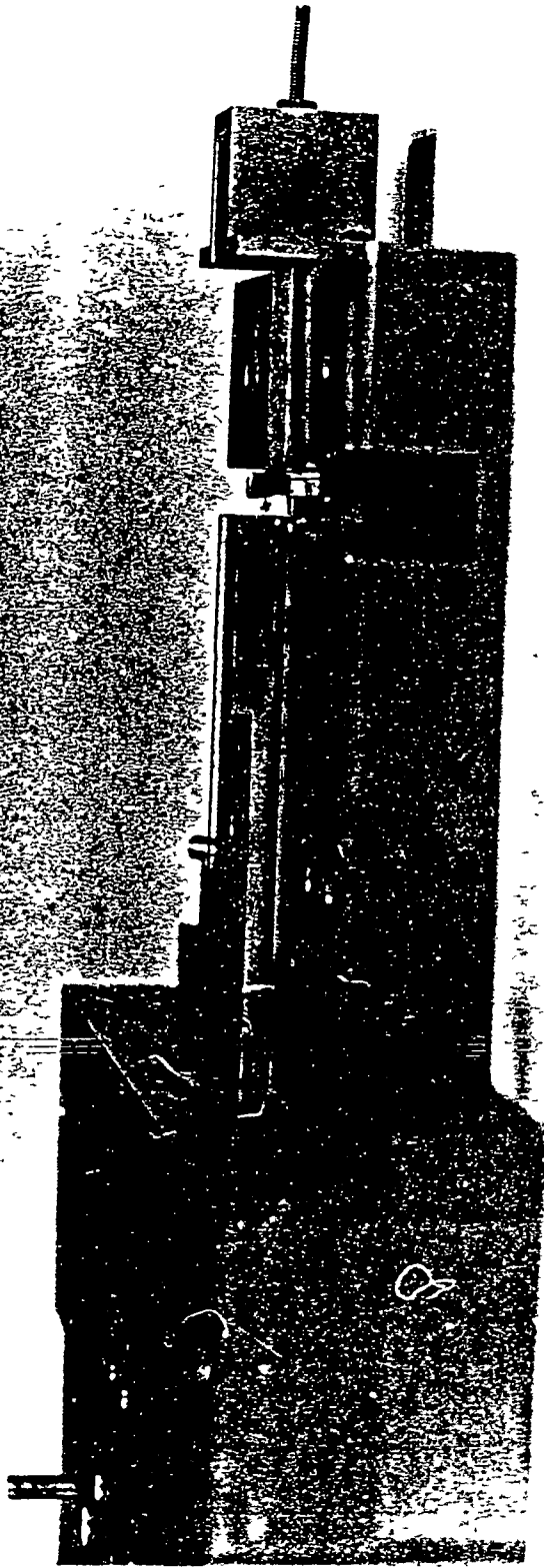
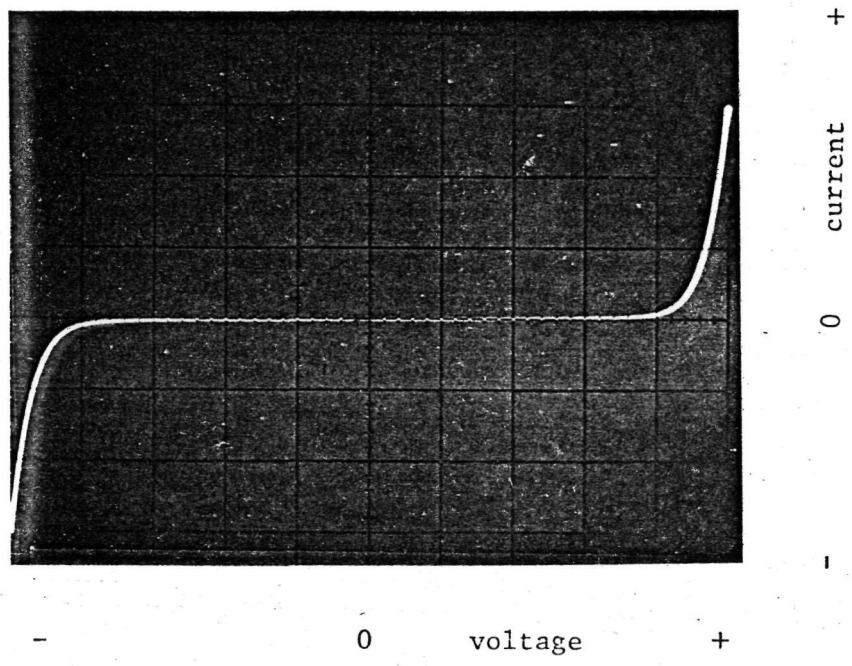Figure 4-. LO Filter and Model Diodes-Photograph
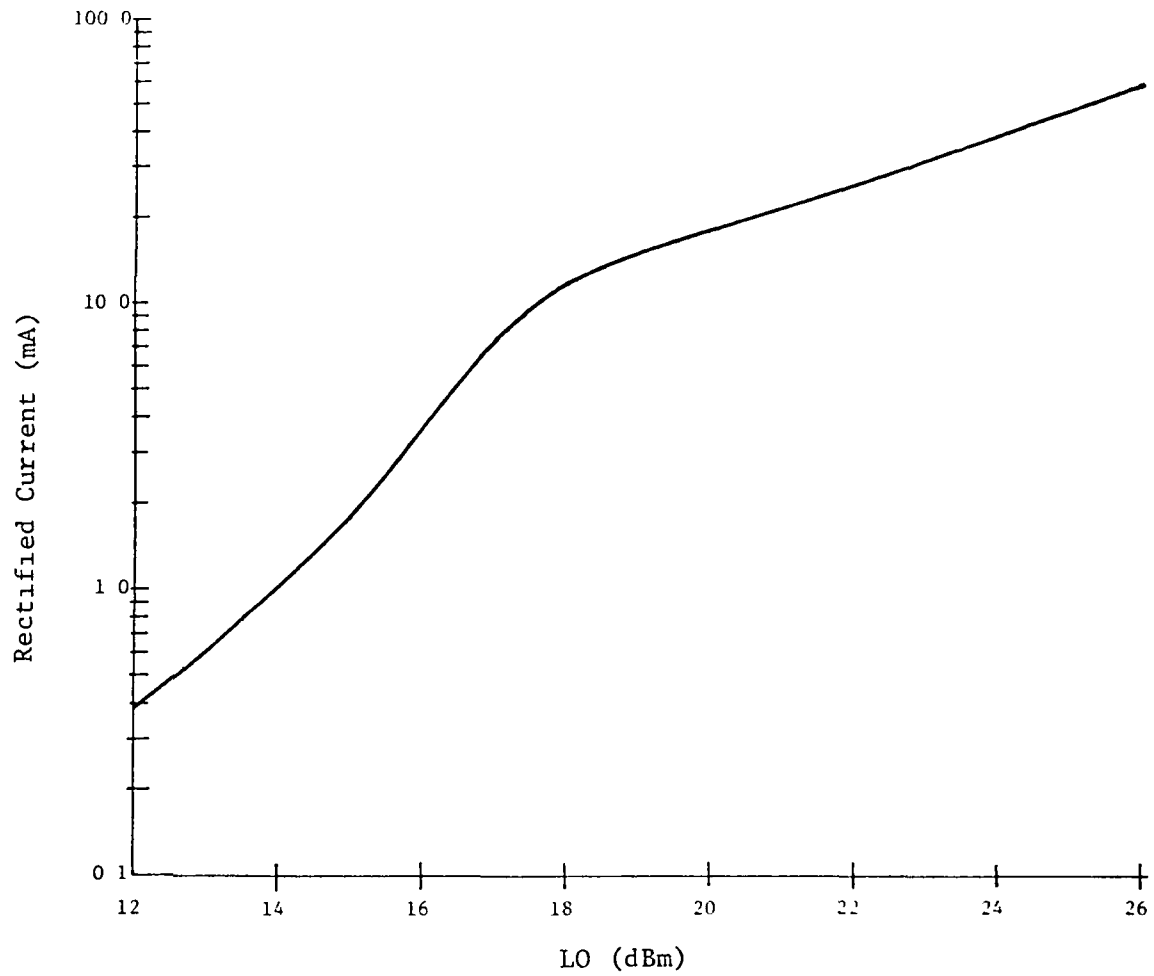
Figure 46. Diode Pair I/V Characteristics

Figure 47. Rectified Current vs. LO Power

SUMMARY

The filter circuits have now been finalized. The model stripline circuit performs its job in the mixer very well. The LO power is delivered to the diodes, the signal power stays in the diode pair, and the IF power is transmitted to the If port. Conversion loss is typically 6dB and noise figure is typically 8dB for the model.

The next task is the development of a fourth harmonic mixer circuit. Preliminary measurements on a similar mixer using fourth harmonic pumping yielded from 7 to 10dB conversion loss (SSB) across the same IF band with the same diodes as those used in the model A second harmonic mixer. This would correspond to pumping the 183GHz mixer with an LO of 45GHz.

Fabrication of the final 183GHz circuits will begin immediately. Scribing techniques necessary for cutting the stripline quartz substrate after the circuits are made have been developed. Some circuits will be fabricated here at Georgia Tech and some will be made at NASA GSFC.

Part I of this report gave preliminary data on the individual stripline filters and showed the design techniques used in developing them.

Part II finalized their design and gives the design procedures necessary to optimize the integrated circuit in the subharmonic mixer. This part also gives test data showing how well each circuit performs its individual task as well as overall mixer performance.

ATTACHMENTS

Vendor Data

1. Alpha   GaAs Diodes

2. RHG   Low Noise IF Preamplifier

Gallium Arsenide
### Schottky Barrier
Mixer Diodes

DATA SHEET
10100

| Frequency Band | Type Number | | Electrical Characteristics | | | Package Outline |
| | Polarity | NF [1] dB | F_{co} [2] (GHz) | C_j @ 0V pf | |
	Reversible	Max	Typ	Typ	
Packaged					
X	DMK–6600A	4 5	1000	0 15	207–001
X	DMK–6601A	4 5	1000	0 15	247–001
X	DMK–6600	5 0	700	0 15	207–001
X	DMK–6601	5 0	700	0 15	247–001
Ku	DMK–6602A	4 8	1000	0 10	207–001
Ku	DMK–5068A	4 8	1000	0 10	247–001
Ku	DMK–6602	5 3	700	0 10	207–001
Ku	DMK–5068	5 3	700	0 10	247–001
Ka	DMK–6603A	5 5	800	0 05	207–001
Ka	DMK–4058A	5 5	800	0 05	247–001
Ka	DMK–6603	6 0	500	0 05	207–001
Ka	DMK–4058	6 0	500	0 05	247–001
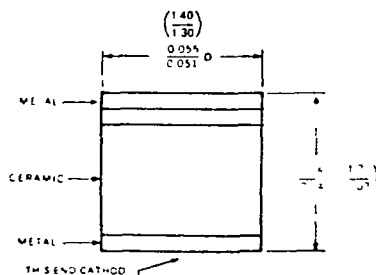
247-001

Notes

Maximum operating temperature = 150°C

Note 1 Single sideband noise figure measured with L O – 7 mW and including N_{if} = 1 0 dB

Note 2 $F_{co} = \dfrac{1}{2\pi R_s C_{j0}}$
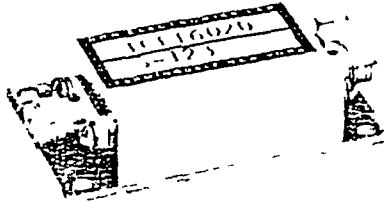
Note 3 Noise figure is determined by lot sampling

132

HYBRID IC PREAMPLIFIERS

■ LOW NOISE   ■ HIGH POWER   ■ SMALL SIZE

FIXED GAIN MODELS

• 2 db noise figures   • Bandwidths to 300 MHz

ICFT SERIES

Model	Center Freq (MHz)	Band width (MHz)	Power Gain (db)	Noise Figure (db)	Price
ICFT2006	20	6	30	2	$145
ICFT3010	30	10	30	2	95
ICFT6010	60	10	30	2	95
ICFT6020	60	20	30	2	125
ICFT6040	60	40	30	2	195
ICFT7030	70	30	30	2	195
ICFT12040	120	40	25	2 5	225
ICFT16050	160	50	25	3 0	225
ICFT300	10 to 300		25	2 to 100 MHz 4 to 250 MHz	225

NOTES
1 Input and output impedance 50'' VSWR 1 5 1 typical
2 Power out   0 dbm at 1 db compression
3 Power   12 VDC at 15 ma to 70 MHz 30 ma above 70 MHz
4 Connectors S'1A

The ICFT Series of preamplifiers are low noise hybrid IC units utilizing thin film techniques They have been designed to provide sufficient gain to overcome second stage noise effects in receiving systems

---

GENERAL

All units utilize hybrid integrated thin film techniques on an alumina substrate

Power Input	RFI filters with solder pins
Size	1 ½' x 1 ¼' x ½'
Weight	1 5 o (typ)
Environment	Parts materials and workmanship follow the guidelines of MIL E 5100 and MIL F IC 160

SPECIAL OPTIONS

1 All units are available in phase and gain matched sets
   Fixed gain models   and 0 5 db
   Variable gain models   and 1 db
2 Input impedance other than 50 ohms and crystal current monitor
   are available on special order

Double balanced mixers for RF and IF amplifiers are available
See catalog

RHG ELECTRONICS LABORATORY, INC.